

**T.C.
DİCLE ÜNİVERSİTESİ
FEN BİLİMLERİ ENSTİTÜSÜ**

**EXPERIMENTAL AND COMPUTATIONAL
STUDY OF VARIOUS CHEMICAL PROCESSES**

A Thesis submitted in part fulfilment for the degree of Doctor of Philosophy

At The University of Dicle, Graduate School of Science

by

Şafak ÖZHAN KOCAKAYA (BSc, MSc)

**DİYARBAKIR
June 2009**

**T.C.
DİCLE ÜNİVERSİTESİ
FEN BİLİMLERİ ENSTİTÜSÜ**

**EXPERIMENTAL AND COMPUTATIONAL
STUDY OF VARIOUS CHEMICAL PROCESSES**

A Thesis submitted in part fulfilment for the degree of Doctor of Philosophy

At The University of Dicle, Graduate School of Science

by

Şafak ÖZHAN KOCAKAYA (BSc, MSc)

Supervised by Prof. Dr. Necmettin PİRİNÇÇİOĞLU

**DİYARBAKIR
June 2009**

Table of Contents

Özet	i
Abstract	iv
Acknowledgements	vii
Abbreviations	viii
Figure and Table List	ix

Chapter 1 A Brief Introduction to Computational Modelling in Chemistry

1.1 Introduction	1
1.1.1 Molecular Modelling	2
1.1.2 Quantum Chemistry	5
1.1.2.1 <i>ab initio</i> Quantum Chemistry Methods	6
1.1.2.2 Density Functional Theory	7
1.1.2.3 Semi-empirical Quantum Chemistry Methods	8
1.1.3 Basis Sets	8
1.1.3.1 Minimal Basis Sets	10
1.1.3.2 Split-Valence Basis Sets	11
1.1.3.3 Plane Wave Basis Sets	12
1.1.4 Molecular Mechanics	12
1.1.4.1 Force Field	13
1.1.5 Molecular Dynamic	14
1.1.6 Molecular Docking	16
1.1.7 Binding Energy	17
1.1.8 Molecular Structure	18
1.1.9 Free Energy	20

1.1.10 Reaction Coordinate	20
1.1.11 Transition State	21
1.2 References	23
Chapter 2 A Theoretical Study of Effects of Polar Substitution on the Activation Barriers for Internal Rotation Around the C-N Bond in <i>p</i> -Substituted Nitrosobenzenes: Comparison of DFT and MP2 Calculations	
2.1 Introduction	25
2.2 Material and Methods	26
2.3 Results and Discussion	27
2.3.1 Linear Free Energy Relationship	30
2.3.2 Solvation	37
2.3.3 Steric Factors	38
2.3.4 Models	40
2.4 Conclusion	41
2.5 Tables	42
2.6 References	48
Chapter 3 A Theoretical Modelling of Polar Substituent Effects on the Alkaline Hydrolysis of <i>p</i> -Substituted Methyl Benzoates	
3.1 Introduction	50
3.2 Material and Method	51
3.3 Results and Discussion	52
3.4 Conclusion	56
3.5 Figures	57

3.6 Tables	60
3.7 References	62
Chapter 4 Theoretical And Experimental comparison Of Calix-[4] Resorcin Aren	
Specificity Towards Neutral And Charged Ligands	
4.1 Introduction	64
4.2 Method	66
4.2.1 Computational Modeling	66
4.2.1.1 Molecular Dynamics Simulations	66
4.2.1.2 Docking Study (Molecular Docking)	67
4.2.1.3 MM/PBSA Calculations	68
4.2.1.4 Quantum Chemical Calculations	70
4.3 Result and Discussion	70
4.3.1 MM/PBSA Calculations	71
4.3.2 Quantum Chemical Calculations	72
4.4 Conclusion	72
4.5 Figures	73
4.6 Tables	80
4.8 References	82
Chapter 5 A Mechanistic Detail of Addition of Aqueous Bromine to Disodium	
Salts of Citroconic and Mesaconic Acids	
5.1 Introduction	86
5.2 Materials	88
5.2.1 Experimental	88
5.2.1.1 General remarks	88

5.3 Method	88
5.3.1 General procedure for bromination of sodium citraconate and sodium mesaconate	85
5.4 Result and Discussion	90
5.5 Conclusions	95
5.6 Figures	96
5.7 References	105
 Chapter 6 Experimental (¹H NMR) and Theoretical Study of Complexes of Chiral Aza-15-Crown-5 Ether with Methyl Esters of Alanine and Valine Salts	
6.1 Introduction	107
6.2 Material and Method	108
6.3 Experimental Section	109
6.3.1 NMR Titration	109
6.3.2 Computational Section	109
6.3.2.1 Molecular Dynamics Simulations	109
6.3.2.2 Docking Study	110
6.3.2.3 MM/PBSA Calculations	111
6.3.2.4 Quantum Chemical Calculations	113
6.4 Results and Discussion	113
6.4.1 NMR Titration	113
6.4.2 Molecular Dynamics (MD)	114
6.4.3 MM/PBSA Method	116
6.4.4 Quantum Mechanical Calculations	117
6.5 Conclusions	117

6.6 Figures	118
6.7 Tables	129
6.7 References	132
Appendix A	135
Appendix B	140
Appendix C	154
<i>Curriculum Vitae(CV)</i>	158

Özet

Organizmalardaki kimyasal işlemlerin çalışılması önemli ve zor bir konudur. Bu işlemlerin atomic seviyede anlaşılması bir çok hastalığın tanımlanması ve tedavisinde yardımcı olabilir. Bilgisayarlı modelleme; kimyasal hız, denge ve moleküler etkileşimleri açıklamada en sık kullanılan araçlardan biridir.

Bu tezin amacı, biyolojik olaylar ile ilgisi olabilecek bazı kimyasal işlemleri deneysel ve bilgisayarlı teknikleri kullanarak incelemek ve açıklamaya çalışmaktır.

Birinci bölümde, kimyada kullanılan bilgisayarlı teknik ve metotlar hakkında kısaca bilgi verilmiştir.

İkinci bölümde, in *p*-süstitüe nitrosobenzen bileşikleri kullanılarak polar süstitüe etkinin C-N bağ etrafındaki dönme aktivasyon bariyerine tesiri DFT and MP2 metotları ile hesapsal olarak araştırıldı ve bu iki yöntem modele uygunlukları açısından karşılaştırıldı. Bağ dönme aktivasyon bariyerleri DFT (density functional theory) ve MP2 (Møller-Plesset) methodları ve 6-31+g(d) basis seti kullanılarak hesaplandı. Aktivasyon bariyerlerinin Hammett sigma değerleri ile doğrusal ilişkili oldukları ve MP2 methodu ile elde edilen sonuçların literatürde varolan deneysel sonuçlara çok yakın değerler verdiği görüldü.

Üçüncü bölümde, polar süstitüe etkinin *p*-süstitüe metil benzoatların alkalın hidroliz reaksiyonlarına tesiri incelendi. Hesaplamalar DFT metodu B3LYP/6-31+g(d) basis seti ile PCM çözücü ortamında (su, methanol ve asetonitril) yapıldı. Elde edilen serbest enerji aktivasyon bariyerinin alkalın hidrolizi geçiş

halinde hesaplanmış olan bağ uzunlukları ile polar Hammett sigma değerleri ve p-süstitüe benzoic asit pKa değerleri ile iyi korelasyon gösterdiği tespit edildi. Kullanılan PCM çözücü ortamlarının serbest enerji ilişkisin dikkate değer bir etkisinin olmadığı görüldü.

Dördüncü bölümde, oktakarboksilat metilresorsinkalix[4]arene bileşiğinin asetat, benzoate, hekzaonate, N-metil nikotinate ligandları ile olan non kovalent etkileşimleri araştırıldı. Farklı yüklü ve nötral esterlerin komplekslerinin modu, moleküler dinamik, MM/PBSA and ve (B3LYP/6-31+G*) metotları ile bağlanma özellikleri incelendi. Bu esterler için ONIOM B3LYP/631+G* seviyesinde hesaplanan bağlanma serbest enerjileri ($\Delta E_{\text{bind}} = -26.47, -27.82, -40.12, -363.76, -370.95$, MM/PBSA metodu ile hesaplanan bağlanma serbest enerjileri ($\Delta E_{\text{bind}} = -2.17, -7.22, -10.27, -15.15, -18.47$ olarak tespit edildi. Sonuç olarak host molekülünün yüklü olan ligandlar ile elektrostatik etkileşimler yaparak çok daha güçlü etkileştiği, nötral ligandlar ile ise van der Waals türü etkileşimler yaparak nispeten daha zayıf bağlanma yaptığı görülmüştür. Bulunan bu sonuçların literatürde var kinetic metot ile hesaplanmış olan deneysel veriler ile paralellik gösterdiği saptanmıştır.

Beşinci bölümde, mesakonik ve sitrakonik asit disodium tuzlarına sulu ortamda brom katılma reaksiyonları detaylı olarak çalışıldı. NMR ve x-ray cihazları ile yapılan ürün analizinde, mesakonat reaksiyonundan, *threo* β -lakton (%56), ve *threo* bromohidrin (%8.5), sitrakonattan ise *erythro* β -lakton (%45), *threo* β -lakton(%21) , *threo* bromohidrin (%6) ve 2,3 dibromo dikarboksilik asit izole

edildi. Bütün ürünlerin regioseçici olarak CH-Br ve CMe-Nu şeklinde gerçekleştiği görüldü. Sonuç olarak, her iki reaksiyon için benzer ürün kompozisyonlarına rastlanmıştır, reaksiyon mekanizması ve ürün oranları detaylı olarak çalışılmıştır.

Son bölümde, chiral aza-15-crown-5 bileşiğinin, alanin ve valin metil esterlerinin hidroklorür tuzları ile verdiği komplekslerin kloroform içindeki bağlanma ile moleküler tanıma ve diskriminasyon özellikleri atomik seviyede çalışılmıştır. Host molekülünün enantiyomerik diskriminasyonu bağlanma sabitleri . ^1H NMR titrasyon metodu kullanılarak deneysel olarak tespit edildi. Hesapsal olarak bağlanma serbest enerjileri -3.32, -3.53, -2.83, ve -2.89, Deneysel bağlanma sabitleri ise 260, 372, 116, 129 M^{-1} olarak belirlendi. Host molekülünün alanin tuzlarını valin tuzlarına göre daha iyi tanıdığı ve daha kuvvetli bağlandığı tespit edildi. Enantiyomerik diskriminasyon faktörü alanin tuzları için 17.36, valin tuzları için 5.22 olarak hesaplandı. Hesapsal çalışmalar, moleküler dinamik, MM/PBSA ve ONIOM (B3LYP/6-31+G*) metotları ve ^1H NMR metodu ile yapılan çalışmaların birbirini destekler nitelikte olduğu görüldü.

Abstract

Studying chemical processes are a very important but very difficult task, mainly those occurring in organisms. Understanding these processes at atomic level will assist scientists recognize and compact many major diseases. Computational modeling is one of the current tools employed in understanding of chemical rates, equilibria and molecular interactions. The aim of the thesis is to use experimental and computational techniques in investigation of some chemical processes, which may be relevant to biological interests.

The first chapter of this thesis gives a brief introduction to computational techniques and methodologies applied in chemistry and biochemistry.

The second chapter describes comparison of DFT and MP2 calculations in the study of effects of polar substitution on the activation barriers for internal rotation around the C-N bond in *p*-substituted nitrosobenzenes. The activation barriers for internal rotation were calculated using the density functional theory (DFT) and second-order Møller-Plesset (MP2) methods with 6-31+g(d) basis set. The activation barriers were well-correlated with Hammett sigma values and MP2 method produces better and comparable results with few available experimental values.

In the third chapter a detail mechanistic study of polar substituted effects on the alkaline hydrolysis of substituted methyl benzoates using B3LYP/6-31+g(d) computational method in PCM solvents (water, methanol and acetonitril) is given. The results indicate that activation free energies and bond lengths going from ground state to transition state for alkaline hydrolysis of methyl substituted benzoic acids are well-correlated with polar Hammett sigma constants and pKa's of

substituted benzoic acids. It was found that the PCM solvents did not have any significant effect on the free energy relationship.

The fourth chapter examines the nonmode of complexation of an octacarboxylatedmethlresorcincalix[4]arene with acetate, benzoic hegzagonate, N-methylnikotinate and methyl isonicotinate. The binding free energies respectively, ($\Delta E_{\text{bind}} = -26.47, -27.82, -40.12, -363.76, -370.95$, calculated by MM/PBSA and ($\Delta E_{\text{bind}} = -2.17, -7.22, -10.27, -15.15, -18.47$, kcal/mol calculated by ONIOM (B3LYP/6-31+G*) methods. The results showed the host binds to charged guests via electrostatic interactions while it binds to neutral guests via van der Waals interactions. The calculated binding constants are consistent with previously found experimental results by kinetic method.

In the fifth chapter experimental description is detailed for the mechanisms of aqueous bromine addition to disodium salts of citraconic and mesaconic acids. Product analysis by NMR and x-ray reveals that citraconate generates *erythro* β -lactone and *erythro* bromohydrin with expected stereo with overall *syn* addition and regiochemistry forming CMe-Nu bond rather CH-Nu bond. Surprisingly, it also generates *threo* β -lactone, which is the major product of the addition reaction of mesaconate with overall *anti* addition, a traceable amount of 2,3-dibromo acids with overall *anti* addition. However, the addition reaction of mesaconate yields the expected *threo* β -lactone and *threo* bromohydrin with overall *syn* addition but also *erythro* bromohydrin with overall *anti* addition. It was found that the addition

reactions of both free acids produce similar product composition. A rational mechanistic detail was proposed for the reactions.

The final chapter gives insight at atomic level concerning the molecular recognition and discrimination properties of a chiral aza-15-crown-5 with methyl esters of alanine and valine hydrochloride salts. Enantiomeric discrimination of the host against salts was studied by ^1H NMR titration. The binding free energies are calculated as $-(\Delta E_{\text{bind}} = 3.32, -3.53, -2.83, \text{ve } -2.89, \text{ experimental results; } 260, 372, 116, 129 \text{ M}^{-1})$. The results indicated that the host binds and discriminates alanine salts better than valine salts. Enantiomeric discrimination factors are calculated as 17.36 ve 5.22 for alanin and valine salt pair, respectively. The molecular dynamics, MM/PBSA and ONIOM (B3LYP/6-31+G*) calculations are consistent with ^1H NMR results.

ACKNOWLEDGEMENT

I am deeply indebted to my supervisor Prof. Dr. Necmettin PİRİNÇÇİOĞLU for his encouragement, guidance and support throughout my studies.

I would also like to thank prof. J. Grant BUCHAHAN and Ian H. WILLIAMS For their advisors and valuenable discussion for Chapter 5.

I would like to thank F. Marry MAHON for x-Ray spectrums.

I shall express my best graditus fort he memeber of the comitee of my thesis especially Prof. Dr. Viktorya AVİYENTE for their contributions and advises.

This Project was supported By Dicle University Reasearch Council (DUAPK-02-FF-20 and DUBAP-05-FF-31)

I would like to thank Arş. Gör. Ahmet Cenk ANDAÇ for guidance me molecular mechanic calculations and also for his friendship.

I would like to thank Bircan, Elif, Nevin and Selami for their providing me a friendly environment and support.

My deepest gratitude goes to my family for their unflagging loves and supports throughout my life.

I would like to give my special thanks to my husband Şefik and my son Sait Baran whose patient love enabled me to complete this work.

Abbreviations

DFT	Density functional theory
MP2	Møller Plesset methods
IRC	Intrinsic Reaction Coordinate
TS	Transition State
PCM	Polarizable Continuum Model
AMBER	Assisted Model Building with Energy Refinement
PBC	periodic boundary conditions
GAFF	The general AMBER Force Field
PME	The particle Mesh Ewald Method
AM1-Bcc	Austrian Model with Bond Change Correction
QM	Quantum mechanic
MM	Molecular mechanic
MD	Molecular Dynamic
RMSD	Root-Mean- Square deviation
NMODE	Normal mode analysis
ns	nano second
^1H NMR	Proton nuclear magnetic resonance spectroscopy
ϵ	effective charge
B	The Brønsted coefficient, a measure of the sensitivity rate for equilibrium change in basicity of nucleophile
σ	Hammett constants
δ	Chemical shift value parts per million relative to tetramethylsilane

Figure and Table List

1- Figure 2.1	26
2- Figure 2.2	27
3- Table 2.1	29
4- Figure 2.3	33
5- Table 2.2	35
6- Figure 2.5	39
7- Figure 2.6	39
8- Figure 2.7	40
9- Figure 2.8	40
10- Table 2.5.1	42
11- Table 2.5.2	46
12- Table 2.5.3	47
13- Figure 3.1	52
14- Figure 3.5.1	57
15- Figure 3.5.2	57
16- Figure 3.5.3	58
17- Figure 3.5.4	58
18- Figure 3.5.5	59
19- Table 3.6.1	60
20- Table 3.6.2	61
21- Figure 4.5.1	73
22- Figure 4.5.2	74
23- Figure 4.5.3	75

24- Figure 4.5.4	76
25- Figure 4.5.5	77
26- Figure 4.5.6	78
27- Figure 4.5.7	79
28- Table 4.6.1	80
29- Table 4.6.2	81
30- Figure 5.6.1	96
31- Figure 5.6.2	97
32- Figure 5.6.3	98
33- Figure 5.6.4	99
34- Figure 5.6.5	100
35- Figure 5.6.6	101
36- Figure 5.6.7	101
37- Figure 5.6.8	102
38- Figure 5.6.9	102
39- Figure 5.6.10	103
40- Figure 5.6.11	103
41- Figure 5.6.12	104
42- Figure 5.6.13	104
43- Figure 6.6.1	118
44- Figure 6.6.2	118
45- Figure 6.6.3	119
46- Figure 6.6.4	120
47- Figure 6.6.5	121

48- Figure 6.6.6	122
49- Figure 6.6.7	123
50- Figure 6.6.8	124
51- Figure 6.6.9	125
52- Figure 6.6.10	126
53- Figure 6.6.11	127
54- Figure 6.6.11	128
55- Table 6.7.1	129
56- Table 6.7.2	130
57- Table 6.7.3	131
58- Table 4.6.3	135
59- Table 4.6.4	136
60- Table 4.6.5	137
61- Table 4.6.6	138
62- Table 4.6.7	139
63- Table 5.7.1	140
64- Table 5.7.2	141
65- Table 5.7.3	141
66- Table 5.7.4	142
67- Table 5.7.5	142
68- Table 5.7.6	143
69- Table 5.7.7	144
70- Table 5.7.8	145
71- Table 5.7.9	145

72- Table 5.7.10	146
73- Table 5.7.11	147
74- Table 5.7.12	148
75- Table 5.7.13	148
76- Table 5.7.14	149
77- Table 5.7.15	149
78- Table 5.7.16	150
79- Table 5.7.17	151
80- Table 5.7.18	151
81- Table 5.7.19	152
82- Table 5.7.20	152
83- Table 6.6.4	154
84- Table 6.6.5	155
85- Table 6.6.6	156
86- Table 6.6.7	157

Chapter 1

A Brief Introduction to Computational Modelling in Chemistry

Chapter 2

A Theoretical Study of Effects of Polar Substitution on the Activation Barriers for Internal Rotation Around the C-N Bond in *p*-Substituted Nitrosobenzenes: Comparison of DFT and MP2 Calculations

Chapter 3

A Theoretical Modelling of Polar Substituent Effects on the Alkaline Hydrolysis of p-Substituted Methyl Benzoates

Chapter 4

Theoretical Study of Binding Properties of Octa-carboxylated calix[4]resorcinarene with Neutral and Charged Esters

Chapter 5

A Detail Mechanistic Study of Addition of Aqueous Bromine to Disodium Salts of Citraconic and Mesaconic Acids

Chapter 6

Experimental (¹H NMR) and Theoretical Study of Enantiomeric Discrimination of Methyl Esters of Alanine and Valine Salts by Chiral Aza-15-Crown-5 Ether

Appendix A

Appendix B

Appendix C

1.1. Introduction

The term *theoretical chemistry* may be defined as a mathematical description of chemistry, whereas *computational chemistry* is usually used when a mathematical method is sufficiently well developed and they can be automated for implementation on a computer. Note that the words *exact* and *perfect* do not appear here, as very few aspects of chemistry can be computed exactly. Almost every aspect of chemistry, however, can be included in a qualitative or approximate quantitative computational scheme.¹

Molecules consist of nuclei and electrons, so the methods of quantum mechanics apply. Computational chemists often attempt to solve the non-relativistic Schrödinger equation, with relativistic corrections added, although some progress has been made in solving the fully relativistic Schrödinger equation. It is, in principle, possible to solve the Schrödinger equation, in either its time-dependent form or time-independent form as appropriate for the problem in hand, but this in practice is not possible except for very small systems.² Therefore, careful approximation approaches are considered to achieve the best trade-off between accuracy and computational cost. The properties of molecules that contain no more than 10-40 electrons can be routinely and accurately modeled. The treatment of larger molecules that contain a few dozen electrons is computationally tractable by approximate methods such as density functional theory (DFT). However, it has been doubted that the method may not be sufficient to describe complex chemical reactions, such as those in biochemistry. Large molecules are rather studied by semi-empirical methods and even larger ones are treated with classical mechanic methods called molecular mechanics.³

In theoretical chemistry, chemists, physicists and mathematicians develop algorithms and computer programs to predict atomic and molecular properties and reaction paths for chemical transformations. Computational chemists, in contrast, may simply apply existing computer programs and methodologies to specific chemical questions. The followings are the basic subjects where the computational chemistry can be applied.

- 1- To find a starting point for a laboratory synthesis, or to assist in understanding experimental data, such as the position and source of spectroscopic peaks.
- 2- To predict the possibility of so far entirely unknown molecules or to explore reaction mechanisms that are not readily studied by experimental means.
- 3- It may assist the experimental chemist or it can challenge the experimental chemist to find entirely new chemical objects.
- 4- To predict the molecular structure of molecules by the use of the simulation of forces to find stationary points on the energy hypersurface as the position of the nuclei is varied
- 5- To identify correlations between chemical structures and properties (QSPR and QSAR).
- 6- To help in the efficient synthesis of compounds.
- 7- To design molecules that interact in specific ways with other molecules.

1.1.1 Molecular Modelling

Molecular modelling is a collective term, referring to theoretical approaches and computational techniques to model or mimic the behaviour of molecules. The techniques are used in the fields of computational chemistry, biology and materials

science and study molecular systems ranging from small chemical systems to large biological molecules and material assemblies. The simplest calculations can be performed by hand, but inevitably computers are required to perform molecular modeling of any reasonably sized system. The common feature of molecular modeling techniques is to describe the atomistic level of the molecular systems; the lowest level of information is a small group of atoms.

Molecular mechanics is synonymous with molecular modeling, and refers to the use of classical mechanics/Newtonian mechanics to describe the physical basis behind the models. Molecular models typically describe atoms, nucleus and electrons collectively as point charges with an associated mass. The interactions between neighbouring atoms are defined by spring-like interactions and van der Waals forces. The Lennard-Jones potential is commonly used to describe van der Waals forces. The electrostatic interactions are computed based on Coulomb's law. Atoms are assigned coordinates in Cartesian space or in internal coordinates, and can also be assigned velocities in dynamical simulations. The atomic velocities are related to the temperature of the system which is a macroscopic quantity. The collective mathematical expression is known as a potential function and is related to the system internal energy, a thermodynamic quantity equal to the sum of potential and kinetic energies. Methods which minimize the potential energy are known as energy minimization techniques while methods that model the behaviour of the system with propagation of time are known as molecular dynamics.

$$E = E_{bonds} + E_{angle} + E_{dihedral} + E_{non-bonded} \quad (1.1)$$

$$E_{non-bonded} = E_{electrostatic} + E_{van\ der\ Waals} \quad (1.2)$$

This function which is referred to as a potential function, computes the molecular potential energy as a sum of energy terms in equation 1.1 that describe the deviation of bond lengths, bond angles and torsion angles away from equilibrium values is related equation 1.2 to non-bonded pairs of atoms describing van der Waals and electrostatic interactions. The set of parameters consisting of equilibrium bond lengths, bond angles, partial charge values, force constants and van der Waals parameters are collectively known as a force field. Different implementations of molecular mechanics use slightly different mathematical expressions, and therefore, different constants for the potential function. The common force fields have been developed by using high level quantum calculations and fitting to the experimental data. Energy minimization techniques are used to find positions of zero gradient for all atoms, in other words, a local energy minimum. Lower energy states are more stable and are commonly considered for their role in chemical and biological processes. A molecular dynamics simulation, involves solving Newton's laws of motion, principally the second law in equation 1.3.

$$F = m a \quad (1.3)$$

Integration of Newton's laws of motion, using different integration algorithms, leads to atomic trajectories in space and time. The force on an atom is defined as the negative gradient of the potential energy function. The energy minimization technique is useful for obtaining a static picture for comparing between states of similar systems, while molecular dynamics provides information about the dynamic processes with the intrinsic inclusion of temperature effects.

The effect of solution to be considered is an important factor in behaviour of molecules and they can be modeled either in vacuum or in the presence of a solvent

such as water. Simulations of systems in vacuum are referred to as *gas-phase* simulations, while those that include the presence of solvent molecules are referred to as *explicit solvent* simulations. In another type of simulation, the effect of solvent is estimated by different empirical mathematical expressions, known as *implicit solvation* simulations.

1.1.2 Quantum Chemistry

Quantum chemistry is a branch of theoretical chemistry, which applies quantum mechanics and quantum field theory to address issues and problems in chemistry. The description of the electronic behavior of atoms and molecules as pertaining to their reactivity is one of the applications of quantum chemistry, which lies on the border between chemistry and physics, and significant contributions have been made by scientists from both fields. It has a strong and active overlap with the field of atomic physics and molecular physics, as well as physical chemistry.

Quantum chemistry mathematically defines the fundamental behavior of matter at the molecular scale. It is, in principle, possible to describe all chemical systems using this theory. In practice, only the simplest chemical systems may realistically be investigated in purely quantum mechanical terms, and approximations must be made for most practical purposes (Hartree-Fock, post-Hartree-Fock or Density functional theory) Hence a detailed understanding of quantum mechanics is not necessary for most chemistry, as the important implications of the theory (principally the orbital approximation) can be understood and applied in simpler terms.

In quantum mechanics the Hamiltonian, or the physical state, of a particle can be expressed as the sum of two operators, one corresponding to kinetic energy and the other to potential energy. The Hamiltonian in the Schrödinger wave equation used in quantum chemistry does not contain terms for the spin of the electron.

Solutions of the Schrödinger equation gives the form of the wave function for atomic orbitals for the hydrogen atom, and the relative energy of the various orbitals. The orbital approximation can be used to understand the other atoms e.g. helium, lithium and carbon.

1.1.2 Quantum Chemistry Methods

1.1.2.1 *ab initio* Method

The programs used in computational chemistry are based on many different quantum-chemical methods that solve the molecular Schrödinger equation associated with the molecular Hamiltonian. Methods that do not include any empirical or semi-empirical parameters in their equations - being derived directly from theoretical principles, with no inclusion of experimental data - are called *ab initio* methods. This does not imply that the solution is an exact one; they are all approximate quantum mechanical calculations. It means that a particular approximation is rigorously defined on first principles (quantum theory) and then solved within an error margin that is qualitatively known beforehand. If numerical iterative methods have to be employed, the aim is to iterate until full machine accuracy is obtained. The simplest type of *ab initio* electronic structure calculation is the Hartree-Fock (HF) scheme, in which the Coulombic electron-electron repulsion is not specifically taken into account. Only its average effect is included in the calculation. As the basis set size is

increased the energy and wave function tend to a limit called the Hartree-Fock limit. Many types of calculations, known as post-Hartree-Fock methods, begin with a Hartree-Fock calculation and subsequently correct for electron-electron repulsion, referred to also as electronic correlation. As these methods are pushed to the limit, they approach the exact solution of the non-relativistic Schrödinger equation. In order to obtain exact agreement with experiment, it is necessary to include relativistic and spin orbit terms, both of which are only really important for heavy atoms. In all of these approaches, in addition to the choice of method, it is necessary to choose a basis set. This is set of functions, usually centered on the different atoms in the molecule, which are used to expand the molecular orbital with the LCAO ansatz. *ab initio* methods need to define a level of the method) and a basis set.

The Hartree-Fock wave function is a single configuration or determinant. In some cases, particularly for bond breaking processes, this is quite inadequate and several configurations need to be used. Here the coefficients of the configurations and the coefficients of the basis functions are optimized together. The total molecular energy can be evaluated as a function of the molecular geometry, in other words the potential energy surface.

1.1.2.2 Density Functional Theory

Density functional theory (DFT) methods are often considered to be *ab initio* methods determined to the molecular electronic structure, even though many of the most common functional use parameters derived from empirical data, or from more complex calculations. This means that they could also be called semi-empirical methods. It is best to treat them as a class on their own. In DFT, the total energy is

expressed in terms of the total electron density rather than the wave function. In this type of calculation, there is an approximate Hamiltonian and an approximate expression for the total electron density. DFT methods can be very accurate for little computational cost. The drawback is, that unlike *ab initio* methods, there is no systematic way to improve the methods by improving the form of the functional.

1.1.2.3 Semi-empirical Quantum Chemistry Methods

Semi-empirical quantum chemistry methods are based on the Hartree-Fock formalism, but make many approximations and obtain some parameters from empirical data. They are very important in computational chemistry for treating large molecules where the full Hartree-Fock method without the approximations is too expensive. The use of empirical parameters appears to allow some inclusion of correlation effects into the methods.

Semi-empirical methods follow what are often called empirical methods where the two-electron part of the Hamiltonian is not explicitly included. For π -electron systems, this was the Hückel method proposed by Erich Hückel, and for all valence electron systems, the Extended Hückel method proposed by Roald Hoffmann.

1.1.3 Basis Sets

A basis set in chemistry is a set of functions used to create the molecular orbitals, which are expanded as a linear combination of such functions with the weights or coefficients to be determined. Usually these functions are atomic orbital, in that they

are centered on atoms, but functions centered in bonds or lone pairs have been used as have pairs of functions centered in the two lobes of a p orbital.

In modern computational chemistry, quantum chemical calculations are typically carried out within a finite set of basis functions. In these cases, the wave functions under consideration are all represented as vectors, the components of which refer to coefficients in a linear combination of the basis functions in the basis set used. The operators are then represented as matrices, (rank two tensors), in this finite basis.

It is common to use a basis composed of a finite number of atomic orbitals, centered at each atomic nucleus within the molecule when performing the molecular calculation. Initially, these atomic orbitals were typically Slater orbitals which corresponded to a set of functions which decayed exponentially with distance from the nuclei. Later, it was realized that these Slater-type orbitals could in turn be approximated as linear combinations of Gaussian orbitals instead. Calculation of overlap and other integrals with Gaussian basis functions easier leading to huge computational savings.

Hundreds of basis sets consisted of Gaussian-type orbitals (GTOs) have been developed. The smallest of these are called *minimal basis sets*, and they are typically composed of the minimum number of basis functions required to represent all of the electrons on each atom while the largest of once can contain literally dozens to hundreds of basis functions on each atom.

The most common addition to minimal basis sets is probably the addition of polarization functions, denoted by an asterisk, *. Two asterisks, **, indicate that polarization functions are also added to light atoms (hydrogen and helium). These are

auxiliary functions with one additional node. For example, the only basis function located on a hydrogen atom in a minimal basis set would be a function approximating the 1s atomic orbital. When polarization is added to this basis set, a p-function is also added to the basis set. Thus, adding some additional needed flexibility within the basis set and hence effectively allowing molecular orbitals involving the hydrogen atoms to be more asymmetric about the hydrogen nucleus. This is an important outcome when considering accurate representations of bonding between atoms, because of the bonded atom changes makes the energetic environment of the electrons spherically asymmetric. Similarly, d-type functions can be added to a basis set with valence p orbital, and f-functions to a basis set with d-type orbital, and so on. Another, more precise notation indicates exactly which and how many functions are added to the basis set, such as (p, d).

Another common addition to basis sets is diffuse functions, denoted by a plus sign, +. Two plus signs indicate that diffuse functions are also added to light atoms (hydrogen and helium). These are very shallow Gaussian basis functions, which more accurately represent the "tail" portion of the atomic orbitals, which are distant from the atomic nuclei. These additional basis functions can be important when considering anions and other large, "soft" molecular systems.

1.1.3.1 Minimal Basis Sets

A common naming convention for minimal basis sets is *STO-XG*, where X is an integer. This X value represents the number of Gaussian primitive functions comprising a single basis function. In these basis sets, the same number of Gaussian primitives comprise core and valence orbitals. Minimal basis sets typically give

rough results that are insufficient for research-quality publication, but are much cheaper than their larger counterparts. Here is a list of commonly used minimal basis sets: STO-2G, STO-3G, STO-6G, STO-3G* - Polarized version of STO-3G.

1.1.3.2 Split-Valence Basis Sets

The notation for these *split-valence* basis sets is typically $X\text{-}YZg$. In this case, X represents the number primitive Gaussians comprising each core atomic orbital basis function. The Y and Z indicate that the valence orbitals are composed of two basis functions each, the first one composed of a linear combination of Y primitive Gaussian functions, the other composed of a linear combination of Z primitive Gaussian functions. In this case, the presence of two numbers after the hyphens implies that this basis set is a *split-valence double-zeta* basis set. Split-valence triple- and quadruple-zeta basis sets are also used, denoted as $X\text{-}YZWg$, $X\text{-}YZWVg$, etc. Here is a list of commonly used split-valence basis sets: 3-21g, 3-21g* (Polarized), 3-21+g (Diffuse functions), 3-21+g* - With polarization *and* diffuse functions, 6-31g, 6-31g*, 6-31+g*, 6-31g(3df, 3pd), 6-311g, 6-311g*, 6-311+g*, SV(P) SVP. Double, triple, quadruple zeta basis sets the existence of multiple basis functions corresponding to each atomic orbital, including both valence orbitals and core orbitals or just the valence orbitals, are called double, triple, or quadruple-zeta basis sets. Commonly used multiple zeta basis sets are given as follows: cc-pVDZ - Double-zeta MC pVTZ - Triple-zeta, cc-pVQZ - Quadruple-zeta, cc-pV5Z - Quintuple-zeta, etc. aug-cc-pVDZ, etc. - Augmented versions of the preceding basis sets with added diffuse functions, TZVPP- Triple-zeta, QZVPP - Quadruple-zeta.

The 'cc-p' at the beginning of some of the above basis sets stands for 'correlation consistent polarized' basis sets. They are double/triple/quadruple/quintuple-zeta for the valence orbitals only (the 'V' stands for valence) and include successively larger shells of polarization (correlating) functions (d, f, g, etc.) that can yield convergence of the electronic energy to the complete basis set limit. They are the current state of the art for correlated or post Hartree-Fock calculations.

1.1.3.3 Plane Wave Basis Sets

In addition to localized basis sets, plane wave basis sets can also be employed in quantum chemical simulations. Typically, the use of a finite number of plane wave functions are done, below a specific cutoff energy which is chosen for a certain calculation. They are quite popular in calculations involving periodic boundary conditions. It is much easier to code and carry out certain integrals and operations with plane wave basis functions, compared with their localized counterparts; furthermore, as all functions in the basis are mutually orthogonal, plane wave basis sets do not exhibit basis set superposition error. However, they are less well suited to gas-phase calculations.

1.1.4 Molecular Mechanics

The term molecular mechanics, refers to the use of Newtonian mechanics to model molecular systems. Molecular mechanics calculates the potential energy of all systems using force fields. Molecular mechanics can be used to study small molecules as well as large biological systems or material assemblies with many thousands to millions of atoms. A force field, set of parameters and functions

forming a data base of compounds are used for parameterization is crucial to the success of molecular mechanics calculations so a force field parameterized against a specific class of molecules, for instance proteins, would be expected to only have any relevance when describing other molecules of the same class.

All-atomistic molecular mechanics methods have the following properties: Each atom is simulated as a single particle and Each particle is assigned a radius (typically the van der Waals radius), polarizability, and a constant net charge. Bonded interactions are treated as "springs" with an equilibrium distance equal to the experimental or calculated bond length.⁶

Molecular Mechanic and Molecular Dynamic (MD) are related but different. Main purpose of MD is modeling of molecular motions, although it is also applied for optimization, for example using simulated annealing. MM implements more "static" energy minimization methods to study the potential energy surfaces of different molecular systems. However, MM can also provide important dynamic parameters, such as energy barriers between different conformers or steepness of a potential energy surface around a local minimum. MD and MM are usually based on the same classical force fields. But MD may also be employ on quantum chemical methods like DFT. MM is also loosely used to define a set of techniques in molecular modeling.³⁶

1.1.4.1 Force Field

In the context of molecular mechanics, a force field refers to the functional form and parameter sets used to describe the potential energy of a system of particles (typically but not necessarily atoms). Force field functions and parameter sets are

derived from both experimental work and high-level quantum mechanical calculations. "All-atom" force fields provide parameters for every atom in a system, including hydrogen, while "united-atom" force fields treat the hydrogen and carbon atoms in methyl and methylene groups as a single interaction center. "Coarse-grained" force fields, which are frequently used in long-time simulations of proteins, provide even more abstracted representations for increased computational efficiency.¹¹

1.1.5 Molecular Dynamic

Molecular dynamics (MD) is a form of computer simulation where atoms and molecules are allowed to interact for a period of time under known laws of physics. Because in general molecular systems consist of a large number of particles, it is impossible to find the properties of such complex systems analytically. MD simulation circumvents this problem by using numerical methods. It represents an interface between laboratory experiments and theory and can be understood as a virtual experiment.⁷

Molecular dynamics is a multidisciplinary field. Its laws and theories stem from mathematics, physics and chemistry. MD employs algorithms from computer science and information theory. It was originally conceived within theoretical physics in the 1950's, but it's mostly applied today in materials science and biomolecules.

Even though we know that matter consists of interacting particles in motion at least since Boltzmann in the 19th Century, many still think of molecules as rigid museum models. Richard Feynman said in 1963 that "everything that living things

do can be understood in terms of the jiggling and wiggling of atoms." ⁸ One of MD's key contributions is creating awareness that molecules like proteins and DNA are machines in motion. MD probes the relationship between molecular structure, movement and function.

Before it became possible to simulate molecular dynamics with computers, some undertook the hard work of trying it with physical models such as macroscopic spheres. The idea was to arrange them to replicate the properties of a liquid. Here's a quote from J.D. Bernal from 1962: "... I took a number of rubber balls and stuck them together with rods of a selection of different lengths ranging from 2.75 to 4 inch. I tried to do this in the first place as casually as possible, working in my own office, being interrupted every five minutes or so and not remembering what I had done before the interruption." ⁹ Fortunately, now computers keep track of bonds during a simulation.

MD has also been termed as "statistical mechanics by numbers" and "Laplace's vision of Newtonian mechanics" of predicting the future by animating nature's forces. It is tempting to describe it as a virtual microscope. However, long MD simulations are mathematically ill conditioned. This generates cumulative numerical errors. This fact alone should dispel any illusions that the method acts like a molecular microscope that allows us to look at the actual trajectories a molecule would follow in time. Nevertheless, molecular dynamics techniques allow detailed time and space resolution into representative behavior in phase space.¹⁰

More formally, MD is a special discipline of molecular modelling and computer simulation. Based on molecular mechanics, it addresses numerical solutions of Newton's equations of motion i.e. Hamiltonian mechanics on an atomistic or similar

model of a molecular system to obtain information about its equilibrium and dynamic properties. The main justification of the MD method is that statistical ensemble averages are equal to time averages of the system. This is called the Ergodic hypothesis.

1.1.6 Molecular Docking

In the field of molecular modeling, docking is a method which predicts the preferred orientation of one molecule to a second when bound to each other to form a stable complex.¹² Knowledge of the preferred orientation in turn may be used to predict the strength of association or binding affinity between two molecules using for example scoring functions.

The associations between biologically relevant molecules such as proteins, nucleic acids, carbohydrates, and lipids play a central role in signal transduction. Furthermore, the relative orientation of the two interacting partners may affect the type of signal produced . Therefore docking is useful for predicting both the strength and type of signal produced.

Docking is frequently used to predict the binding orientation of small molecule drug candidates to their protein targets in order to in turn predict the affinity and activity of the small molecule. Hence docking plays an important role in the rational design of drugs. Given the biological and pharmaceutical significance of molecular docking, considerable efforts have been directed towards improving the methods used to predict docking .¹³

Molecular docking can be thought of as a problem of “*lock-and-key*”, where one is interested in finding the correct relative orientation of the “*key*” which will

open up the “*lock*” (where on the surface of the lock is the key hole, which direction to turn the key after it is inserted, etc.). Here, the protein can be thought of as the “*lock*” and the ligand can be thought of as a “*key*”. Molecular docking may be defined as an optimization problem, which would describe the “*best-fit*” orientation of a ligand that binds to a particular protein of interest. However since both the ligand and the protein are flexible, a “*hand-in-glove*” analogy is more appropriate than “*lock-and-key*”. During the course of the process, the ligand and the protein adjust their conformation to achieve an overall “*best-fit*” and this kind of conformational adjustments resulting in the overall binding is referred to as “*induced-fit*”.^{14,15}

The focus of molecular docking is to computationally stimulate the molecular recognition process. The aim of molecular docking is to achieve an optimized conformation for both the protein and ligand and relative orientation between protein and ligand such that the free energy of the overall system is minimized.

1.1.7 Binding Energy

Binding energy is the mechanical energy required to disassemble a whole into separate parts. A bound system has a lower potential energy than its constituent parts; this is what keeps the system together. The usual convention is that this corresponds to a *positive* binding energy.¹⁶

In general, binding energy represents the mechanical work which must be done in acting against the forces which hold an object together, while disassembling the object into component parts separated by sufficient distance that further separation requires negligible additional work. Electron binding energy is a measure

of the energy required to free electrons from their atomic orbits.

Nuclear binding energy is derived from the strong nuclear force and is the energy required to disassemble a nucleus into free unbound neutrons and protons, strictly so that the relative distances of the particles from each other are infinite (essentially far enough so that the strong nuclear force can no longer cause the particles to interact).¹⁷

At the atomic level, the atomic binding energy of the atom derives from electromagnetic interaction and is the energy required to disassemble an atom into free electrons and a nucleus.

In bound systems, if the binding energy is removed from the system, it must be subtracted from the mass of the unbound system, simply because this energy has mass, and if subtracted from the system at the time it is bound, will result in removal of mass from the system. System mass is not conserved in this process because the system is not closed during the binding process.¹⁸

1.1.8 Molecular Structure

The total energy of structure is determined by approximate solutions of the time-dependent Schrödinger equation, usually with no relativistic terms included, and making use of the Born-Oppenheimer approximation which, based on the much higher velocity of the electrons in comparison with the nuclei, allows the separation of electronic and nuclear motions, and simplifies the Schrödinger equation. This leads to the evaluation of the total energy as a sum of the electronic energy at fixed nuclei positions plus the repulsion energy of the nuclei. A notable exception are certain approaches called direct quantum chemistry, which treat electrons and nuclei

on a common footing. Density functional methods and semi-empirical methods are variants on the major subject. For very large systems the total energy is determined using molecular mechanics.¹⁹

A given molecular formula can represent a number of molecular isomers. Each isomer is a local minimum on the potential energy surface produced from the total energy (electronic energy plus repulsion energy between the nuclei) as a function of the coordinates of all the nuclei. A stationary point is a geometry such that the derivative of the energy with respect to all displacements of the nuclei is zero. A local energy minimum is a stationary point where all such displacements lead to an increase in energy. The local minimum corresponding to the lowest energy is called the global minimum and corresponds to the most stable isomer. If there is one particular coordinate change that leads to a decrease in the total energy in both directions, the stationary point is a transition structure and the coordinate is the reaction coordinate. This process of determining stationary points is termed as geometry optimization.²⁰

To determine molecular structures and geometry optimization routine only when efficient methods for calculating the first derivatives of the energy with respect to all atomic coordinates are available. Evaluation of the related second derivatives makes it possible to predict vibrational frequencies if harmonic motion is assumed. In some ways more importantly it allows the characterisation of stationary points. The frequencies are associated with the eigenvalues of the matrix of second derivatives. If the eigenvalues are all positive, then the frequencies are all real and the stationary point is a local minimum. If one eigenvalue is negative (an imaginary frequency), then the stationary point corresponds to a transition structure. If more

than one negative eigenvalues are observed the stationary point is a more complex one, and usually of little interest. When spotted, it is necessary to move the search away from it, if we are looking for local minima and transition structures.²¹

1.1.9 Free Energy

The free energy of a reaction determines if a chemical reaction will take place, the kinetics will then tell how fast the reaction is. A reaction can be very exothermic but will not happen in practice if the reaction is too slow. If a reactant can react to form two different products, the thermodynamically most stable product will generally form except in special circumstances when the reaction is said to be under kinetic reaction control.²² The Curtin-Hammett principle applies when determining the product ratio for two reactants interconverting rapidly each going to a different product.²³ It is possible to make predictions about reaction rate constants for a reaction from Free-energy relationships. The kinetic isotope effect is a difference in the rate of a chemical reaction when an atom in one of the reactants is replaced by one of its isotopes. Chemical kinetics provide information on residence time and heat transfer in a chemical reactor in chemical engineering and the molar mass distribution in polymer chemistry.²⁴

1.1.10 Reaction Coordinate

In chemistry, a reaction coordinate is an abstract one-dimensional coordinate which represents progress along a reaction pathway. It is usually a geometric parameter that changes during the conversion of one or more molecular entities. Reaction coordinates are often plotted against free energy to demonstrate in some schematic

form the potential energy profile (an intersection of a potential energy surface) associated to the reaction.²⁵

In the formalism of transition-state theory the reaction coordinate is that coordinate in set of curvilinear coordinates obtained from the conventional ones for the reactants which, for each reaction step, leads smoothly from the configuration of the reactants through that of the transition state to the configuration of the products. The reaction coordinate is typically chosen to follow the path along the gradient (path of shallowest ascent/deepest descent) of potential energy from reactants to products. For example, in the homolytic dissociation of molecular hydrogen, an apt coordinate system to choose would be the coordinate corresponding to the bond length.²⁶

1.1.11 Transition State

The transition state of a chemical reaction is a particular configuration along the reaction coordinate. It is defined as the state corresponding to the highest energy along this reaction coordinate. At this point, assuming a perfectly irreversible reaction, colliding reactant molecular history of concept. A collision between reactant molecules may or may not result in a successful reaction. The outcome depends on factors such as the relative kinetic energy, relative orientation and internal energy of the molecules. Even if the collision partners form an activated complex they are not bound to go on and form products, and instead the complex may fall apart back to the reactants.²⁷

The concept of a transition state has been important in many theories of the rate at which chemical reactions occur. This started with the transition state theory

(also referred to as the Activated Complex Theory), which was first developed around 1935 and which introduced basic concepts in chemical kinetics which are still used today.²⁸

Because of the rules of quantum mechanics, the transition state cannot be captured or directly observed; the population at that point is zero. However, cleverly manipulated spectroscopic techniques can get us as close as the timescale of the technique will allow us. Femtosecond IR spectroscopy was developed for precisely that reason, and it is possible to probe molecular structure extremely close to the transition point. Often along the reaction coordinate reactive intermediates are present not much lower in energy from a transition state making it difficult to distinguish between the two.²⁹

1.2 References

1. Schaefer, H. F.; Leach, A. R., *Massachusetts, Addison-Wesley Publishing Co.* **1972**, 146.
2. Boys, S. F.; Cook G. B.; Reeves, C. M.; Shavitt, I., *Nature* **1956**, 8, 2, 1207.
3. Richards, W. G.; Walker T. E. H; Hinkley, R. K., *Oxford, Clarendon Press*, **1971**.
4. Patel, S.; MacKerell, Jr. AD; Brooks III, C. L., *J. Comput. Chem.*, **2004**, 1504.
5. Wainwright, T. E., *J. Chem. Phys.* **1959**, 31, 2, 459.
6. Bernal, J. D., *The Bakerian lecture, 1962, The structure of liquids. Proc. Soc.*, **1964** 280, 299.
7. Allinger, N., *J. Am. Chem. Soc.*, **1977**, 99, 8127.
8. Lenguer, T.; Rarey, M., *Opin. Struct. Biol.*, **1996**, 6, 3, 402.
9. Kitchen, D. B.; Decornez, H.; Furr, J. R.; *Nature reviews*, **2004**, 3, 11, 935.
10. Jogensen, W. L.; *Science*, **1991**, 254, 5030, 954.
11. Wei, B. Q.; Weaver, L. H.; Ferrari, A. M.; Matthews, B. W.; Schoichet, B. K., *J. Mol. Biol.*, **2004**, 337, 5, 1161.
12. Preuss, H., *Int. J. Quantum Chem.*, **1968**, 2, 651.
13. Buenker, R. J.; Peyerimhoff, S. D., *Chem. Phys. Lett.*, **1969**, 3, 37.
14. Schaefer, H. F., *Quantum Chem., Oxford, Clarendon Press.*, **1984**.
15. Bernal, J. D., *The structure of liquids. Proc. R. Soc.* **1964**, 280, 299.
16. Alder, B. J.; Wainwright, T. E., *J. Chem. Phys.* **1959**, 31, 2, 459.
17. Tuckerman, M.E.; Berne, B.J.; Martyna, G.J.; *J. Chem. Phys.* **1991**, 94, 10, 6811.
18. Sugita, Y.; Okamoto, Y., *Chem Phys Letters*, **1999**, 314, 141.
19. Streett, W. B.; Tildesley, D. J.; Saville, G., *Mol. Phys.* **1978**, 35, 3, 639.
20. Brenner, D. W., *Phys. Rev. B.*, 2, 15, 9458, 10, 1103, *Phys Rev B.* **1990**, 42, 9458.

21. Duin, A. V.; Dasgupta, S.; Lorant, F.; Goddard, W. A., *III. J. Phys. Chem.* **2001**, 105, 9398.
22. Daw, M. S.; Foiles, S. M.; Baskes, M. I., *Mat. Sci. And Engr. Rep.* **1993**, 9, 251.
23. Cleri, F.; Rosato, V., *Phys. Rev.* **1993**, 48, 22.
24. Lamoureux, G; Harder, E; Vorobyov, R. B.; MacKerell, A.D.; *Chem. Phys. Lett.* **2006**, 418, 245.
25. Billeter, S. R.; Webb, S. P.; Agarwal, P. K.; Iordanov, T.; Hammes-Schiffer, S., *J. Am. Chem. Soc.*, **2001**, 123, 11262.
26. Ding, F.; Borreguero, J. M.; Buldyrey S.V.; Stanley, H. E.; Dokholyan, N.V., *J. Am. Chem. Soc.* **2003**, 53, 220.
27. Paci, E.; Vendruscolo, M. ; Karplus, M., *Biophys J.*, **2002**, 83, 3032.
28. Box, V. G., *J. Mol. Model.*, **1997**, 3, 3, 124.
29. Box, V. G., *Heterocycles*, **1998**, 48, 11, 2389.

2.1 Introduction

Rotamers are a set of conformers and the rotation barrier is the activation energy required to jump from one conformer to another. This will produce a racemic mixture of conformations that may or may not have different reactivities in situations such as enzymatic reactions in which molecular shape is usually a key factor of operation. Conformational isomerism only occurs around single bonds as a consequence of the requirement of breaking one or more pi bonds to rotate substituents about a sigma bond axis in double and triple bonded atoms. So it becomes very important to estimate the activation barrier of bond rotation in different systems in order to foresee, for example, the reactivity of one rotamer over the others and also their interaction with other molecules.

Polar substituent effect is one of the most powerful tools in the elucidation of reaction mechanisms.^{1,2} This effect is observed in rates and equilibria, which is caused by the changes in the electronic structures going from reactant to transition states in rates or from reactant to product states in equilibria. Despite the successful application of polar substitution effects on to rates and equilibria,³ very little is known about the effects on bond rotation.⁴⁻⁸

The present work represents a theoretical approach to study the effect of polar substitution on the activation barriers of internal rotation of the C-N bond in *p*-substituted nitrosobenzene systems. Calculations were conducted by B3LYP density functional theory and MP2 Møller Plesset perturbation theory with the basis 6-31+g(d). PCM was used as solvation model. Nitroso compounds are chosen for the sake of simplicity and the availability of experimental results for comparisons.^{7,8} And it is known that the activation barrier is an indication of self-dimerisation tendencies

in these compounds. The lower barrier means the more tendency for dimerisation. It is also important to predict the structural properties of substituted nitrosobenzenes because they are of great interest. The compounds included in the study are illustrated in Figure 2.1.

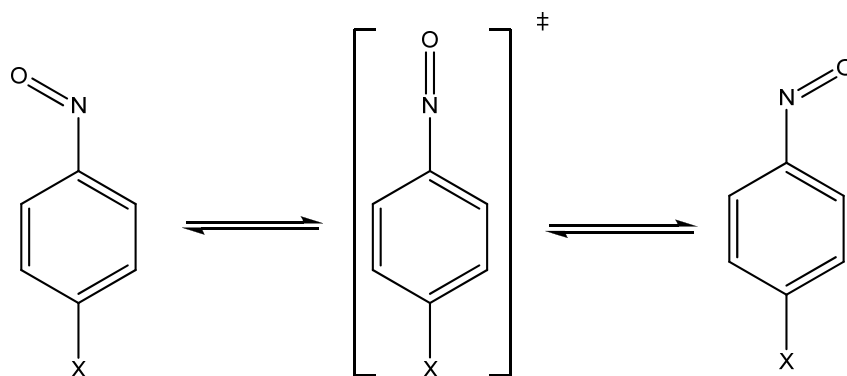


Figure 2.1 X= NO₂, CN, COMe (Ac), Cl, F, H, Me, MeO, OH and NH₂

2.2 Material Methods

All calculations were performed by means of the GAUSSIAN 03 programme⁹ using the B3LYP density functional theory and perturbation theory the MP2 with the 6-31+G(d) basis (with six Cartesian d functions on non-hydrogen atoms), together with the PCM method for aqueous and chloroform solvation using $\epsilon = 78.4$ and 4.90 respectively, and UA0 (Simple United Atom Topological Model) for the molecular cavity. Convergence in the SCF procedure was typically achieved using geometry optimisations used default convergence criteria. TS's were located either performing transition state search on the geometry obtained from the highest energy point from scanning rotation around C-N bond or fixing the torsional angle between the -NO group or phenyl-ring at 90° followed opt=(ts,call). Some of them were obtained from ts=QST2. All transition structures were characterised as possessing a single imaginary frequency corresponding to the transition vector (or reaction coordinate

mode) for a particular chemical transformation, in contrast to energy minima with all-real vibrational frequencies. IRC calculations confirmed the identity of the energy minima adjacent to each saddle point.

2.3 Results and Discussion

Nitrosobenzene is a planar molecule as indicated by NMR.⁷ Overlap between the phenyl pi-system and nitrogen's lone-pair electrons endows the planar forms (**I** and **III**) with greater stability than the nonplanar form (**II**). Structure **II** represents a transition state for rotation about the C-N bond as seen in Figure 2.2.

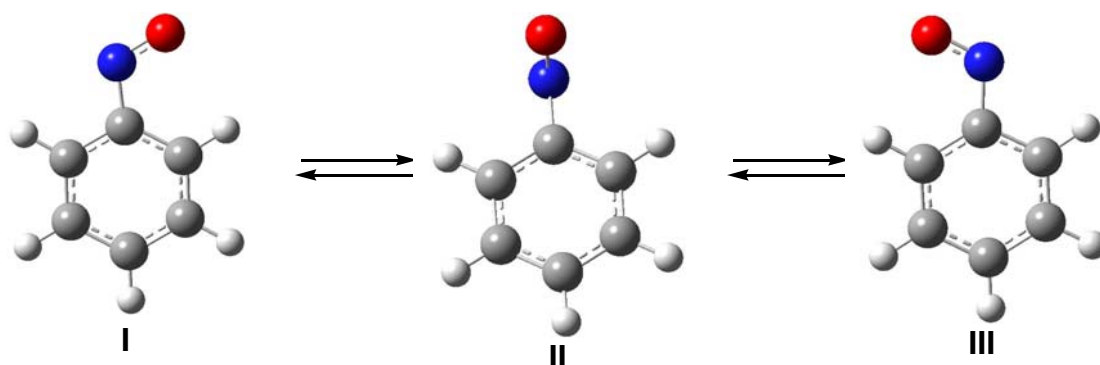


Figure 2.2 Structures of nitrosobenzene optimised by B3LYP/6-31+g(d) in chloroform. **I** and **III** are identical and correspond to the ground states and **II** corresponds to transition state

The difference in energy between these two forms will be denoted as ΔG^\ddagger and represents the barrier to rotation of the -NO group. The rotation barriers around C-N bonds in *p*-substituted nitrosobenzene were investigated by DFT and MP2 calculations using 6-31+g(d) basis set in vacuum and PCM solvents. Geometry

optimizations corresponding to ground, transition and product states by different theory and in different media are presented in supplementary material. The activation barriers are summarized in Table 1. The activation free energy barriers obtained from DFT calculations are in the ranges of 8-19 kcal/mol in water (PCM), 8-17 kcal/mol in chloroform (PCM) and 8-14 kcal/mol in vacuum. The barriers obtained from MP2 calculations are in the ranges of 7-11 kcal/mol in vacuum and 8-10 kcal/mol in chloroform (PCM). It is notable that reasonably good agreement was observed between the MP2 calculations and the few available experimental values with regard to the activation free energies for internal rotation barriers (see Table 2.1) within the limit of errors. It had previously reported that MP2 somehow yields better values for the activation barriers for the internal rotation of C-O bond in substituted phenols.⁶ The activation barriers for closely related guanidinium compounds are in the range of 10-13 kcal/mol.⁴ B3LYP/6-311+g(d,p) level of theory was employed to calculate the activation barrier of *p*-methoxynitrosobenzene and it was unfortunately found that the value (16.46 kcal/mol) was even higher than the one obtained at B3LYP/6-31+g(d) level with reference to the experimental value (9.81 kcal/mol). So it was decided that MP2 is the method of choice for predicting internal rotation barriers of substituted nitrosobenzenes.

Table 2.1 Activation free energies (ΔG^\ddagger)^a in kcal/mol calculated for *p*-substituted nitrosobenzene by DFT and MP2 methods with 6-31+g(d) basis sets. Inputs in the each column in the second row with negative sign represent imaginary frequencies corresponding to the transition state of the respective transformation.

	σ^b	ΔG^\ddagger B3LYP/6-31+g(d)			ΔG^\ddagger MP2/6-31+g(d)			exp ⁱ
		Water ^c	Explicit ^d	GAS ^e	CHCl ₃ ^f	GAS ^g	CHCl ₃ ^h	
NO ₂	0.778	7.99	7.52	8.07	8.02	8.25	5.82	
	(0.740)	-174.14	-180.56	-178.83	-176.94	-167.56	-171.24	
CN	0.660	8.02	j	8.66	8.72	8.59	8.27	
	(0.674)	-185.55		-188.73	-188.01	-171.71	-177.17	
Ac	0.502	9.04	8.50	8.71	8.97	7.67	7.51	
	(0.567)	-188.23	-186.37	-188.36	-189.96	-171.4	-177.05	
Cl	0.227	10.88	10.44	10.11	10.66	8.67	8.20	8.11 (7.51)
	(0.035)	-210.63	-211.12	-206.13	-210.87	-180.86	-189.39	
F	0.062	11.46	11.06	10.58	11.19	8.50	8.36	8.52
	(-0.247)	-217.12	-217.28	-211.82	-216.84	-183.92	-182.5	
H	0	10.76	9.48	9.64	10.44	7.94	8.13	8.21
		-212.9	-205.75	-202.94	-211.48	-180.2	-188.36	
Me	-0.170	12.96	10.31	10.14	9.81	7.99	8.65	8.54 (8.21)
	(-0.256)	-225.14	-215.73	-211.78	-222.72	-183.32	-194.27	
MeO	-0.268	14.23	12.69	12.25	13.63	9.73	10.03	9.81 (10.31)
	(-0.647)	-249.74	-242.96	-233.07	-246.85	-194.01	-205.31	
OH	-0.37	14.61	12.49	12.03	13.70	9.62	10.03	
	(-0.853)	-254.59	-240	-232.06	-248.5	-193.93	-202.29	
NH ₂	-0.66	18.66	14.77	13.77	17.13	9.94	11.19	
	(-1.111)	-291.12	-266.2	-250.84	-291.12	-199.43	-217.23	

^a ΔG^\ddagger correspond to activation barriers which are defined as the difference between energies reported as G_{TS} and G_{GS} which are sum of electronic and thermal free energies of transition and ground states which includes zero-point thermal and

entropic terms at 298 K and 1 atm multiplied by 627.5. Those in solution (with non-electrostatic terms) include the total electronic energy polarised by the dielectric continuum together with the cavitation dispersion and repulsive terms within PCM.

^b σ_p values are taken from McDaniel DH, Brown HC (1958) An extended table of Hammett substituent constants based on the ionization of substituted benzoic acids. *J. Org. Chem.* 23, 420-427. The values within brackets correspond to σ_p^+ values and they are taken from Swain CG, Lupton Jr EC (1968) Field and resonance components of substituent effects. *J. Am. Chem. Soc.* 90, 4328.

^cPCM in water

^dInvolving an explicit water in vacuum

^eIn vacuum

^fPCM in chloroform

^gIn vacuum

^hPCM in chloroform

ⁱExperimental values taken from reference 7b. Those within bracket are from Cox RH, Hamada M (1979) A ¹³C NMR investigation of restricted rotation and dimerization in *p*-substituted nitrosobenzenes. *Org. Magn. Reson.* 12, 322-325.

^jThe transition state could not be located.

2.3.1 Linear Free Energy Relationship: It is expected that electron-donating groups would increase the barrier of internal rotation of the C-N bond in nitrosobenzenes and this would be seen by the correlation of the activation barriers with polar substituted Hammett constants. It was indeed found that calculated activation barriers by DFT and MP2 methods for the internal rotation of the C-N

bond in *p*-substituted nitrosobenzene were well-correlated with polar Hammett sigma values. The correlation of Hammett sigma constants with the barrier to rotation about the C-N bond ΔG^\ddagger produces the following regression (Eqs. 1-2). It is quite obvious that all data fit comparably well with σ^+ rather than with σ , meaning that there is a strong resonance effect on the activation barriers.

B3LYP/6-31+g(d) in water

$$\Delta G^\ddagger \text{ (kcal/mol)} = (-6.89 \pm 0.68) \times \sigma + 12.39 \pm 0.31 \quad r^2 = 0.93 \quad (1)$$

$$\Delta G^\ddagger \text{ (kcal/mol)} = (-5.04 \pm 0.46) \times \sigma^+ + 11.31 \pm 0.29 \quad r^2 = 0.94 \quad (2)$$

B3LYP/6-31+g(d) in vacuum with explicit water

$$\Delta G^\ddagger \text{ (kcal/mol)} = (-4.70 \pm 0.71) \times \sigma + 10.86 \pm 0.29 \quad r^2 = 0.86 \quad (3)$$

$$\Delta G^\ddagger_{\text{rot}} \text{ (kcal/mol)} = (-3.55 \pm 0.33) \times \sigma^+ + 10.11 \pm 0.20 \quad r^2 = 0.94 \quad (4)$$

B3LYP/6-31+g(d) in vacuum

$$\Delta G^\ddagger \text{ (kcal/mol)} = (-3.98 \pm 0.45) \times \sigma + 10.96 \pm 0.20 \quad r^2 = 0.91 \quad (5)$$

$$\Delta G^\ddagger \text{ (kcal/mol)} = (-2.74 \pm 0.23) \times \sigma^+ + 10.09 \pm 0.14 \quad r^2 = 0.95 \quad (6)$$

B3LYP/6-31+g(d) in chloroform

$$\Delta G^\ddagger \text{ (kcal/mol)} = (-5.41 \pm 0.94) \times \sigma + 11.64 \pm 0.42 \quad r^2 = 0.81 \quad (7)$$

$$\Delta G^\ddagger \text{ (kcal/mol)} = (-4.10 \pm 0.55) \times \sigma^+ + 10.78 \pm 0.34 \quad r^2 = 0.87 \quad (8)$$

MP2/6-31+g(d) in vacuum

$$\Delta G^\ddagger \text{ (kcal/mol)} = (-1.15 \pm 0.45) \times \sigma + 8.78 \pm 0.20 \quad r^2 = 0.45 \quad (9)$$

$$\Delta G^\ddagger \text{ (kcal/mol)} = (-0.97 \pm 0.28) \times \sigma^+ + 8.58 \pm 0.17 \quad r^2 = 0.60 \quad (10)$$

MP2/6-31+g(d) in chloroform

$$\Delta G^\ddagger \text{ (kcal/mol)} = (-3.44 \pm 0.35) \times \sigma + 8.70 \pm 0.15 \quad r^2 = 0.93 \quad (11)$$

$$\Delta G^\ddagger \text{ (kcal/mol)} = (-2.50 \pm 0.24) \times \sigma^+ + 8.17 \pm 0.15 \quad r^2 = 0.94 \quad (12)$$

MP2/6-31+g(d) in chloroform

(only electron donating groups, H, F, Cl, Me, MeO, OH and NH₂)

$$\Delta G^\ddagger \text{ (kcal/mol)} = (-2.65 \pm 0.26) \times \sigma^+ + 8.06 \pm 0.15 \quad r^2 = 0.96 \quad (13)$$

MP2/6-31+g(d) in chloroform-experimental^{7b}

$$\Delta G^\ddagger \text{ (kcal/mol)} = (-2.67 \pm 0.07) \times \sigma^+ + 8.08 \pm 0.06 \quad r^2 = 0.99 \quad (14)$$

The magnitude of the slope in equations of the free energy relationships is basically an indication of the competition of interaction of charge in transition state

between polar substituents and environment, namely solvents when rates or equilibria are measured.³ The larger the slope less interaction of the transition state with environment and hence, more pronounced effect of substituents. The sign of the slope gives generally evidence about the type of the charge developed in transition state. The slope means positive charge development in going from ground state to transition state. The negative slopes calculated by DFT in different environments are -5.04, -4.10, -3.55 and -2.74 in water, chloroform, with explicit water in vacuum and in vacuum. Similar results are computed by MP2. They are -1.15 and -2.50 in vacuum and in chloroform as seen. It is always a question in mind if the theoretical methods chosen would provide comparable results with those of experimental ones. A striking outcome produced from MP2 calculations is that they give a very similar free energy relationship with experimental results. The slope derived for only electron donating groups including parent nitrosobenzene (Eq. 13) has a quite close parameters derived from experimental data (Eq. 14) where *para* substituents are H, Cl, Br, I, Me, MeO, NMe₂ and NEt₂ [7b]. This means that as stated earlier MP2 is the method to employ to predict the activation barrier of internal bond rotation at least for C-N bond in substituted nitrosobenzenes.

The results, the magnitudes of the slopes, normally contradict with simple electrostatic interaction of solvent molecules with transition state structures involving charge developing where polar solvent like water reduces the effect of polar substituents. Therefore the magnitude of the slope in polar solvents will be smaller than that in less polar ones. So it can be deduced that the slopes can not be accounted for charge changes in the effect of polar substituent on the internal rotation of the C-N bonds in substituted nitrosobenzenes. This was supported by the finding that

calculated Mulliken charges on oxygen do not significantly change with polar Hammett constants (See Figure 2.3). So what could be accounted for the strong dependency of activation barriers on Hammett sigma constants, namely the slopes of free energy relationships? This question will be answered in details late in the text.

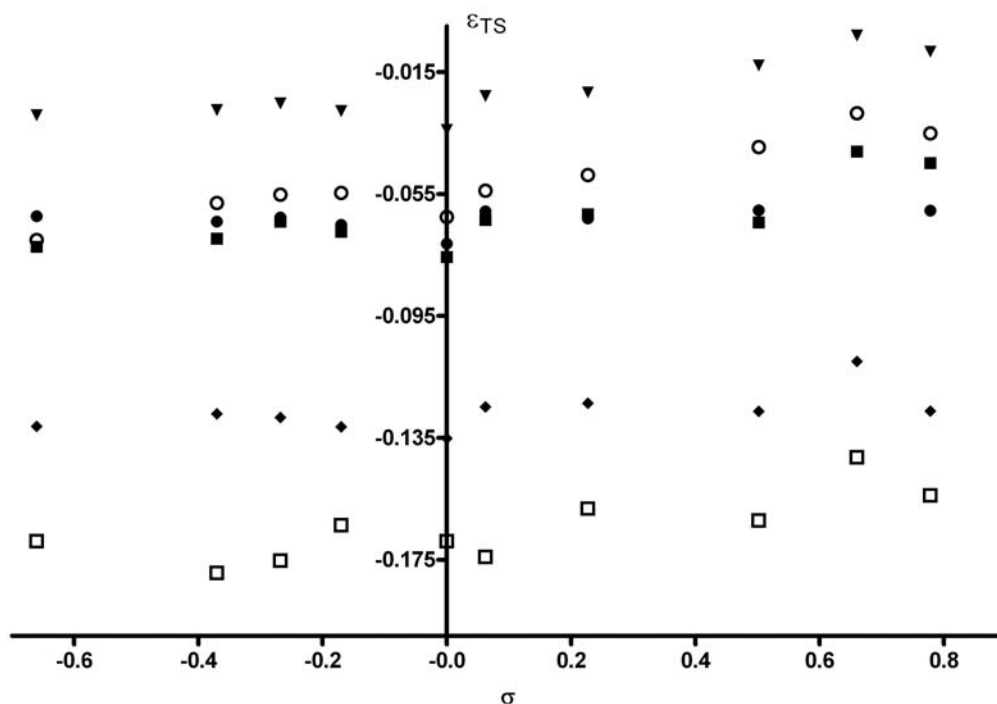


Figure 2.3 Dependence of Mulliken charges on oxygen atoms in the transition states of *p*-substituted nitrosobenzenes on polar Hammett constants calculated by DFT and MP2 methods at 6-31+g(d) level in different environment. Semi-solid diamonds represent DFT calculations in vacuum diamonds represent MP2 calculations in vacuum solid circles represent DFT calculations with explicit water in vacuum solid squares represent DFT calculations in PCM (water) open circles represent DFT calculations in PCM (chloroform) open squares represent DFT calculations in PCM (chloroform)

The other most important result gained from the slope derived from the linear free energy relationships, which indicates the bond changes going from ground state to transition state. The calculated C-N bond length changes going from ground states to transition states showed a strong correlation with the substituent Hammett constants as indicated by the regression statistics (Eqs. 15-26). The data are presented in Table 2. They show that bond changes are rather correlated with Hammett σ^+ , meaning a strong resonance effect as seen in the dependency of activation free energies on Hammett constants. A similar trend in the magnitude of the slopes of dependency of bond changes on Hammett constants with the activation barriers were found, meaning that the more electron donating group the shorter the C-N bond length. This is consistent with the results obtained for the activation free energies. So it can be concluded that the strong dependence of activation barriers for internal rotation of the C-N bond on polar substituents is mainly due to the double bond character of the C-N bond in the ground state of the structure with more electron donating groups. For example, the calculated C-N bond length by MP2 in chloroform for *p*-nitronitrosobenzene in the ground state is 1.4399 Å whereas this bond is 1.4111 Å for *p*-aminonitrosobenzene. So there is a 0.0288 Å of difference between two bonds, which corresponds to 5.37 kcal/mol of difference in the activation free energies of two compounds.

Table 2.2 C-N bond lengths in ground (first row) and transition (second row) states calculated for *p*-substituted nitrosobenzene by DFT and MP2 methods with 6-31+g(d) basis sets.

X	B3LYP/6-31+g(d)			MP2/6-31+g(d)		
	Water ^a	Explicit ^b	GAS ^c	CHCl ₃ ^d	GAS ^e	CHCl ₃ ^f
NO ₂	1.4366	1.4395	1.4486	1.4407	1.4461	1.4399
	1.4634	1.4645	1.4678	1.4644	1.4612	1.4592
CN	1.4322	1.4353	1.4450	1.4366	1.4458	1.4391
	1.4642		1.4686	1.4653	1.4610	1.4587
AC	1.4290	1.4323	1.4429	1.4332	1.4433	1.4364
	1.4622	1.4626	1.4661	1.4632	1.4592	1.4570
Cl	1.4192	1.4254	1.4363	1.4244	1.4401	1.4319
	1.4649	1.4655	1.4696	1.4661	1.4601	1.4576
F	1.4167	1.4234	1.4345	1.4223	1.4398	1.4318
	1.4659	1.4665	1.4709	1.4672	1.4608	1.4579
H	1.4195	1.4274	1.4383	1.4254	1.4422	1.4334
	1.4634	1.4643	1.4684	1.4647	1.4595	1.4568
Me	1.4129	1.4216	1.4331	1.4191	1.4382	1.4288
	1.4627	1.4633	1.4675	1.4675	1.4585	1.4557
MeO	1.4013	1.4124	1.4242	1.4084	1.4309	1.4204
	1.4639	1.4645	1.4692	1.4692	1.4589	1.4560
OH	1.4001	1.4137	1.4256	1.4084	1.4330	1.4210
	1.4640	1.4654	1.4670	1.4654	1.4595	1.4562
NH ₂	1.3815	1.4037	1.4174	1.3929	1.4277	1.4111
	1.4626	1.4641	1.4691	1.4641	1.4584	1.4551

^aPCM in water

^bInvolving an explicit water in vacuum

^cIn vacuum

^dPCM in chloroform

^eIn vacuum

^fPCM in chloroform

B3LYP/6-31+g(d) in water

$$\Delta C-N (\text{\AA}) = (-0.0355 \pm 0.0030) \times \sigma + 0.0524 \pm 0.0014 \quad r^2 = 0.95 \quad (15)$$

$$\Delta C-N (\text{\AA}) = (-0.0256 \pm 0.0018) \times \sigma^+ + 0.0463 \pm 0.0012 \quad r^2 = 0.97 \quad (16)$$

B3LYP/6-31+g(d) in vacuum with explicit water

$$\Delta C-N (\text{\AA}) = (-0.0239 \pm 0.0028) \times \sigma + 0.0426 \pm 0.0012 \quad r^2 = 0.91 \quad (17)$$

$$\Delta C-N (\text{\AA}) = (-0.0179 \pm 0.0011) \times \sigma^+ + 0.0389 \pm 0.0007 \quad r^2 = 0.98 \quad (18)$$

B3LYP/6-31+g(d) in vacuum

$$\Delta C-N (\text{\AA}) = (-0.0209 \pm 0.0024) \times \sigma + 0.0354 \pm 0.0011 \quad r^2 = 0.90 \quad (19)$$

$$\Delta C-N (\text{\AA}) = (-0.0157 \pm 0.0012) \times \sigma^+ + 0.0321 \pm 0.0008 \quad r^2 = 0.95 \quad (20)$$

B3LYP/6-31+g(d) in chloroform

$$\Delta C-N (\text{\AA}) = (-0.0315 \pm 0.0029) \times \sigma + 0.0470 \pm 0.0013 \quad r^2 = 0.94 \quad (21)$$

$$\Delta C-N (\text{\AA}) = (-0.0232 \pm 0.0016) \times \sigma^+ + 0.0420 \pm 0.0010 \quad r^2 = 0.97 \quad (22)$$

MP2/6-31+g(d) in vacuum

$$\Delta C-N (\text{\AA}) = (-0.0109 \pm 0.0018) \times \sigma + 0.0218 \pm 0.0008 \quad r^2 = 0.82 \quad (23)$$

$$\Delta C-N (\text{\AA}) = (-0.0084 \pm 0.0009) \times \sigma^+ + 0.0201 \pm 0.0006 \quad r^2 = 0.92 \quad (24)$$

MP2/6-31+g(d) in chloroform

$$\Delta C-N (\text{\AA}) = (-0.0160 \pm 0.0024) \times \sigma + 0.0289 \pm 0.0011 \quad r^2 = 0.86 \quad (25)$$

$$\Delta C-N (\text{\AA}) = (-0.0121 \pm 0.0014) \times \sigma^+ + 0.0263 \pm 0.0008 \quad r^2 = 0.91 \quad (26)$$

It would not be surprised to see the dependence of force constant and imaginary frequency corresponding to the transition vector (or reaction coordinate mode) on polar Hammett constants since it would be expected that the force constant and thus the imaginary frequency is basically a measure of the strength of the C-N bond in the transition state. It was in fact found that the imaginary frequencies are well-correlated with Hammett constants as indicated in Eqs. 27-38. The data are reported in Table 2.1.

B3LYP/6-31+g(d) in water

$$\nu_i (\text{cm}^{-1}) = (57.22 \pm 4.56) \sigma + -225.7 \pm 3.3 \quad r^2 = 0.93 \quad (27)$$

$$\nu_i (\text{cm}^{-1}) = (77.62 \pm 7.747) \sigma^+ + -213.5 \pm 2.8 \quad r^2 = 0.96 \quad (28)$$

B3LYP/6-31+g(d) in vacuum with explicit water

$$\nu_1 (\text{cm}^{-1}) = (58.63 \pm 7.27) \sigma + -219.1 \pm 3.1 \quad r^2 = 0.90 \quad (29)$$

$$\nu_1 (\text{cm}^{-1}) = (44.08 \pm 3.32) \sigma^+ + -209.7 \pm 2.0 \quad r^2 = 0.96 \quad (30)$$

B3LYP/6-31+g(d) in vacuum

$$\nu_1 (\text{cm}^{-1}) = (49.07 \pm 5.26) \sigma + -213.4 \pm 2.2 \quad r^2 = 0.93 \quad (31)$$

$$\nu_1 (\text{cm}^{-1}) = (36.73 \pm 2.12) \sigma^+ + -205.6 \pm 1.3 \quad r^2 = 0.98 \quad (32)$$

B3LYP/6-31+g(d) in chloroform

$$\nu_1 (\text{cm}^{-1}) = (22.87 \pm 2.36) \sigma^+ + -184.1 \pm 1.0 \quad r^2 = 0.93 \quad (33)$$

$$\nu_1 (\text{cm}^{-1}) = (17.15 \pm 0.75) \sigma^+ + -180.4 \pm 0.5 \quad r^2 = 0.99 \quad (34)$$

MP2/6-31+g(d) in vacuum

$$\nu_1 (\text{cm}^{-1}) = (68.39 \pm 6.67) \sigma + -212.5 \pm 2.2 \quad r^2 = 0.94 \quad (35)$$

$$\nu_1 (\text{cm}^{-1}) = (50.55 \pm 3.62) \sigma^+ + -212.5 \pm 2.2 \quad r^2 = 0.97 \quad (36)$$

MP2/6-31+g(d) in chloroform

$$\nu_1 (\text{cm}^{-1}) = (31.07 \pm 3.79) \sigma + -192.3 \pm 1.6 \quad r^2 = 0.91 \quad (37)$$

$$\nu_1 (\text{cm}^{-1}) = (22.50 \pm 2.91) \sigma^+ + -187.5 \pm 1.8 \quad r^2 = 0.90 \quad (38)$$

2.3.2 Solvation: An explicit water molecule was deliberately introduced to form hydrogen bond with nitroso group in order to see the effect of solvation explicitly on the barrier. The structures of the ground, transition and product states including the explicit water are illustrated in Figure 4 for the internal rotation of C-N bond in nitrosobenzene. The results are shown in Table 1. It implies that the explicit water molecule increases the activation barrier of electron donating groups compared to that in vacuum. This is an accepted outcome since it would be expected that the solvent molecules will attract electrons from the ring and consequently the nitroso group will relatively draw more electrons from the ring, thus increasing the barrier. In another word, the results hint that the electron withdrawing capacity of nitroso group is enhanced with the explicit water. To rule out the possibility of the steric factor implemented by the solvent on the activation barrier, an explicit methanol molecule was also introduced in a similar manner but just for *p*-

methoxynitrosobenzene by B3LYP. It was found that the explicit methanol produces similar results to that of water. This may be attributed to the fact that water molecule by forming hydrogen bond with nitroso group causes more transmission of electrons from the ring. The C-N bond lengths produce a supporting evidence for this explanation. Data in Table 2 show that C-N lengths with an explicit water are quite close those in water (PCM) and much shorter than those in vacuum, implying the existence of an electronic effect.

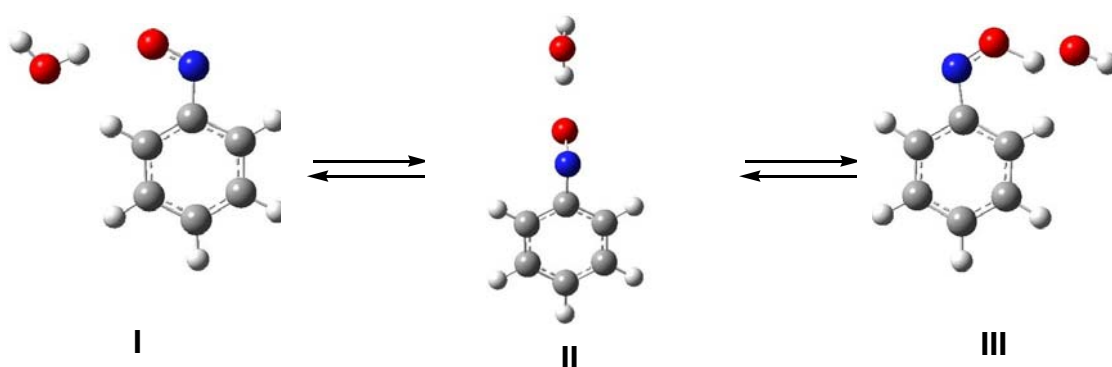


Figure 2.4 Structures of nitrosobenzene involving and explicit water molecule optimised by B3LYP/6-31+g(d) in chloroform. **I** and **III** are identical and correspond to the ground states and **II** corresponds to transition state

2.3.3 Steric Factors: Calculations were carried out by MP2 method in vacuum to see the steric effect on the activation barrier by introducing methyl, ethyl and methoxy groups at position 2. The structures are shown in Figure 5. The results are presented in supplementary material. Activation free energy barriers in kcal/mol are represented in Figure 6. Reverse reactions for three systems are all have lower activation energy barriers compared to forward reactions, which may be ascribed to steric effect. On the other hand, the barriers for forward reactions of 2-methyl and 2-

ethylnitrosobenzenes are similar and but higher than that of 2-methoxynitrosobenzene. This means that introducing methoxy group at *ortho* position causes inductive effect by withdrawing electron from the ring instead of donating as in the case of *p*-substituted, thus leading a longer C-N bond (1.4609 Å), and hence a lower activation barrier. The C-N bond length and activation barrier for *p*-methoxynitrosobenzene is 1.4589 Å (See Table 2) and 9.75 kcal/mol so there is a difference of 2.03 kcal/mol between *ortho* and *para* substituted metoxy.

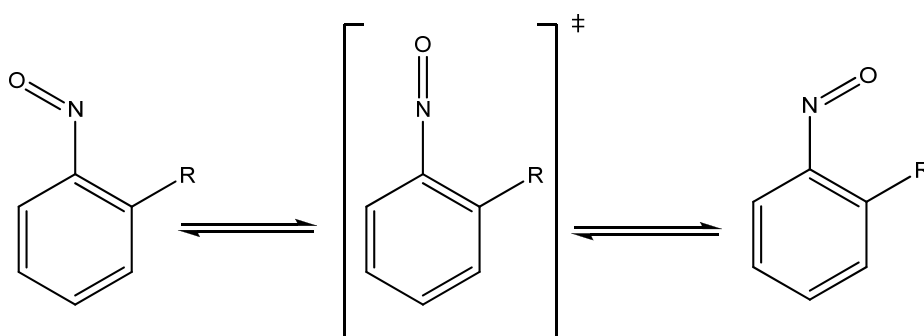


Figure 2.5 R=methyl (1); R=ethyl (2); R=methoxy (3)

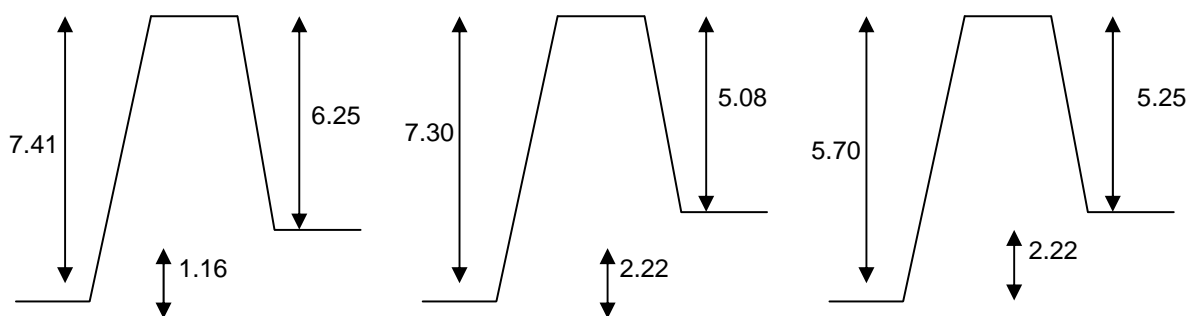


Figure 2.6 The values correspond to activation barriers (ΔG^\ddagger) in kcal/mol. Profile on the right corresponds to the 2-methylnitrosobenzene; the one in the middle corresponds to 2-ethylnitrosobenzene and the one on the left corresponds to 2-methoxynitrosobenzene. For each profile the values on the right correspond to the forward reaction and those on the left correspond to the reverse reaction.

2.3.4 Models: To see the individual contribution of resonance and inductive effects, several models were built and their rotation barriers were computed. The compounds chosen for this purposes are listed in Figure 7. The data, recorded in supplementary material, are presented in Figure 8. They show that nitrosocyclohexane and nitrosoethane have a very similar and small activation barrier compared to nitrosoethene whose activation barrier is close to those of aromatic ones, even larger than that of nitrosobenzene. This suggests that simple conjugation increases the barrier almost eight times, correspond ton on-conjugated systems, basically due to the resonance effect.

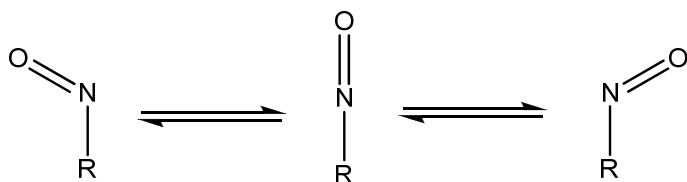


Figure 2.7 R=cyclohexyl (4); R=ethyl (5); R=vinyl (6)

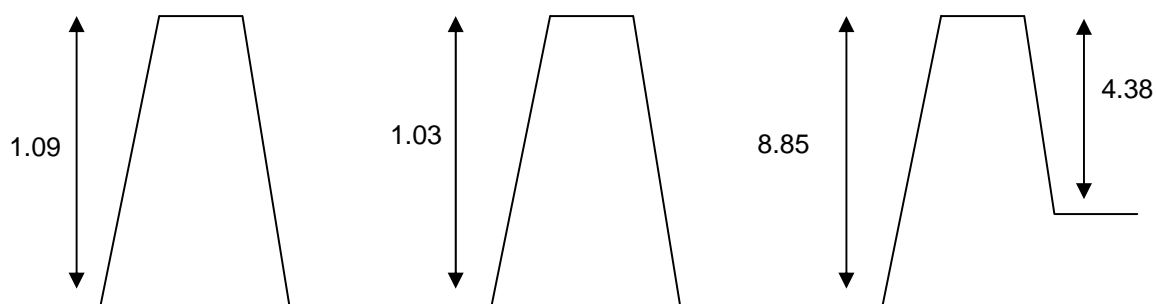


Figure 2. 8 The values correspond to activation barriers (ΔG^\ddagger) in kcal/mol. Profile on the right corresponds to nitrosocyclohexane; the one in the middle corresponds to nitrosoethane and the one on the left corresponds to nitrosoethen

2.4 Conclusion

DFT and MP2 methods at 6-31+g(d) level of theory were used to predict the activation barriers for internal rotation of the C-N bond in *p*-substituted nitrosobenzenes. It was found that electron donating groups increase the barriers which are well correlated with Hammett sigma σ^+ rather than σ , and indication of strong resonance effect. The effect of solvation (PCM solvents) on the activation barrier including introducing an explicit water molecule was also studied. The result showed that the more polar the solvent the larger the barrier. This was ascribed to the interaction of solvent molecule with nitroso group, hence the electron donating groups will increase the barrier and consequently the slope will be larger in pure polar solvents. The results indicate that MP2 is the choice of the method to predict the activation barriers for the internal rotation of C-N bond with comparable results with few available experimental values.

Tables 2.5

Table 2.5.1. Calculations for the rotation of C-N bond in *p*-substituted nitrosobenzene computed by DFT and MP2 with basis set of 6-31 + (d).^{a,b}

X	E_{GS}	E_{TS}	$E_{GS,zp}$	$E_{TS,zp}$	G_{GS}	G_{TS}	ΔE^\ddagger	ΔE^\ddagger	ΔG^\ddagger	\square^c
NO₂	-566.061175	-566.048367	-565.961706	-565.949593	-565.996723	-565.983859	8.04	7.60	8.07	-178.83
	-566.076770	-566.064129	-565.978343	-565.966388	-566.013546	-566.000812	7.93	7.50	7.99	-174.14
	-642.491234	-642.475677	-642.368113	-642.353731	-642.408704	-642.396723	9.76	9.02	7.52	-180.56
	-564.482281	-564.471226	-564.383865	-564.373189	-564.383865	-564.373189	6.94	6.70	6.70	-167.56
	-566.071922	-566.059207	-565.973104	-565.961062	-566.008189	-565.995416	7.98	7.56	8.02	-176.94
	-564.491972	-564.481322	-564.394096	-564.383692	-564.428025	-564.418748	6.68	6.53	5.82	-171.24
CN	-453.798032	-453.784032	-453.702403	-453.689168	-453.735659	-453.721859	8.79	8.30	8.66	-188.73
	-453.814093	-453.800054	-453.719316	-453.705970	-453.752477	-453.738530	8.81	8.37	8.75	-185.55
	-530.228317		-530.108961		-530.147760					-191.92
	-452.476539	-452.465243	-452.383643	-452.371920	-452.418619	-452.404928	7.09	7.36	8.59	-171.71
	-453.809296	-453.795269	-453.714193	-453.700884	-453.747380	-453.733476	8.80	8.35	8.72	-188.01
	-452.486969	-452.476051	-452.394618	-452.383321	-452.429374	-452.416202	6.85	7.09	8.27	-177.17
AC	-514.206221	-514.192320	-514.071730	-514.058560	-514.107599	-514.093721	8.72	8.26	8.71	-188.36
	-514.220677	-514.206392	-514.087097	-514.073485	-514.123073	-514.10866	8.96	8.54	9.04	-188.23
	-590.636178	-590.620071	-590.477793	-590.463132	-590.519163	-590.505612	10.11	9.20	8.50	-186.37
	-512.672129	-512.660952	-512.539368	-512.527647	-512.576418	-512.564191	7.01	7.35	7.67	-171.4

	-514.216074	-514.201861	-514.082142	-514.068618	-514.118057	-514.103765	8.92	8.49	8.97	-189.96
	-512.681073	-512.670067	-512.547909	-512.537078	-512.584362	-512.572391	6.91	6.80	7.51	-177.05
CI	-821.151091	-821.134626	-821.063464	-821.047844	-821.096130	-821.080014	10.33	9.80	10.11	-206.13
	-821.162090	-821.144495	-821.075416	-821.058590	-821.108087	-821.090752	11.04	10.56	10.88	-210.63
	-897.581801	-897.562202	-897.470311	-897.452168	-897.508483	-897.491846	12.30	11.38	10.44	-211.12
	-819.494347	-819.481744	-819.408818	-819.395663	-819.441819	-819.427997	7.91	8.25	8.67	-180.86
	-821.158705	-821.141418	-821.071674	-821.055190	-821.104341	-821.087355	10.85	10.34	10.66	-210.87
	-819.501131	-819.488584	-819.415336	-819.403166	-819.448502	-819.435442	7.87	7.64	8.20	-189.39
F	-460.798092	-460.780822	-460.709042	-460.692661	-460.740765	-460.723906	10.84	10.28	10.58	-211.82
	-460.809804	-460.791204	-460.721784	-460.703998	-460.753494	-460.735225	11.67	11.16	11.46	-217.12
	-537.228958	-537.208561	-537.116064	-537.097138	-537.153454	-537.135832	12.80	11.88	11.06	-217.28
	-459.489287	-459.476274	-459.401505	-459.388814	-459.433737	-459.420190	8.17	7.96	8.50	-183.92
	-460.806244	-460.788028	-460.717837	-460.700486	-460.749556	-460.731716	11.43	10.89	11.19	-216.84
	-459.496651	-459.483708	-459.409588	-459.397080	-459.441800	-459.428480	8.12	7.85	8.36	-182.5
H	-361.556042	-361.540306	-361.458727	-361.443875	-361.489181	-361.473813	9.87	9.32	9.64	-202.94
	-361.567445	-361.549995	-361.471120	-361.454483	-361.501571	-361.484422	10.95	10.44	10.76	-212.9
	-437.986568	-437.968191	-437.865377	-437.848517	-437.901451	-437.886346	11.53	10.58	9.48	-205.75
	-360.461251	-360.449300	-360.365258	-360.353525	-360.396236	-360.383583	7.50	7.36	7.94	-180.2
	-361.563931	-361.546955	-361.467238	-361.451111	-361.497687	-361.481048	10.65	10.12	10.44	-211.48
	-360.468265	-360.456115	-360.373034	-360.361108	-360.404132	-360.391170	7.62	7.48	8.13	-188.36

Me	-400.875974	-400.858890	-400.751218	-400.735064	-400.784755	-400.768599	10.72	10.14	10.14	-211.78
	-400.887179	-400.867847	-400.763320	-400.744880	-400.796893	-400.776239	12.13	11.57	12.96	-225.14
	-477.306922	-477.287132	-477.158206	-477.140014	-477.197217	-477.180789	12.42	11.42	10.31	-215.73
	-399.634208	-399.621559	-399.510523	-399.497712	-399.543092	-399.530355	7.94	8.04	7.99	-183.32
	-400.883511	-400.864989	-400.759377	-400.741692	-400.791212	-400.775586	11.62	11.10	9.81	-222.72
	-399.640881	-399.627752	-399.517330	-399.504483	-399.550922	-399.537130	8.24	8.06	8.65	-194.27
MeO	-476.086749	-476.066476	-475.956584	-475.937387	-475.990410	-475.970895	12.72	12.05	12.25	-233.07
	-476.100814	-476.077438	-475.971542	-475.949182	-476.005357	-475.982685	14.67	14.03	14.23	-249.74
	-552.518254	-552.494796	-552.364036	-552.342384	-552.403321	-552.383095	14.72	13.59	12.69	-242.96
	-474.658866	-474.643925	-474.529646	-474.514983	-474.564322	-474.548823	9.38	9.20	9.73	-194.01
	-476.096379	-476.073918	-475.966753	-475.945347	-476.000564	-475.978850	14.09	13.43	13.63	-246.85
	-474.667205	-474.651646	-474.538584	-474.523376	-474.573143	-474.557164	9.76	9.54	10.03	-205.31
OH	-436.780839	-436.760899	-436.679389	-436.660582	-436.711185	-436.692015	12.51	11.80	12.03	-232.06
	-436.805199	-436.781313	-436.705646	-436.682742	-436.737424	-436.714148	14.99	14.37	14.61	-254.59
	-513.212544	-513.189088	-513.087056	-513.065508	-513.124370	-513.104464	14.72	13.52	12.49	-240
	-435.502977	-435.488365	-435.403398	-435.389026	-435.436049	-435.420717	9.17	9.02	9.62	-193.93
	-436.797047	-436.774519	-436.696720	-436.675258	-436.728514	-436.706679	14.14	13.47	13.70	-248.5
	-435.518080	-435.502584	-435.419813	-435.404690	-435.452417	-435.436440	9.72	9.49	10.03	-202.29
NH₂	-416.919991	-416.897558	-416.806161	-416.784604	-416.838164	-416.816217	14.08	13.53	13.77	-250.84
	-416.945544	-416.915343	-416.833236	-416.803879	-416.865227	-416.835488	18.95	18.42	18.66	-291.12

-493.352408	-493.325902	-493.214563	-493.189663	-493.252178	-493.228646	16.63	15.62	14.77	-266.2
-415.663669	-415.647920	-415.550337	-415.535109	-415.582695	-415.566852	9.88	9.56	9.94	-199.43
-416.936982		-416.824300		-416.856551					-291.12
-415.677947	-415.660322	-415.565865	-415.548644	-415.598160	-415.580325	11.06	10.81	11.19	-217.23

a) Energies reported as E_{GS} and E_{TS} are total free energies of ground and transition states which exclude zero-point term. Energies reported as E_{GS-zp} and E_{TS-zp} are sum of electronic and zero-point energies of ground and transition states. Energies reported as G_{GS} and G_{TS} are sum of electronic and thermal free energies of ground and transition states which includes zero-point, thermal and entropic terms at 298 K and 1 atm. Those in solution (with non-electrostatic terms) include the total electronic energy polarised by the dielectric continuum together with the cavitation, dispersion and repulsive terms within PCM. The activation barriers of rotation about the C-N bond ($\Delta E_{rot}^{\ddagger}$, $\Delta E_{rot-zp}^{\ddagger}$ and $\Delta G_{rot}^{\ddagger}$) are defined as the difference between the energy of the transition state and that of the equilibrium geometry multiplied by 627.5.

b) The first row: B3LYP/6-31+g(d)-vacuum; the second row: B3LYP/6-31+g(d)-PCM (water); the third row: B3LYP/6-31+g(d) with an explicit HOH in vacuum; the fourth row: MP2/6-31+g(d); the fifth row: B3LYP/6-31+g(d)-PCM (chloroform); the sixth row: MP2/6-31+g(d)-PCM (chloroform)

c) Imaginary frequencies corresponding to the transition vector.

Table 2.5.2 Activation free energies in kcal mol⁻¹ calculated for *p*-substituted nitrosobenzene by DFT and MP2 methods with 6-31+g(d) basis sets. Data are taken from Table 2.6.1.

	ΔG^\ddagger B3LYP/6-31+g(d)				ΔG^\ddagger MP2/6-31+g(d)			
	$\sigma^{a,b}$	PCM ^c	gas-hoh ^d	gas ^e	PCM ^f	gas ^g	PCM ^h	exp ⁱ
NO ₂	0.79	7.99	7.52	8.07	8.02	8.25	5.82	
CN	0.66	8.02		8.66	8.72	8.59	8.27	
Ac	0.50	9.04	8.50	8.71	8.97	7.67	7.51	
Cl	0.23	10.88	10.44	10.11	10.66	8.67	8.20	8.11
F	0.06	11.46	11.06	10.58	11.19	8.50	8.36	8.52
H	0	10.76	9.48	9.64	10.44	7.94	8.13	8.21
Me	-0.17	12.96	10.31	10.14	9.81	7.99	8.65	8.54
MeO	-0.27	14.23	12.69	12.25	13.63	9.73	10.03	9.81
OH	-0.34 ^b	14.61	12.49	12.03	13.70	9.62	10.03	
NH ₂	-0.66	18.66	14.77	13.77	17.13	9.94	11.19	

a) *The Effect of Structure upon the Reactions of Organic Compounds. Benzene Derivatives* Louis P. Hammett J. Am. Chem. Soc.; **1937**; 59(1); 96-103

b) L.P.Hammett, *Physical Organic Chemistry*, McGraw-Hill Book Co., Inc., New York, NY, 1940, Chaps. III,IV,VII.

c) PCM in water

d) Involving an explicit water in vacuum

e) In vacuum

f) PCM in chloroform

g) In vacuum

h) PCM in chloroform

i) Experimental valuse taken from reference 13.

Table 2.5.3 C-N bond lengths in ground (first row) and transition (second row) states calculated for *p*-substituted nitrosobenzene by DFT and MP2 methods with 6-31+g(d) basis sets. For a-h see Table 2.6.2.

X	$\sigma^{a,b}$	B3LYP/6-31+g(d)			MP2/6-31+g(d)		
		PCM ^c	gas-hoh ^d	gas ^e	PCM ^f	gas ^g	PCM ^h
NO ₂	0.79	1.4366	1.4395	1.4486	1.4407	1.4461	1.4399
		1.4634	1.4645	1.4678	1.4644	1.4612	1.4592
CN	0.66	1.4322	1.4353	1.4450	1.4366	1.4458	1.4391
		1.4642		1.4686	1.4653	1.4610	1.4587
AC	0.50	1.4290	1.4323	1.4429	1.4332	1.4433	1.4364
		1.4622	1.4626	1.4661	1.4632	1.4592	1.4570
Cl	0.23	1.4192	1.4254	1.4363	1.4244	1.4401	1.4319
		1.4649	1.4655	1.4696	1.4661	1.4601	1.4576
F	0.06	1.4167	1.4234	1.4345	1.4223	1.4398	1.4318
		1.4659	1.4665	1.4709	1.4672	1.4608	1.4579
H	0	1.4195	1.4274	1.4383	1.4254	1.4422	1.4334
		1.4634	1.4643	1.4684	1.4647	1.4595	1.4568
Me	-0.17	1.4129	1.4216	1.4331	1.4191	1.4382	1.4288
			1.4633	1.4675	1.4675	1.4585	1.4557
MeO	-0.27	1.4013	1.4124	1.4242	1.4084	1.4309	1.4204
		1.4639	1.4645	1.4692	1.4692	1.4589	1.4560
OH	-0.34	1.4001	1.4137	1.4256	1.4084	1.4330	1.4210
		1.4640	1.4654	1.4670	1.4654	1.4595	1.4562
NH ₂	-0.66	1.3815	1.4037	1.4174	1.3929	1.4277	1.4111
		1.4626	1.4641	1.4691	1.4641	1.4584	1.4551

2.6 References

1. Hammett, L. P. *J. Am. Chem. Soc.* **1937**, 59, 96.
2. Hammett, L. P. *Trans Faraday Soc.* **1938**, 34, 156.
4. Botto, R. E.; Schwartz, J. H.; Roberts, J. D. *Proc. Nati. Acad. Sci. USA*, **1980**, 77, 23.
5. Smith, B. D.; Goodenough-Lashua, D.A. M.; DÕSouza, C. J. E.; Kieran, J.; Norton, L. M.; Tung, S.; James, C., *Tetrahedron Lett.* 45, **2004**, 2747.
6. Gross, K. C.; Seybold, P. G. *Int. J. Quantum Chem.* **2001**, 85, 569.
7. a) Fletcher, A.; Gowenlock, B. G.; Orrell, K. G. *J. Chem. Soc. Perkin Trans. 2*, **1997**, 2201 b) Fletcher D. A.; Gowenlock B. G., Orrell K. G. *J. Chem. Soc.* **1998**, 797.
8. Irle, S.; Krygowski, T. M.; Niu, J. E.; Schwarz W. H. E. *J. Org. Chem.* **1995**, 60(21), 6744.
9. Gaussian 03, Revision C.02, Frisch, M. J.; Trucks, G. W.; Schlegel, H. B.; Scuseria, G. E.; Robb, M. A.; Cheeseman, J. R.; Montgomery, Jr., J. A.; Vreven, T.; Kudin, K. N.; Burant, J. C.; Millam, J. M.; Iyengar, S. S.; Tomasi, J.; Barone, V.; Mennucci, B.; Cossi, M.; Scalmani, G.; Rega, N.; Petersson, G. A.; Nakatsuji, H.; Hada, M.; Ehara, M.; Toyota, K.; Fukuda, R.; Hasegawa, J.; Ishida, M.; Nakajima, T.; Honda, Y.; Kitao, O.; Nakai, H.; Klene, M.; Li, X.; Knox, J. E.; Hratchian, H. P.; Cross, J. B.; Bakken, V.; Adamo, C.; Jaramillo, J.; Gomperts, R.; Stratmann, R. E.; Yazyev, O.; Austin, A. J.; Cammi, R.; Pomelli, C.; Ochterski, J. W.; Ayala, P. Y.; Morokuma, K.; Voth, G. A.; Salvador, P.; Dannenberg, J. J.; Zakrzewski, V. G.; Dapprich, S.; Daniels, A. D.; Strain, M. C.; Farkas, O.; Malick, D. K.; Rabuck, A. D.; Raghavachari, K.; Foresman, J. B.; Ortiz, J. V.; Cui, Q.; Baboul, A. G.; Clifford,

S.; Cioslowski, J.; Stefanov, B. B.; Liu, G.; Liashenko, A.; Piskorz, P.; Komaromi, I.; Martin, R. L.; Fox, D. J.; Keith, T.; Al-Laham, M. A.; Peng, C. Y.; Nanayakkara, A.; Challacombe, M.; Gill, P. M. W.; Johnson, B.; Chen, W.; Wong, M. W.; Gonzalez, C.; and Pople, J. A.; Gaussian, Inc., Wallingford CT, **2004**.

3.1. Introduction

Studying mechanism of organic reactions is an important task in understanding very complicated biochemical transformations as well as in synthetic organic chemistry. Measuring the extent of changes in bonds between atoms or electrical charge on atoms in reacting bonds during a reaction provides significant information about the mechanism of a reaction. Substantial changes in electrical charge on atoms in reacting bonds are observed.^{1a-d} Development of charge is a result of an energy change, so that any interaction with charge will be seen in energy change, reflected in the reactivity of the reaction. Polar substituent effect is one of the most powerful tools in elucidation of mechanism of organic reactions. The application of this method to a wide range of system including enzymatic reactions are reported in details by Williams.^{2a-d} The effect of polar substituent is measured by a number of similar methods, Hammett, Bronsted and Taft.^{3,4a,b}

$$\text{Log } (k_X/k_H) = \rho \sigma_X + C_1 \quad (3.1)$$

$$\text{Log } (k_X/k_H) = \beta \text{p}K_X + C_2 \quad (3.2)$$

$$\text{Log } (k_X/k_{Me}) = \rho^* \sigma_X^* + \delta E_X \quad (3.3)$$

The aim of this study is to investigate the effect of polar substituents and PCM-solvents on the alkaline hydrolysis of substituted methyl benzoates. Despite a very sophisticated experimental details of polar substituted effect on rates if these types is no considerably theoretical study of this effect.⁵⁻⁷ The reason to study these series is that a full experimental details regarding the mechanism has been documented.⁸ The work involves a density functional investigation of polar substituted effect on the alkaline hydrolysis of methyl benzoates.

3.2 Material and Method

All calculations were performed by means of the Gaussian03 program^{9,10} using the B3LYP density functional theory with the 6-31+G(d) basis (with six Cartesian d functions on non-hydrogen atoms), together with polarizable continuum model (PCM) in water, methanol and acetonitril solvents using $\epsilon = 78.4, 56.6$ and 37.5 respectively, and UA0 (Simple United Atom Topological Model) for the molecular cavity. Convergence in the SCF procedure was typically achieved using geometry optimizations using default convergence criteria. TSs were located by performing transition state search on the geometry obtained from the highest energy point from scanning $\text{HO}^{\delta-} \cdots \text{CPh}=\text{O}(\text{OMe})$ bond followed `opt=(ts,calcall)` from `ts=QST2`. All transition structures were characterized as possessing a single imaginary frequency corresponding to the transition vector (or reaction coordinate mode) for a particular chemical transformation, in contrast to energy minima with all-real vibrational frequencies. IRC calculations confirmed the identity of the energy minima adjacent to each saddle point. The activation free energies reported as ΔG^{\ddagger} are defined as the difference between the free energy of the transition state and that of corresponding equilibrium geometry multiplied by 627.5 for each species.

3.3. Results and Discussion

There has been a question for the alkaline hydrolysis of carboxylic acid ester processes via a concerted or step-wise (addition/ elimination) mechanism. Linear free energy relationships, simply Hammett correlations are successful tools to determine and consequently distinguish this mechanism. Alkaline hydrolysis of methyl benzoates produces a slope (ρ) which corresponds to a step-wise mechanism since S_N2 like concerted mechanism would produce a smaller dependence on polar substituents.¹¹

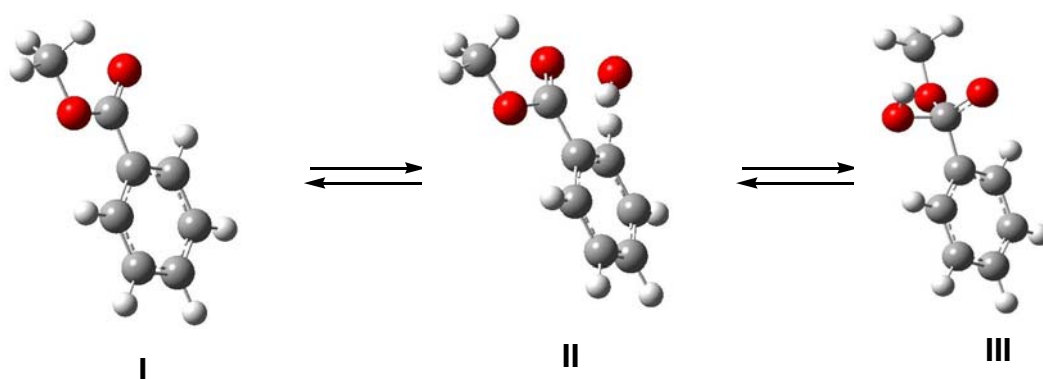


Figure 3.1 Structures of methyl benzoate optimised by B3LYP/6-31+g(d) in water. **I** identical and correspond to the ground states, **II** corresponds to transition state and **III** corresponds to intermediate.

The activation energy (including zero-point energy) and free energy of each reaction is derived from the difference in the energy of ground state of reacting species and transition state multiplied by 627.5 and they are summarized in Table 3.6.1. They indicate that there around 6 kcal mol⁻¹ free energy difference in activation barrier between the most electron-withdrawing cyano group and the most electron-donating amino group. This implies that there is a strong dependence of transition state structure on polar substituents, which is generally reflected in the

linear free energy relationship, mostly derived by various methods as mentioned earlier.

The theoretical calculations indicates that activation energies for the alkaline hydrolysis of substituted methyl benzoates in different PCM solvents show a strong correlation with Hammett sigma constant and pK_a of benzoic acid. The results are illustrated in equation 3.3.1-3.3.9.

As mentioned earlier Hammett correlations produce a positive slope for a mechanism proceeding through a transition state with the negative charge build up and the Bronsted correlation produce the other way around where the rate constant is corrected against Hammett sigma values and pK_a 's.

Methanol

$$\Delta E \text{ (kcal mol}^{-1}\text{)} = (-4.649 \pm 0.195) \sigma + 9.646 \pm 0.078 \quad R^2 = 0.9930 \quad (3.3.1)$$

Acetonitrile

$$\Delta E \text{ (kcal mol}^{-1}\text{)} = (-4.628 \pm 0.144) \sigma + 9.731 \pm 0.055 \quad R^2 = 0.9952 \quad (3.3.2)$$

Water

$$\Delta E \text{ (kcal mol}^{-1}\text{)} = (-4.593 \pm 0.240) \sigma + 9.454 \pm 0.092 \quad R^2 = 0.9866 \quad (3.3.3)$$

Water

$$\Delta G^\ddagger \text{ (kcal mol}^{-1}\text{)} = (-4.79 \pm 0.40) \sigma + 14.11 \pm 0.15 \quad R^2 = 0.9659 \quad (3.3.4)$$

Methanol

$$\Delta G^\ddagger \text{ (kcal mol}^{-1}\text{)} = (-4.90 \pm 0.30) \sigma + 14.47 \pm 0.12 \quad R^2 = 0.9852 \quad (3.3.5)$$

Acetonitril

$$\Delta G^\ddagger \text{ (kcal mol}^{-1}\text{)} = (-4.84 \pm 0.51) \sigma + 14.53 \pm 0.20 \quad R^2 = 0.9466 \quad (3.3.6)$$

Since the activation energies are directly correlated with Hammett constants and pK_a 's, so that is why Hammett correlations produce negative slopes Brønsted produced positives. Because, $\ln K$ is proportional $\Delta G^\ddagger/RT$. The other evidence for the

step-wise mechanism is that the alkaline hydrolysis of substituted benzoates proceeds via a tetrahedral intermediate. The correlation is presented in Figure 3.5.1-3.5.3.

Water

$$\Delta G^\ddagger \text{ (kcal mol}^{-1}\text{)} = (4.70 \pm 0.37) \text{ p}K_a - 5.71 \pm 1.57 \quad R^2 = 0.9703 \quad (3.3.7)$$

Methanol

$$\Delta G^\ddagger \text{ (kcal mol}^{-1}\text{)} = (4.80 \pm 0.29) \text{ p}K_a - 5.79 \pm 1.25 \quad R^2 = 0.9853 \quad (3.3.8)$$

Acetonitril

$$\Delta G^\ddagger \text{ (kcal mol}^{-1}\text{)} = (4.75 \pm 0.47) \text{ p}K_a - 5.49 \pm 2.01 \quad R^2 = 0.9528 \quad (3.3.9)$$

As mentioned in the introduction of the text, there is a substantial bond change between the atoms where bond breaking/forming occurs going from the ground state to the transition state of a reaction. This can be experimentally measured by driving the linear free energy regression from the effect of polar substitution on the rate.¹¹ Therefore, a correlation of bond change with polar Hammett constant or *pKa* values from the ground to the transition state of the reaction is expected. Calculated bond lengths of O=C-OMe in the ground and in transition states are illustrated in Table 3.6.2. The difference as represented by $\Delta\text{C-OMe}$ referees bond change from ground state to transition state is correlated with the *pKa*'s of substituted benzoic acid a slightly better than Hammett sigma constants. The results are shown in Eqs. 3.3.10-3.3.15 and Figures 3.5.4 and 3.5.5.

Water

$$\Delta\text{C-OMe (Å)} = (-0.005458 \pm 0.001454)\sigma + 0.02170 \pm 0.0006022 \quad R^2=0.7790 \quad (3.3.10)$$

Methanol

$$\Delta\text{C-OMe (Å)} = (-0.004611 \pm 0.001948) \sigma + 0.02131 \pm 0.0008822 \quad R^2=0.6514 \quad (3.3.11)$$

Acetonitril

$$\Delta\text{C-OMe (Å)} = (-0.007306 \pm 0.001240) \sigma + 0.02460 \pm 0.0004756 \quad R^2=0.8741 \quad (3.3.12)$$

Water

$$\Delta C\text{-OMe } (\text{\AA}) = (-0.005235 \pm 0.001567) pK_a - 0.04401 \pm 0.006671 \quad R^2=0.7362 \quad (3.3.13)$$

Methanol

$$\Delta C\text{-OMe } (\text{\AA}) = (-0.004701 \pm 0.001831) pK_a - 0.04129 \pm 0.007752 \quad R^2=0.6873 \quad (3.3.14)$$

Acetonitril

$$\Delta C\text{-OMe } (\text{\AA}) = (-0.006935 \pm 0.001504) pK_a - 0.05410 \pm 0.006393 \quad R^2=0.8095 \quad (3.3.15)$$

The effect of solvent on properties of structure quantum chemical calculations values QM/MM is employed based on continuum solvation models. A similar result is observed in the effect of solvent on the reactivity of reaction. It is a well-known phenomenon that transition state–solvent interaction dramatically affects chemical reactivity. Their influence on energies, structures and other properties have been reported¹² and have been documented. To describe this effect theoretically, continuum solvation models are often used. The conductor-like polarizable continuum model¹³ (C-PCM) is a generalization of polarizable continuum model (PCM).²³ This model treats the solvent as a continuum dielectric, which reacts against the solute charge distribution generating reaction field. Thus any change of molecular or electronic structure within solvent induces an external force. However if it is known that depended upon the mechanism solvents compete with polar substitute to interact with charges developed in transition state and this is consequently reflected in the equation of linear free energy relationship. The more polar the solvent the smaller the slope will be in the equation (ρ or β). The correlations in Eqs. 3.3.1-3.3.15 indicate that PCM solvents do not have any influence on the reactivity of alkaline hydrolysis of substituted benzoates. This may be ascribed to the fact that the continuum solvation model ignores solute-solvent

interactions. Thus the effect of explicit solvation will not be observed by computational modeling.

3.4. Conclusion

Activation free energy barriers and bond change for the alkaline hydrolysis of methyl *p*-substituted benzoates obtained by DFT calculations at B3LYP/6.31+g(d) level in water, methanol and acetonitril solvents (PCM) showed a relatively good correlation with Hammett sigma constants and *pKa*'s of corresponding benzoic acid. It was found that PCM solvents did not influence the linear free energy regressions as expected in those derived from experimental calculations.

3.5 Figures

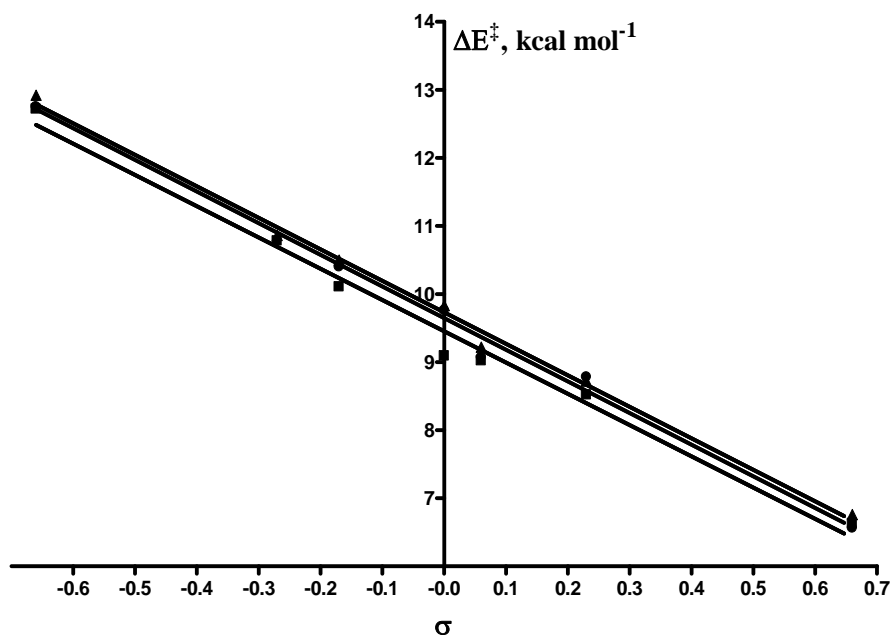


Figure 3.5.1 Dependence of ΔE^\ddagger (kcal mol⁻¹) on Hammett sigma constants σ for alkaline hydrolysis of methyl *p*-substituted benzoate calculated by B3LYP/6-31+g(d) in PCM solvents (■ water, $R^2=0.9866$, ● methanol, $R^2=0.9930$ and ▲ acetonitril, $R^2=0.9952$).

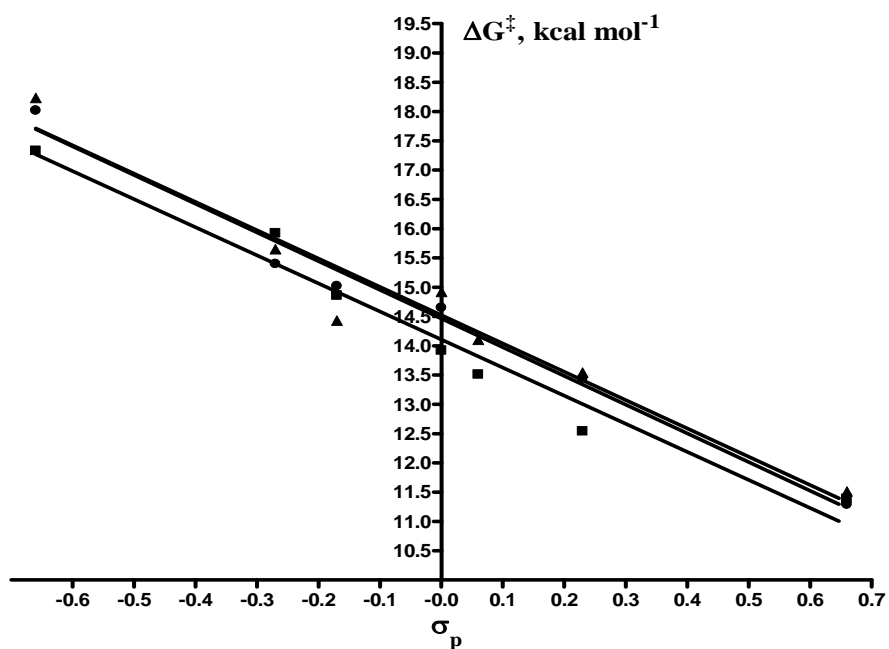


Figure 3.5.2 Dependence of ΔG^\ddagger (kcal mol⁻¹) on Hammett sigma constants for alkaline hydrolysis of methyl *p*-substituted benzoate calculated by B3LYP/6-31+g(d) in PCM solvents (■ water, $R^2=0.9659$, ● methanol, $R^2=0.9852$ and ▲ acetonitril, $R^2=0.9466$).

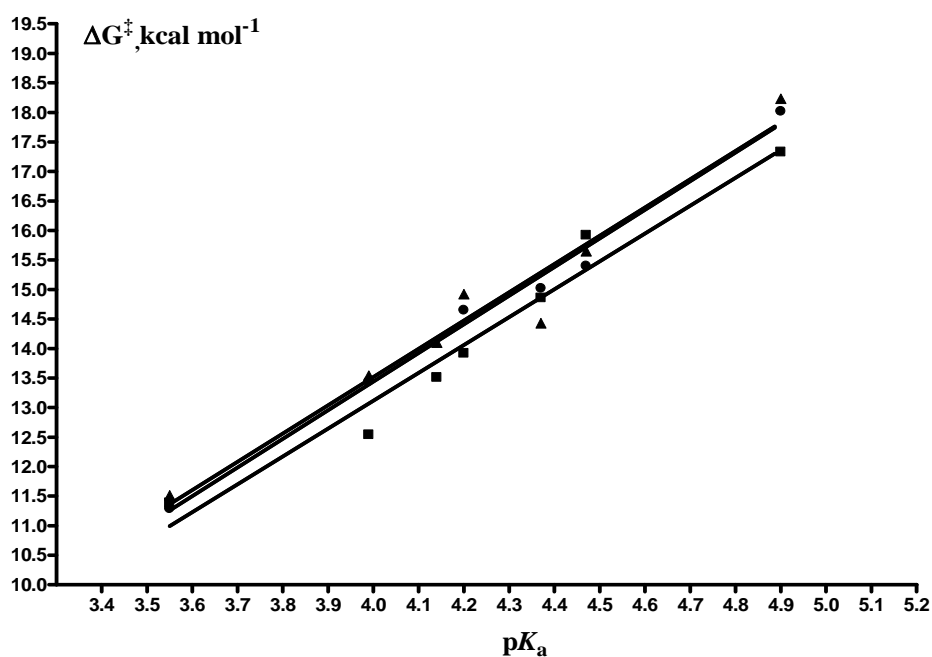


Figure 3.5.3 Dependence of ΔG^\ddagger (kcal mol^{-1}) on $\text{p}K_a$'s of substituted benzoic acids for alkaline hydrolysis of methyl *p*-substituted benzoate calculated by B3LYP/6-31+g(d) in PCM solvents (■ water, $R^2=0.9703$ ● methanol, $R^2=0.9853$ and ▲ acetonitril, $R^2=0.9528$).

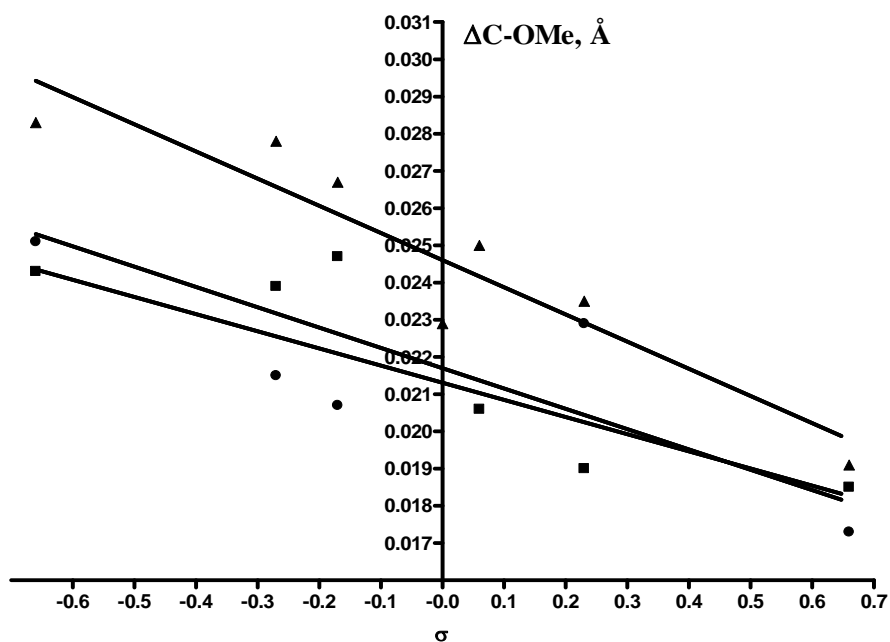


Figure 3.5.4 Dependence of C-OMe bond length change (\AA) on Hammett sigma constants for alkaline hydrolysis of methyl *p*-substituted benzoate calculated by B3LYP/6-31+g(d) in PCM solvents (■ water, $R^2=0.7790$, ● methanol, $R^2=0.6514$ and ▲ acetonitril, $R^2=0.8741$).

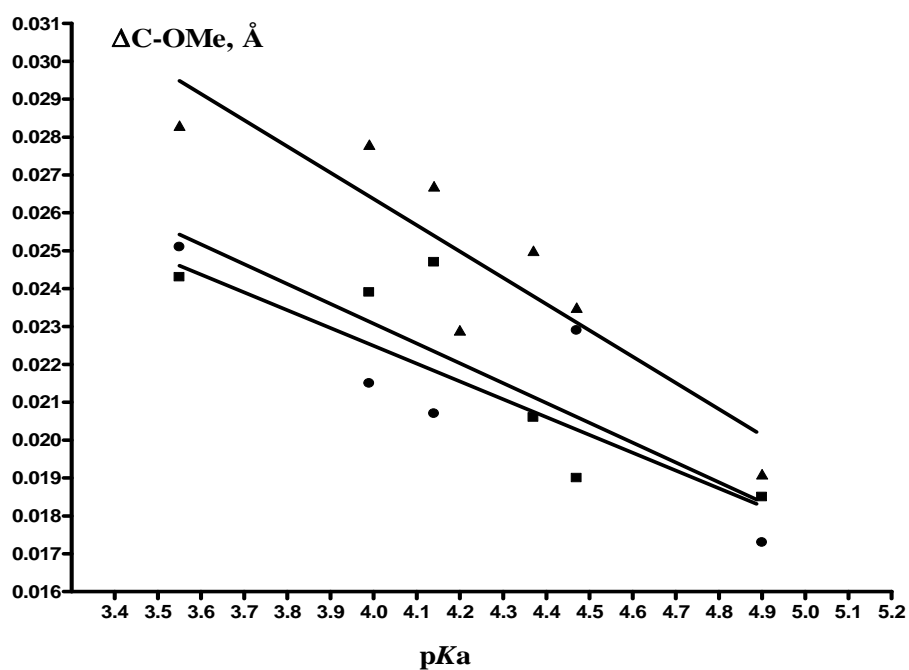


Figure 3.5.5 Dependence of C-OMe bond length change (\AA) on pK_a 's of substituted benzoic acids for alkaline hydrolysis of methyl *p*-substituted benzoate calculated by B3LYP/6-31+g(d) in PCM solvents (■ water, $R^2= 0.7362$ ● methanol, $R^2= 0.6873$ and ▲ acetonitril $R^2=0.8095$).

3.6 Tables

Table 3.6.1 Energies calculated for the alkaline hydrolysis of methyl substituted benzoates by B3LYP/6-31 + (d) in different PCM-solvents.^{a,b}

E_{GS}	E_{TS}	G_{GS}	G_{TS}	ΔE^\ddagger	ΔG^\ddagger	V (cm ⁻¹) ^c
-628.342406	-628.331835	-628.238187	-628.220034	6.63	11.39	-193.73
-628.339312	-628.328853	-628.235068	-628.217072	6.56	11.29	-188.96
-628.339796	-628.329018	-628.235588	-628.217245	6.76	11.51	-174.63
-995.688189	-995.674598	-995.591783	-995.571800	8.52	12.54	-214.7
-995.685258	-995.671763	-995.588694	-995.567281	8.78	13.44	-229.59
-995.685724	-995.671819	-995.589222	-995.567639	8.72	13.54	-235.56
-635.335365	-635.320977	-635.236769	-635.215242	9.02	13.51	-228.99

a) Energies reported as E_{GS} and E_{TS} are in Hartrees and correspond to total free energies of ground and transition states which exclude zero-point term. Energies reported as G_{GS} and G_{TS} are in Hartrees and correspond to sum of electronic and thermal free energies of ground and transition states which includes zero-point, thermal and entropic terms at 298 K and 1 atm. Those in solution (with non-electrostatic terms) include the total electronic energy polarised by the dielectric continuum together with the cavitation, dispersion and repulsive terms within PCM. The activation barriers for alkaline hydrolysis of methyl substituted benzoates (ΔE^\ddagger and ΔG^\ddagger) are in kcal mol⁻¹ and defined as the difference between the energy of the transition state and that of the equilibrium geometry multiplied by 627.5.

b) The first row corresponds to values for the reactions in PCM-water; the second row corresponds to values for the reactions in PCM-methanol and the third row corresponds to values for the reactions in PCM-acetonitril

c) Imaginary frequencies corresponding to the transition vector.

Table 3.6.2 C-OMe (Å) bond length calculated for the alkaline hydrolysis of methyl substituted benzoates by B3LYP/6-31 + (d) in different PCM-solvents. The first row corresponds to values for the reactions in PCM-water; the second row corresponds to values for the reactions in PCM-methanol and the third row corresponds to values for the reactions in PCM-acetonitril.

X	σ^a	pK_a^b	C-OMe (Å) _{GS} ^c	C-OMe (Å) _{TS} ^d	Δ C-OMe (Å) ^e
CN	0.66	3.55	1.3417	1.3602	0.0185
			1.3419	1.3592	0.0173
			1.3417	1.3608	0.0191
Cl	0.23	3.99	1.3447	1.3637	0.0190
			1.3450	1.3679	0.0229
			1.3447	1.3682	0.0235
F	0.06	4.14	1.3456	1.3662	0.0206
			1.3465	1.3592	0.0127
			1.3455	1.3624	0.0169
H	0.0	4.20	1.3463	1.3739	0.0276
			1.3465	1.3719	0.0254
			1.3462	1.3691	0.0229
Me	-0.17	4.37	1.3475	1.3722	0.0247
			1.3477	1.3684	0.0207
			1.3475	1.3742	0.0267
MeO	-0.27	4.47	1.3493	1.3732	0.0239
			1.3495	1.3710	0.0215
			1.3491	1.3769	0.0278
NH₂	-0.66	4.9	1.3538	1.3781	0.0243
			1.3538	1.3789	0.0251
			1.3532	1.3815	0.0283

a) *The Effect of Structure upon the Reactions of Organic Compounds. Benzene Derivatives* Louis P. Hammett J. Am. Chem. Soc.; **1937**; 59(1); 96-103; L.P.Hammett, *Physical Organic Chemistry*, McGraw-Hill Book Co., Inc., New York, NY, 1940, Chaps. III,IV,VII.

b) Refence 30

c) C-OMe (Å) bond lengths in the ground state.

d) C-OMe (Å) bond lengths in the transition state.

e) Bond length change, difference between the length in transition state and ground state.

3.7 References

1. (a) Williams, A. *Biochemistry* **1970**, 3383 (b) Jencks, W. P. *Cold Spring Harbor Symposia Quantitative Biology* **1971**, 36. (c) Williams, A., *Chem. Soc. Rev.*, **1986**, 15, 125. (d) Ingold, C.K.; *Structure and mechanism in Organic Chemistry 2nd edn.* Cornell University Press, Ithaca, New York, **1969**.
2. (a) Williams, A. *Concerted Organic and Bio-Organic Mechanism*, CRC, Boca Raton, **2000**, Chapter 4. (b) Connors, K. A. *Structure Reactivity Relationships: the Study of Reaction Rates in Solution*; VCH: New York, **1990** 311. (c) Hall, A.D.; Williams, A. *J. Chem. Soc., Chem. Commun.* **1985**, 1680. (d) Thea, S.; Harun, M. G.; Williams, A. *J. Chem. Soc., Chem. Commun.*, **1979**, 717.
3. (a) Fortunelli, A.; Tomasi, J. *Chem. Phys. Lett.* **1994**, 231. (b) L. P. Hammett, *Chem. Rev.* **1935**, 17, 125.
4. Maskill, H. *The Physical Basis of Organic Chemistry Oxford University Press, Oxford* **1985**. (b) Connors, K. A. *Structure Reactivity Relationships: the Study of Reaction Rates in Solution VCH: New York* **1990**, 311.
5. Yun-Dong, W.; David, K.; Lai, W. *J. Org. Chem.* **1996**, 61, 7904.
6. Poncek, R.; Van Damme, S. *J. Phys. Org. Chem.* **2007**, 20, 662.
7. Contreras, R.; Andres, J.; Domingo, L. R.; Castillo, R.; Perez, P. *Tetrahedron* **2005**, 61, 417.
8. Jack, F.; Kirsch, W.; Simon, C.; Simon, A. *J. Org. Chem.*, 1968, 33, 127.
9. Frisch, M. J.; Trucks, G. W.; Schlegel, H. B.; Scuseria, G. E.; Robb, M. A.; J. R. Cheeseman, J. A.; Montgomery, Jr.; Vreven, T.; Kudin, K.; Burant, J. C.; Millam, S. S.; Iyengar, J.; Tomasi, V.; Barone, B.; Mennucci, M.; Cossi, G.; Scalmani, N.; Rega, G. A.; Petersson, H.; Nakatsuji, M.; Hada, M.; Ehara, K.; Toyota, R.; Fukuda,

J.; Hasegawa, M.; Ishida, T.; Nakajima, Y.; Honda, O.; Kitao, H.; Nakai, M.; Klene, X.; Li, J. E. ; Knox, H. P.; Hratchian, J. B.; Cross, V.; Bakken, C.; Adamo, J.; Jaramillo, R.; Gomperts, R. E.; Stratmann, O.; Yazyev, A. J.; Austin, R.; Cammi, C.; Pomelli, J. W.; Ochterski, P. Y.; Ayala, K.; Morokuma, G. A.; Voth, P. Salvador, J. J.; Dannenberg, V. G.; Zakrzewski, S.; Dapprich, A. D.; Daniels, M. C.; Strain, O.; Farkas, D. K.; Malick, A. D.; Rabuck, K.; Raghavachari, J. B.; Foresman, J. V.; Ortiz, Q.; Cui, A. G.; Baboul, S.; Clifford, J.; Cioslowski, B. B.; Stefanov, G.; Liu, A.; Liashenko, P.; Piskorz, I.; Komaromi, R. L.; Martin, D. J.; Fox, T.; Keith, M. A.; Al-Laham, C. Y.; Peng, A.; Nanayakkara, M. ;Challacombe, P. M. W.; Gill, B.; Johnson, W. ; Chen, M. W.; Wong, C. G., and Pople, J. A. Gaussian 03, Revision C.02, Gaussian, Inc., Wallingford CT, **2004**.

10. Dennington II, R. ; Keith, T. ; Millam, J. ; Eppinnett, K. ; Hovell, W. L.; and Gilliland, R. ;Semichem, Inc., Shawnee Mission, KS, GaussView, Version 3.09, **2003**.

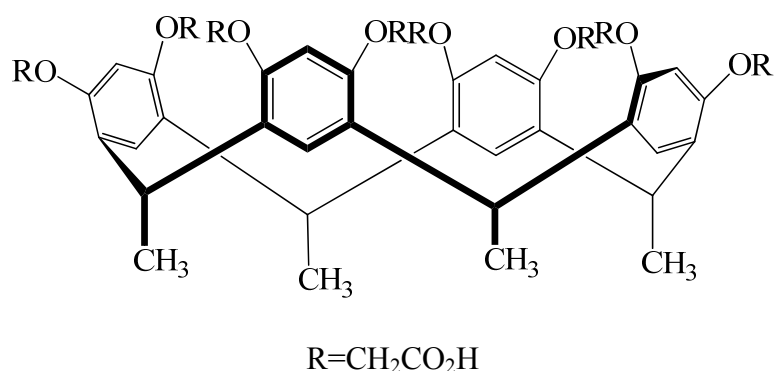
4.1 Introduction

Non-covalent interactions such as electrostatic, hydrogen bonding, hydrophobic, van der Waals and charge transfer are very important driving forces in molecular recognition and thus they are the main factors responsible for the selectivity of bioactive species. They also play a significant role in maintaining protein and DNA structures. However, it is a very difficult task to predict their individual contribution in such processes.

Therefore, information gathered from model studies produces useful insight in understanding of the mode of molecular recognition in biological systems. Hence, using small molecules as models in predicting and realizing the role of non-covalent interactions in macromolecules has become the agenda of Science for almost quarter a century¹⁻⁴. Among the models used calixarenes and calixresorcinarenes hold a key place. They have a similar molecular architecture, that is, both possess a cavity with distinct hydrophobic and hydrophilic sites represented by upper and lower rims of these molecular baskets⁵⁻⁸. By suitable modification of these sites it is quite simple to use these molecules for a wide variety of applications, for example, in designing separation and detection devices for analyses of major biological and environmental interests⁹⁻¹⁷. It has been demonstrated that these compounds and their derivatives can interact with a variety of organic and inorganic species and they can also accommodate many small molecules/ions in their cavity. So such properties have established these hosts as potential in many applications, for example, as chemosensing agents¹⁸.

Molecular dynamics (MD) is one of the current methods used in the understanding of molecular recognition process that occurs in organisms at atomic

level, and consequently free energy calculation have become a powerful tool in estimating quantitative degree of molecular interactions in host-guest chemistry. The method has been developed for the biological systems but it has been used in supramolecular systems of organic structures¹⁹. Molecular mechanics/Poisson-Boltzmann surface area has successfully been employed in predicting the binding free energy of the complexes of macromolecules²⁰.



Host Molecule: Octaethoxycarbonylmethylresorcincalix[4]arene (**1**)

Esters: R-CO₂Ar-4-NO₂

2 (R = Me, *p*-nitrophenyl acetate)

3 (R = Phenyl, *p*-nitrophenyl benzoate)

4 (R = Hexyl, *p*-nitrophenyl hexanoate)

5 (R = 3-*N*-methylpyridinyl, *p*-nitrophenyl *N*-methyl nicotinate)

6 (R = 4-*N*-methylpyridinyl, *p*-nitrophenyl *N*-methyl isonicotinate)

The study involves the investigation of the complexation of the host **1** with *p*-nitrophenyl esters of neutral aliphatic (**2** and **4**) and aromatic (**3**), and charged *N*-methyl isonicotinic (**5**) and nicotinic (**6**) acids using computational modeling. The reason for choosing the host and the guests is that their binding properties have already been studied by kinetic method²¹. Molecular dynamic and quantum mechanic

calculations were employed to predict the mode of complexation and the main driving forces for the binding. Theoretical data produced comparable results with those obtained by kinetics.

4.2 Method

4.2.1 Computational Modeling

4.2.1.1 Molecular Dynamics Simulations

Molecular dynamics (MD) simulations were carried out in a Linux-Cluster system to determine conformations for the each crown ether complex studied. All simulations were conducted by using AMBER (version 9.0)²² suit of programs. These MD experiments were supplemented by quantum mechanics (QM) computations determined at the 6-31+g(d) basis set by Gaussian 03^{23a, b}.

The host and ligands were optimized with Gaussain 03 using semi-empirical AM1 method. AM1-Bcc (Austian model with Bond and charge correction)²⁴ atomic partial charges fort the host and guests were determined by antechamber module of AMBER (v9) package. Charges for the ionizable residues were set at a neutral pH. The complex was solvated in a TIP3PBOX²⁵ water box with dimensions of 10 Å from the solute. 0.4 Å space was initially generated at the boundary of the complex and the solvent molecules during the solvation process. Na⁺ ions were added to neutralize each complex system. The General AMBER Force Field (GAFF)²⁶ was adopted in simulation because it handles small organic molecules.

The entire system was relaxed in four steps over a period of 160 ps. The system was then heated from 0 to 300 K in 100 ps and allowed to equilibration at 300 K for an other 100 ps of MD. Subsequently, MD computations were performed at

through 10 ns and 2 fs of time interval was used for each iteration in all MD studies. The Particle Mesh Ewald (PME) method²⁷ was applied to calculate long-range electrostatics interactions. The SHAKE²⁸ method was applied to constrain all of the covalent bonds involving hydrogen atoms.

To compare bound and unbound structures, additional MD simulations were performed for the host. Root-mean-square deviation (RMSD) analysis for the complex system was carried out on the trajectories by the ptraj module of AMBER (v9). Three dimensional structures were displayed using Chimera (UCSF)²⁹ and VMD³⁰, and RMSD graphics were produced by XMGRACE package program.

4.2.1.2 Docking Study (Molecular Docking)

Molecular docking attempts to arrange molecules in favorable configurations by matching complementary features. This is a difficult task because there are many ways in which complex molecules can be associated. The problem is further complicated by an exponential dependence on molecule size, so that the number of possible configurations explodes when docking involves biological macromolecules such as proteins or nucleic acid polymers. An exhaustive computational analysis of configuration space is not tractable especially for database searching. Current docking methodologies thus invoke either geometry- or energy-based schemes to guide configurational sampling, where the former relies upon the matching of topographical features and the latter upon optimization along a potential energy surface of some kind. As alluded to earlier, however, configurational sampling is only half of the problem. The ranking of each configuration by some measurement of complementarity constitutes the other major hurdle.

In this study, docking studies were performed by Dock 6.0³¹. The initial coordinates of the octacarboxymethylcalix[4]resorcinarene (host), and the respective guests for the docking studies were obtained via MD studies for 5 ns for the host and 1 ns for the guests.

Docking was performed with default settings to obtain a population of possible conformations and orientations for the guests in the binding site. A sphere around the centre of the binding pocket was formed to define as binding pocket for the docking studies. All torsion angles in each compound were allowed to rotate freely. Docking results suggested that several of these derivatives are active host with a significant preference for binding position.

4.2.1.3 MM/PBSA Calculations: This study applies a second-generation form of the Mining Minima³²⁻³⁴ algorithm, termed M2, to analyze the binding reactions of host-guest complexes in an organic solvent. The MM-PB/SA module of AMBER (v9) was applied to compute the binding free energy (ΔG_{bind}) of each complex using the MM/PBSA method. For each complex, a total number of 200 snapshots were extracted from the last 1 ns of the complex trajectories.

During conformational searching and the evaluation of configuration integrals, Welec is computed with a simplified but fast generalized Born model³⁵. The electrostatic solvation energy of each energy-well is then corrected toward a more accurate but time-consuming finite-difference solution of the Poisson equation. The dielectric cavity radius of each atom is set to the mean of the solvent probe radius 1.4 Å for water and the atom's van der Waals radius, and the dielectric boundary between the molecule and the solvent is the solvent-accessible molecular surface³⁶.

The solvation calculations use a water dielectric constant of 80. The MM/PBSA method can be conceptually summarized as:

$$\Delta G_{\text{bind}} = G_{\text{complex}} - [G_{\text{host}} + G_{\text{ligand}}] \quad (4.1)$$

$$G = E_{\text{gas}} + G_{\text{sol}} - TS \quad (4.2)$$

$$E_{\text{gas}} = E_{\text{bond}} + E_{\text{angle}} + E_{\text{torsion}} + E_{\text{vdw}} + E_{\text{ele}} \quad (4.3)$$

$$G_{\text{sol}} = G_{\text{PB}} + G_{\text{SA}} \quad (4.4)$$

$$H = E_{\text{gas}} + G_{\text{sol}} \quad (4.5)$$

$$S_{\text{tot}} = S_{\text{vib}} + S_{\text{trans}} + S_{\text{rot}} \quad (4.6)$$

$$\Delta G = \Delta H - T\Delta S \quad (4.7)$$

where G_{complex} , G_{host} , and G_{ligand} are the absolute free energies of the complex, host and the ligand species respectively as shown equation (4.1). Each of them is calculated by summing an internal energy in gas phase (E_{gas}), a solvation free energy (G_{sol}), and a vibrational entropy term equation (4.2). E_{gas} is Standard force field energy, including strain energies from covalent bonds and torsion angles as well as noncovalent van der Waals and electrostatic energies (4.3). The solvation free energy, G_{sol} , is calculated with a PB/SA model, which dissects solvation free energy as the sum of an electrostatic component (G_{PB}) and a nonpolar component (G_{SA}) as shown equation (4.4), S_{tot} is the total entropy comprising of translational (S_{trans}), vibrational (S_{vib}) and rotational (S_{rot}) entropies as gas phase for each species as shown equation (4.6).

4.2.1.4 Quantum Chemical Calculations: The lowest energy structure for each complex extracted from molecular dynamic simulations was saved as pdb and used for quantum chemical calculations. The ONIOM calculations were performed at B3LYP/6-31+g(d) level for the guests and at AM1 level for the host. The binding energy (ΔE_{bind}) for each complex is calculated from Eq. 4.8.

$$\Delta E_{\text{bind}} = E_{\text{com}} - (E_{\text{host}} + E_{\text{guest}}) \quad (4.8)$$

where E_{com} is the energy of the complex in Hartree, E_{host} is the energy of the host in Hartree and E_{guest} is the energy of the guest in Hartree.

4.3 Results and Discussion

Molecular dynamic calculations were performed to understand the mode of the complexation between the host and the guests and thus to determine the main deriving forces behind the complexes at atomic level. Starting from the right conformation of hosts forms a general problem in MD. In this study the host was computed over a period of 5 ns at 300 K in implicit solvent and the lowest energy conformer was chosen and it was minimized and further computed over 1 ns again. They are shown in Figure 1. It shows that two phenyl rings flip over to form the more stable conformer. It was previously reported that structurally similar compounds³⁷, since they have lower barrier to flip over, have similar structural behaviors. The lowest energy conformer was used to accommodate guests by using Dock 6.0 program as described in the computational modeling section. The obtained structures were computed for MD calculations over a period of 10 ns in explicit water at 300 K as described in experimental section. The root mean-square deviations (RMSD) and energies calculated for each complex are presented in

Figures 4.5.2-4.5.6, indicating that MD calculations produced considerably good results over 10 ns of the period. The docking scores and energies derived from MD calculations are summarized in Table 4.6.1. The results show a parallel agreement with those of experimental ones.

The average structures of the host **1** and its complexes with guests (**2-6**) obtained from MD calculations are demonstrated in Figure 4.5.7. They show that the host holds the guest on the surface of the cavity surrounded by four carboxylates. It seems that in the case of benzoate (**3**) and hexanoate (**4**) the host has undergone deformation upon complexation, probably because of steric effects of phenyl and hexyl groups by increasing the larger van der Waals interaction surface.

4.3.1 MM/PBSA Method: Estimated binding free energies (kcal mol^{-1}) of the host to guests studied by MM/PBSA results are listed in Table 4.6.1. They are quite large than experimental values, particularly those of charged guests. This may be attributed to the fact that the host and some of the guests are charged and the MM/PBSA method utilizes the continuum solvation model where solute-solvent interactions are ignored. Therefore, it is expected that the method would overestimate the binding free energies of such systems. However, it is quite interesting to see that there is a parallel between the binding free energies calculated by MM/PBSA and those of experimental ones. The individual contribution of van der Waals and electrostatic interactions to the free energy of binding are listed in Table 4.6.2. They indicate that the electrostatic interactions are more favorable in the complexation of the host for the charged guests (**5** and **6**) comparing with van der Waals interactions whereas van

der Waals interactions are significantly pronounced in the complexes of the host with neutral esters (2-4) compared with electrostatic interactions, more underlined for 4.

4.3.2 Quantum Mechanical Calculations: The free energies of binding of the host to the guests obtained by ONIOM calculations are presented in Table 4.6.1. They are even larger than those obtained by MM/PBSA compared to the experimental ones. However, they are in parallel with those obtained by MM/PBSA and kinetics. The overestimated binding energies as observed in the MM/PBSA calculation may again be explained in terms of the interactions of charged molecules with the host and the effect of solvation.

4.4 Conclusion

Theoretical calculations have produced relatively comparable results in details to understand the mode of the binding of the octa-carboxymethylcalix[4]arene with *p*-nitrophenyl esters of neutral and charged carboxylic acids. So it can be confidently suggested that a combination of theoretical calculation (MD, MM/PBSA and QM) can be employed to estimate the binding properties of supramolecular structures of these kinds.

4.5 Figures

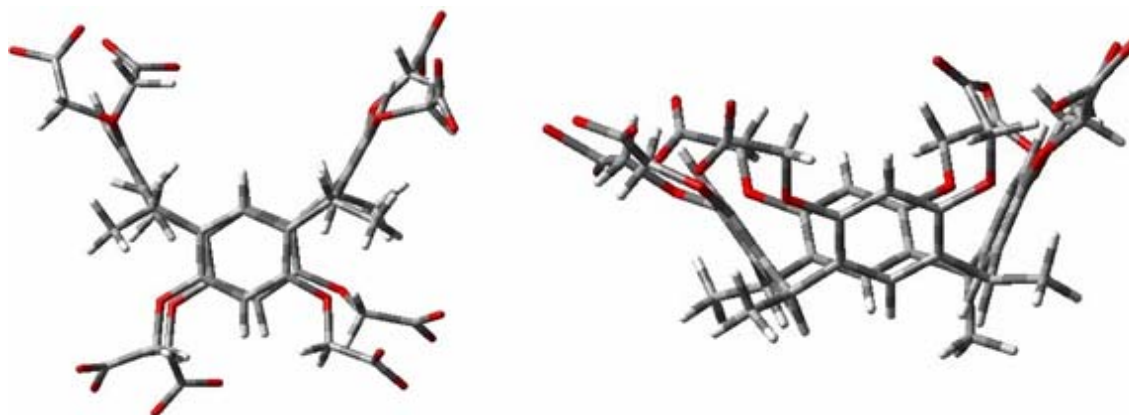


Figure 4.5.1 Graphic representation of two conformations of the host **1** obtained from MD simulation followed by optimization with B3LYP/6-31+g(d) level of theory. -3657.44976544 Hartree for the conformer on the left and -3655.63131093471 Hartree for the conformer on the right.

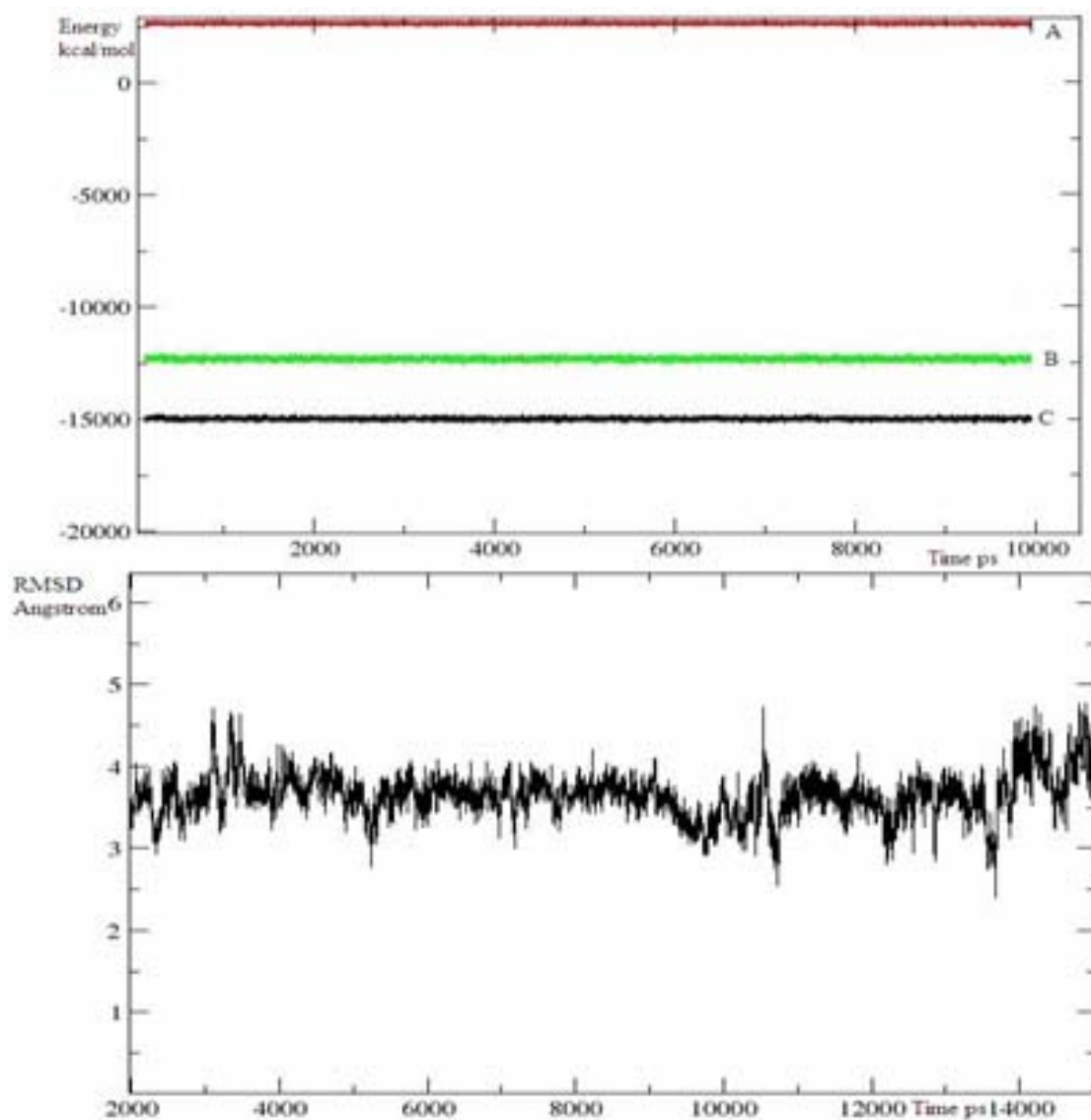


Figure 4.5.2 Root-mean square deviations (RMSD) with reference to minimum energy structure and energy changes observed in MD simulation of the complex of the host **1** with *p*-nitrophenyl acetate **2**. **A** represents kinetic energy, **B** represents total energy and **C** represents potential energy.

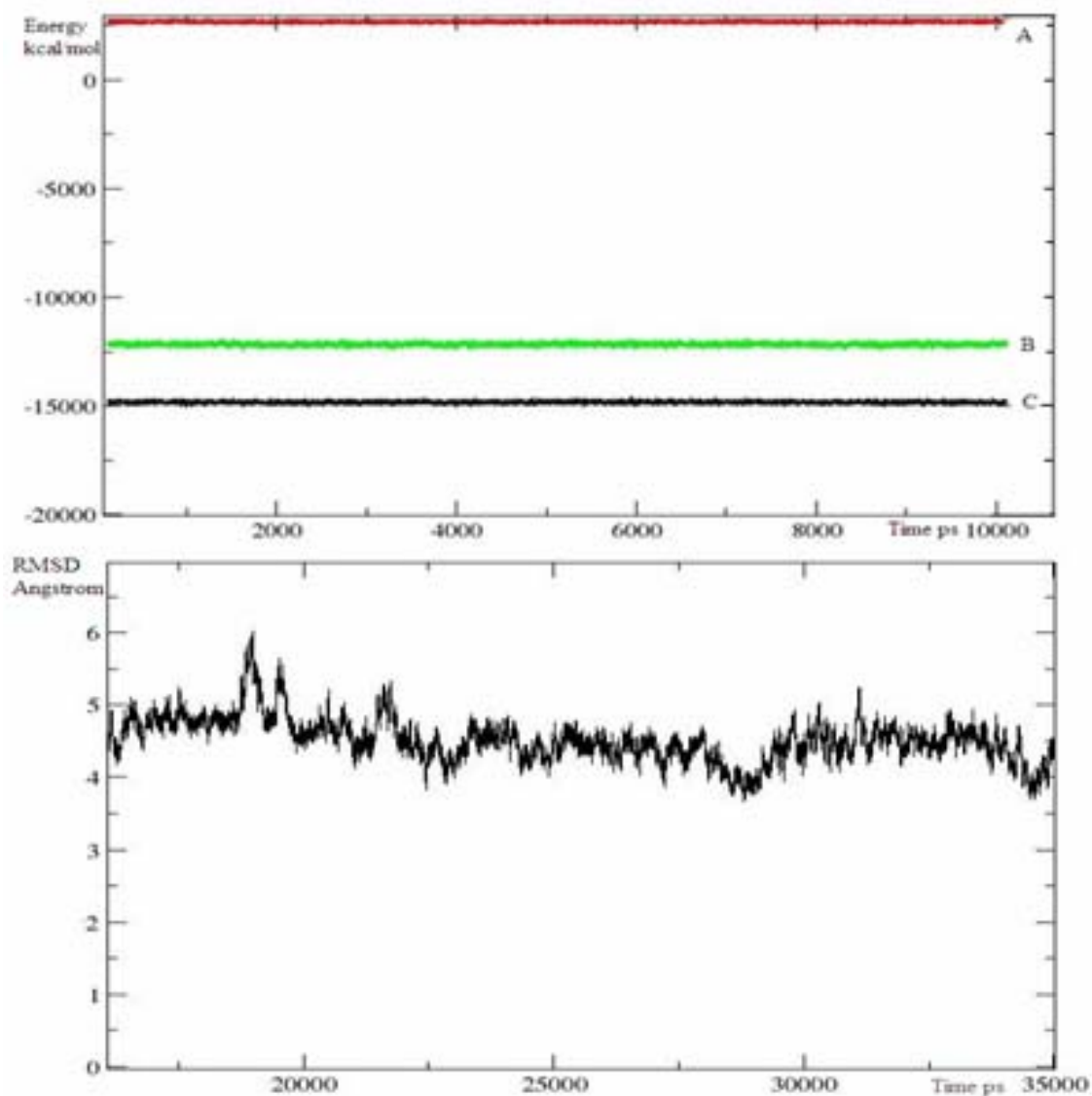


Figure 4.5.3 Root-mean square deviations (RMSD) with reference to minimum energy structure and energy changes observed in MD simulation of the complex of the host **1** with *p*-nitrophenyl benzoate **3**. **A** represents kinetic energy, **B** represents total energy and **C** represents potential energy.

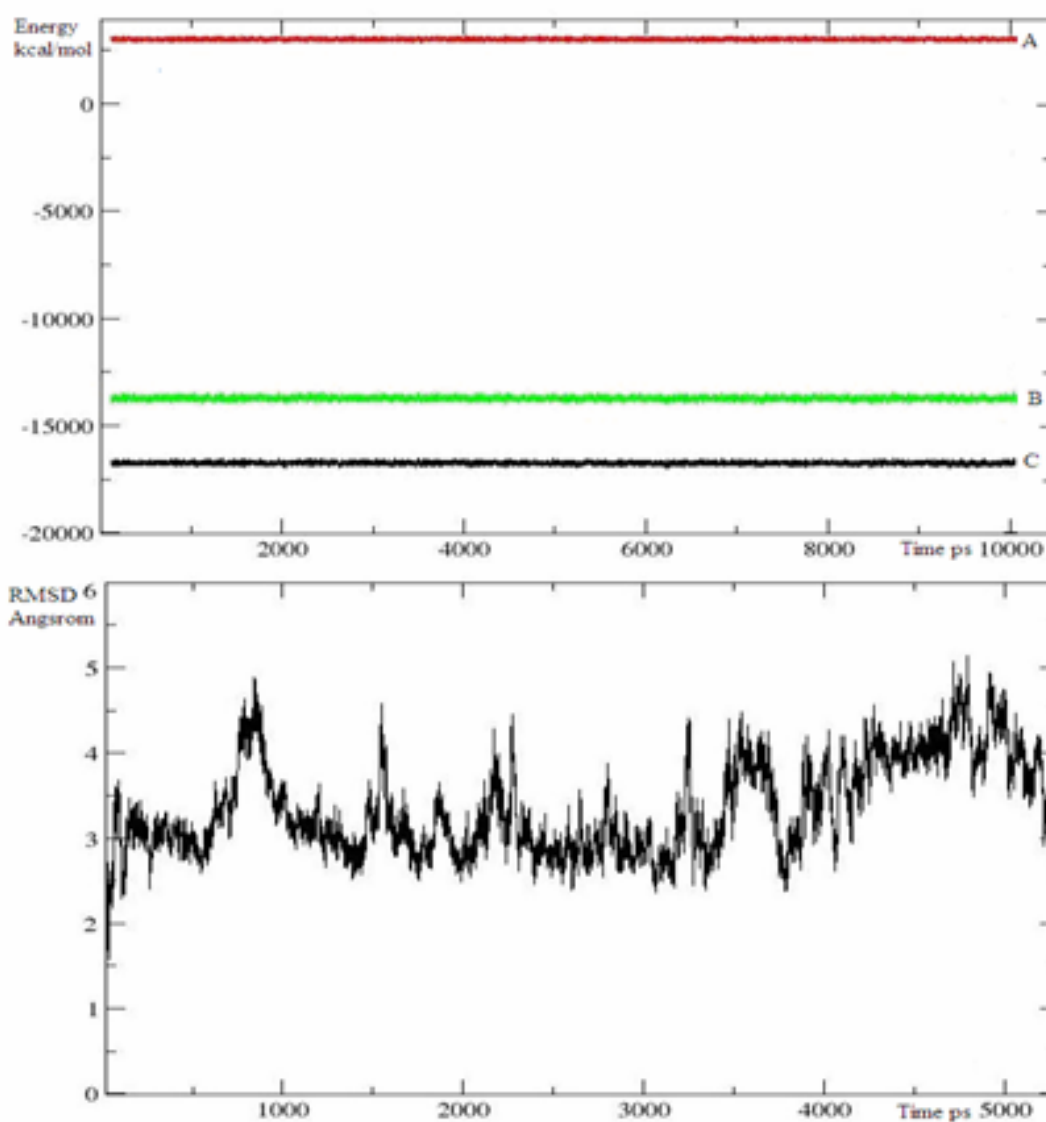


Figure 4.5.4 Root-mean square deviations (RMSD) with reference to minimum energy structure and energy changes observed in MD simulation of the complex of the host **1** with *p*-nitrophenyl hexanoate **4**. **A** represents kinetic energy, **B** represents total energy and **C** represents potential energy.

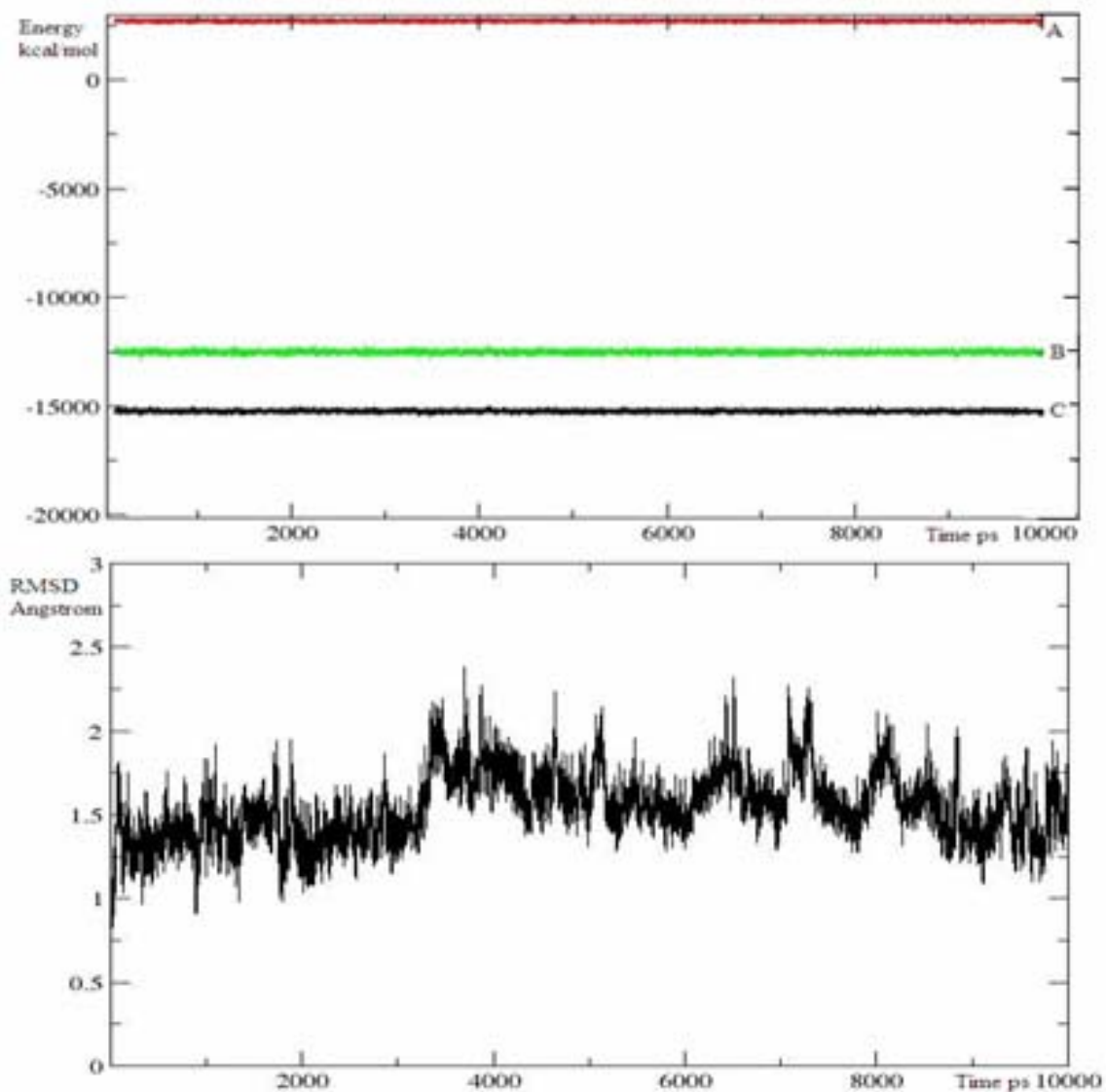


Figure 4.5.5 Root-mean square deviations (RMSD) with reference to minimum energy structure and energy changes observed in MD simulation of the complex of the host **1** with *p*-nitrophenyl isonicotinate **5**. **A** represents kinetic energy, **B** represents total energy and **C** represents potential energy.

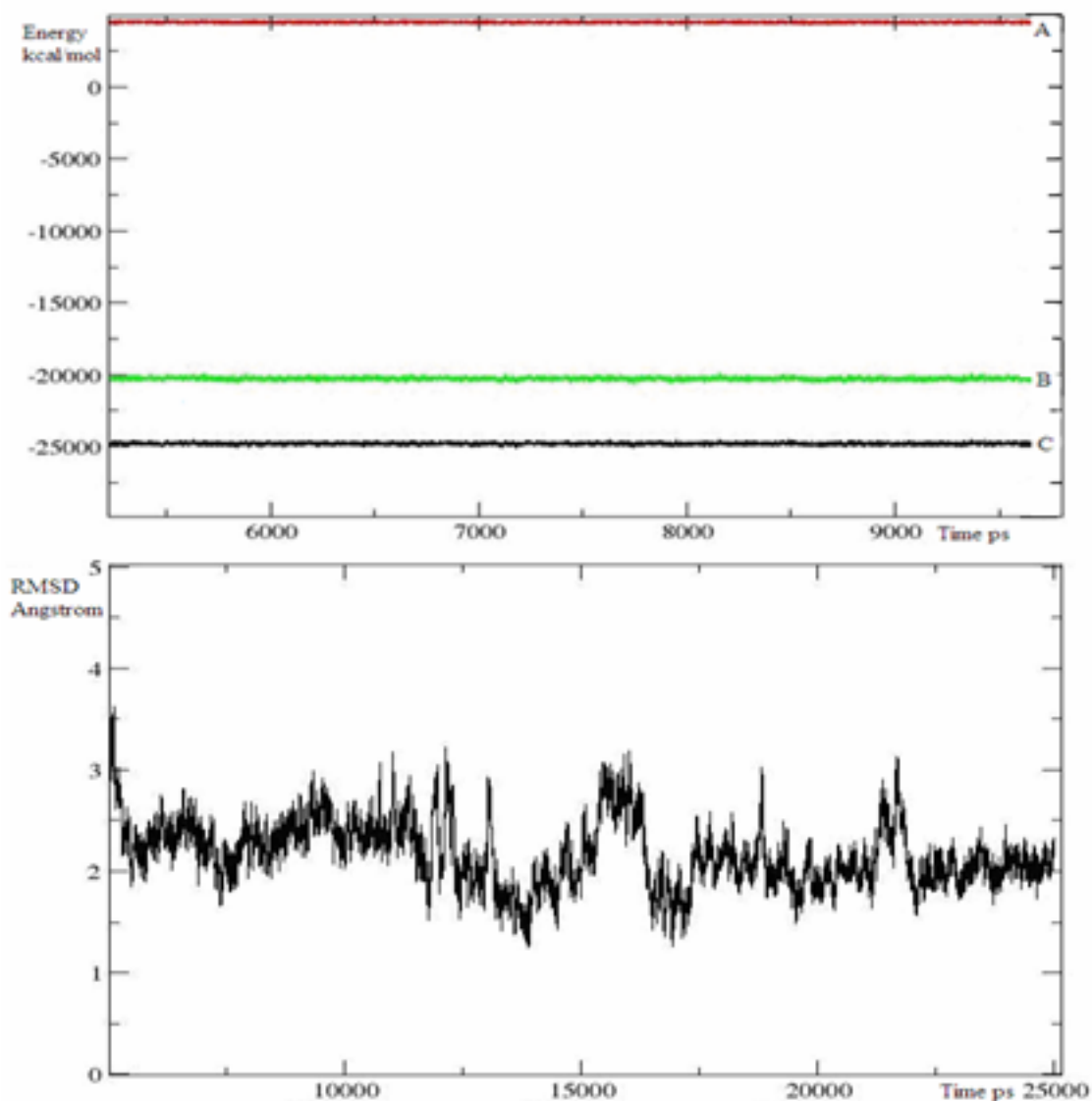


Figure 4.5.6 Root-mean square deviations (RMSD) with reference to minimum energy structure and energy changes observed in MD simulation of the complex of the host **1** with *p*-nitrophenyl nicotinate **6**. **A** represents kinetic energy, **B** represents total energy and **C** represents potential energy.

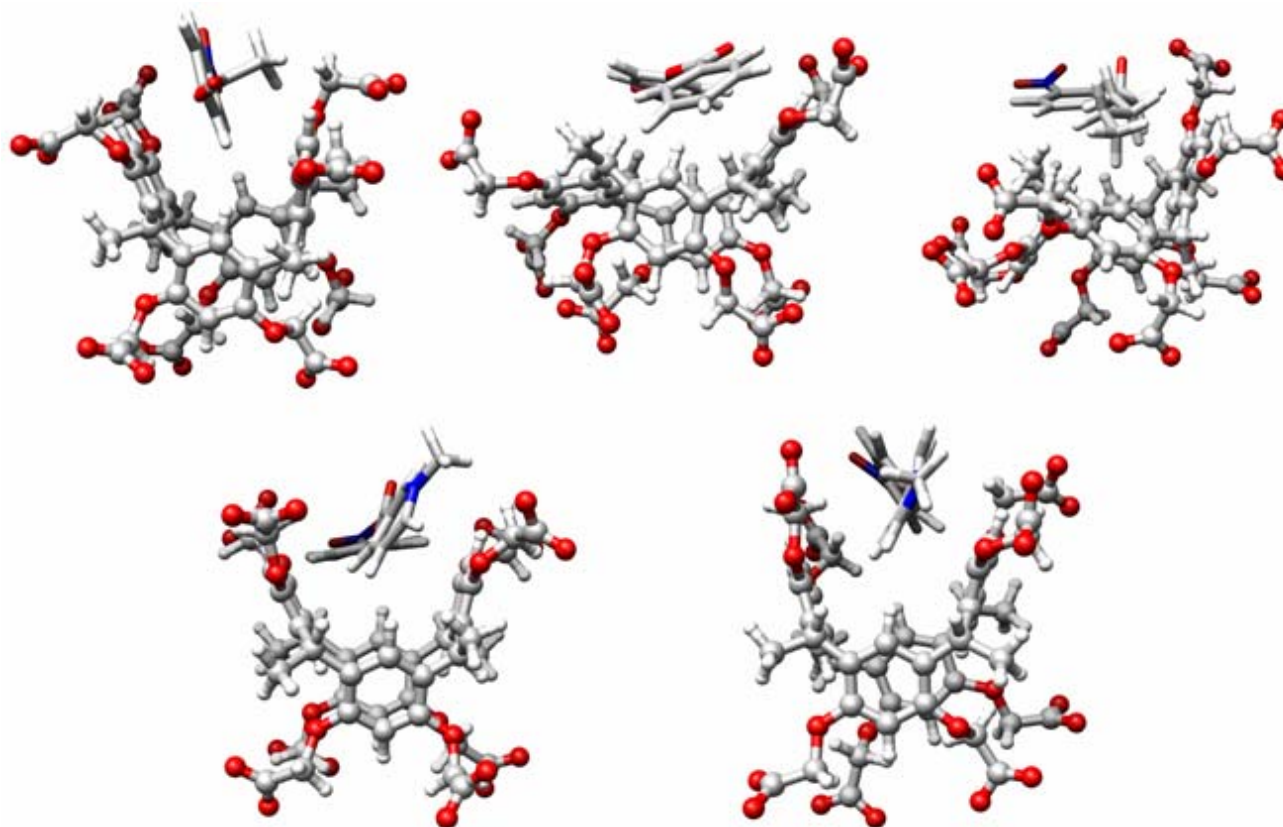


Figure 4.5.7 Graphic representation of the host **1** and its complexes with the guests (**2-6**) obtained by MD calculation. The structures are the average from MD simulations. Pictures on the left, middle and the right in the upper line correspond to acetate, benzoate and hexanoate, respectively. Those on the left and the right in the lower line correspond *N*-methylnicotinate and *N*-methylisonicotinate.

4.6 Tables

Table 4.6.1 Thermodynamic parameters for binding of the host **1** to esters (**2-6**) derived from theoretical calculations.

Guests	MD ^a	DS ^b	$\Delta G_{\text{bind}}^{\text{c}}$	$\Delta E_{\text{bind}}^{\text{d}}$	$\Delta G_{\text{expt.}}^{\text{e}}$	K_{a}^{f}
2	-14975	-21	-2.17	-26.63	-1.33	9.26
3	-14824	-24	-7.22	-27.82	-1.73	18.14
4	-16742	-25	-10.27	-33.68	-2.34	50.51
5	-24227	-39	-15.17	-354.34	-3.36	279.33
6	-24791	-37	-18.49	-369.36	-3.54	380.23

a) Average potential energy including solvent in kcal mol⁻¹ obtained from MD calculations over a period of 10 ns.

b) Docking scores in kcal mol⁻¹.

c) Theoretical binding free energy calculated by MM/PBSA method in kcal mol⁻¹

d) Complexation energy in kcal mol⁻¹ determined by ONIOM (B3LYP/6-31+g(d)//AM1) as described in experimental section.

e) Experimental binding free energy in kcal mol⁻¹ produced from $\Delta G = RT \ln K_{\text{a}}$ where $R = 1.987$ cal mol⁻¹ and $T = 300$ Kelvin.

f) Binding constants of the host to the guests (M⁻¹) taken from reference 21.

Table 4.6.2 The individual contribution of van der Waals and electrostatic terms (in kcal mol⁻¹) to the free energy of binding of the host to the guests calculated by MM/PBSA.

Term	2	3	4	5	6
ELE	1.05	-0.91	1.18	-342.31	-333.31
VDW	-3.36	-10.47	-13.07	-17.80	-16.96

ELE: electrostatic interactions

VDW: van der Waals interactions

4.7 References

1. Cram, D. J. *Angew. Chem. Int. Ed. Engl.* **1988**, 27, 8, 1009.
2. Pedersen, C. J. *Angew. Chem. Int. Ed. Engl.* 1988, 27, 8, 1021.
3. Soares, L. A.; Leal, A.F.V.B.; Fraceto, L.F.; Maia, E.R.; Resck, I.S.; Kato, M. J.; Gil, E.D.; de Sousa, A. R.; da Cunha, L. C.; Rezende, K. R. *J. Incl. Phenom. Macrocycl. Chem.* **2009**, 64, 1-2, 23.
4. Wipff, G.; Kollman, P.A.; Lehn J. M. *J Mol. Struc.- THEOCHEM* **1983**, 93, 153.
5. Gutsche, C. D.; Dhawan, B.; Levine, J. A.; Hyun, N. K.; Bauer, L. J. *Tetrahedron*, **1983**, 39, 3, 409.
6. Böhmer, V. *Angew. Chem. Int. Ed. England* **1995**, 34, 7, 713.
7. Tuntulani, T.; Poompradub, S.; Thavornnyutikarn, P.; Jaiboon, N.; Ruangpornvisuti, V.; Chaichit, N.; Asfari, Z.; Vicens, J. *Tetrahedron Lett.* **2001**, 42, 32, 5541.
8. Baxter, P. N. W. *Comprehensive Supramolecular Chemistry In: Atwood, J.L., Davies, J. E. D.; MacNicol, D.D., Vögtle, F., Lehn, J-M. (eds.), 1996*, 165, Pergamon, Oxford.
9. Ellselami, L.V.; Chartron, F. V.; Conchon, P. C.; Felix, C. G.; Retailleau, L.; Houas, A. J. *Hazardous Materials* **2009**, 166, 2-3, 1195.
10. Hajipour, A. R., Habibi, S.; Ruoho, A. E. *Polimer Int.* **2009**, 58, 6, 630.
11. Hamdi, A.; Sauene, R.; Kim, L.; Ağabeydi, R.; Matihac, L.; Vicens J. *Inc. Phen. Mac. Chem.* **2009**, 64, 1-2, 95.
12. Wei, A.; Tripp, S. L.; Liu, J.; Kasama, T.; Dunin-Borkowski, R. E. *Supr. Mol. Chem.* **2009**, 21, 3-4, 189.
13. Doyle, R.; Breslin, C. B.; Rooney, A. D. *Biochem. Eng. Quarterly* **2009**, 23, 1, 93.

- 14.** Demirtas, H. N.; Bozkurt, S.; Durmaz, M.; Yilmaz, M.; Sirit, A. *Tetrahedron* **2009**, *65*, 15, 3014.
- 15.** Kalenius, E.; Kekaelaenen, T.; Neitola, R.; Beyeh, K.; Rissanen, K.; Vainiotalo, P. *Chem.-Eur. J.* **2008**, *14*, 17, 5220.
- 16.** Mchedlov-Petrossyan N.O, Vodolazkaya, N.A., Vilкова, L.N., Soboleva, O.Y., Kutuzova, L.V.; Rodik, R. V.; Miroshnichenko, S. I., Drapaylo, A. B. *J. Mol. Liq.* **2009**, *145*, 3, 197.
- 17.** Makinen, M.; Kalenius, E.; Neitola, R.; Rissanen, K.; Vainiotalo, P. *Rapid Commun. Mass. Sp.* **2008**, *22*, 9, 1377.
- 18.** Han, J. P., Zang, L.L., Li, H.B., Xie, G.Y. *Sensors and Actuators B-Chemical* **2009**, *137*, 2, 704.
- 19.** Case, D. A.; Cheatham, T. E.; Darden, T.; Gohlke, H.; Luo, R.; Merz, K. M.; Onufriev, A.; Simmerling, C.; Wang, B.; Woods, R. J. *Computat. Chem.* **2008**, *26*, 16, 498.
- 20.** Rodik, R.V.; Boyko, V. I.; Kalchenko V. I. *Calixarenes in Bio-Medical Researches Curr. Med. Chem.* **2009**, *16*, 13, 1630.
- 21.** Cevasco, G.; Galatini, A.; Pirinccioglu, N.; Thea, S.; Williams, A.; *J. Phys. Org. Chem.* **2008**, *21*, 6, 498.
- 22.** Case, D. A.; Darden, T. A.; Cheatham III, T. E.; Simmerling, C. L.; Wang, J.; Duke, R. E.; Luo, R.; Merz, K. M.; Pearlman, D. A.; Crowley, M.; Walker, R. C.; Zhang, W.; Wang, B.; Hayik, S.; Roitberg, A.; Seabra, G.; Wong, K. F.; Paesani, F.; Wu, X.; Brozell, S.; Tsui, V.; Gohlke, H.; Yang, L.; Tan, C.; Mongan, J.; Hornak, V.; Cui, G.; Beroza, P.; Mathews, D. H.; Schafmeister, C.; Ross, W. S. and Kollman, P. A. **2006**, AMBER 9, University of California, San Francisco.

23. a) Frisch, M. J.; Trucks, G. W.; Schlegel, H. B.; Scuseria, G. E.; Robb, M. A.; J. R. Cheeseman, J. A; Montgomery, Jr.; Vreven, T.; Kudin, K.; Burant, J. C.; Millam, S. S.; Iyengar, J.; Tomasi, V.; Barone, B.; Mennucci, M.; Cossi, G.; Scalmani, N.; Rega, G. A.; Petersson, H.; Nakatsuji, M.; Hada, M.; Ehara, K.; Toyota, R.; Fukuda, J.; Hasegawa, M.; Ishida, T.; Nakajima, Y.; Honda, O.; Kitao, H.; Nakai, M.; Klene, X.; Li, J. E. ; Knox, H. P.; Hratchian, J. B.; Cross, V.; Bakken, C.; Adamo, J.; Jaramillo, R.; Gomperts, R. E.; Stratmann, O.; Yazyev, A. J.; Austin, R.; Cammi, C.; Pomelli, J. W.; Ochterski, P. Y.; Ayala, K.; Morokuma, G. A.; Voth, P. Salvador, J. J.; Dannenberg, V. G.; Zakrzewski, S.; Dapprich, A. D.; Daniels, M. C.; Strain, O.; Farkas, D. K.; Malick, A. D.; Rabuck, K.; Raghavachari, J. B.; Foresman, J. V.; Ortiz, Q.; Cui, A. G.; Baboul, S.; Clifford, J.; Cioslowski, B. B.; Stefanov, G.; Liu, A.; Liashenko, P.; Piskorz, I.; Komaromi, R. L.; Martin, D. J.; Fox, T.; Keith, M. A.; Al-Laham, C. Y.; Peng, A.; Nanayakkara, M. ;Challacombe, P. M. W.; Gill, B.; Johnson, W. ; Chen, M. W.; Wong, C. G., and Pople, J. A. Gaussian 03, Revision C.02, Gaussian, Inc., Wallingford CT, **2004.** **b)** Dennington II, R. ; Keith, T. ; Millam, J. ; Eppinnett, K. ; Hovell, W. L.; and Gilliland, R. ;Semichem, Inc., Shawnee Mission, KS, GaussView, Version 3.09, **2003.**

24. Jakalian, A.; Jack, D. B.; Bayly, C. I Abstr. Pap. Am. Chem. S. **2000**, 220, 277.

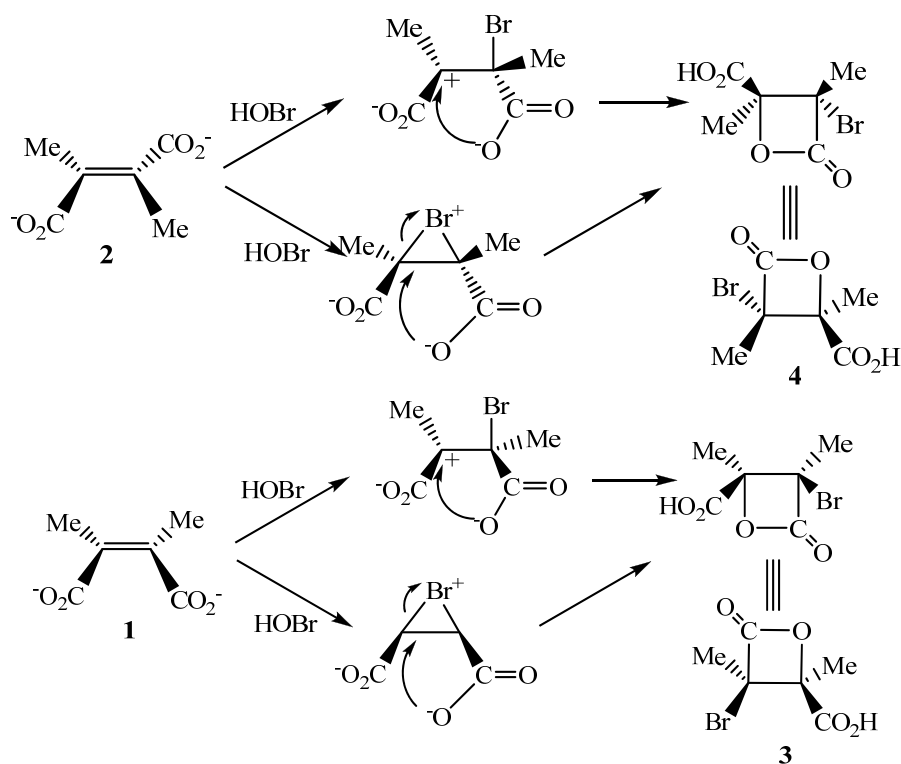
25. Kollman, P. A.; Massova, I.; Reyes, C.; Kuhn, B.; Huo, S.; Lee, M.; Duan, T. Y.; Wang, W.; Donini, O.; Cieplak, P.; Srinivasan, J.; Case, D. A. Acc. Chem. Res. **2000**, 33, 12, 889.

26. Wang, J. M.; Wolf, R. M.; Caldwell, J. W.; Kollman, P. A.; Case, D. A. J. Computat. Chem. **2004**, 25, 9, 1157.

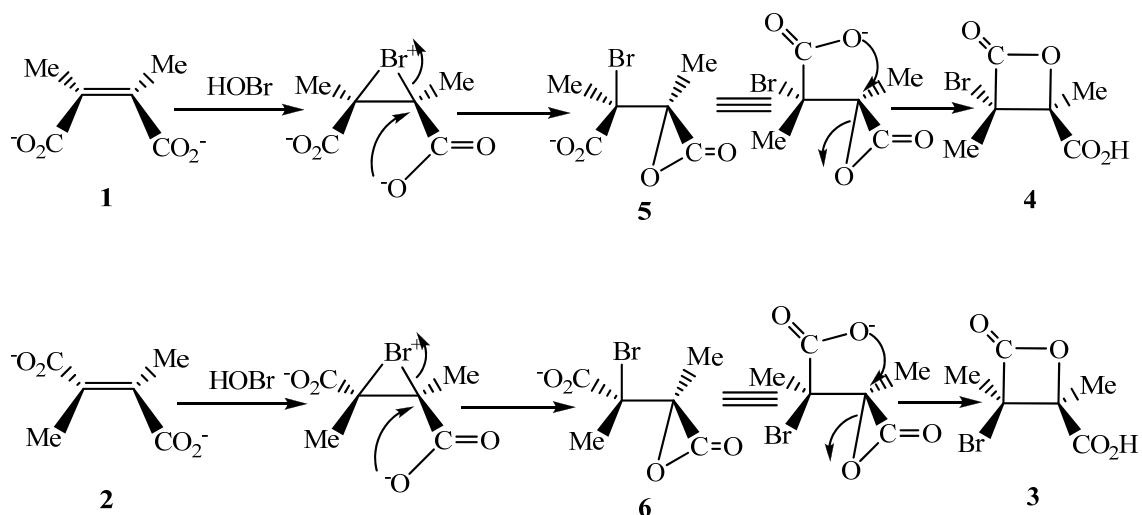
- 27.** Cornell, W. D.; Cieplak, P.; Bayly, C. I.; Gould, I. R.; Merz, K. M.; Ferguson, D. M.; Spellmeyer, D. C.; Fox, T.; Caldwell, J.W.; Kollman, P. A. *J. Am. Chem. Soc.*, **1995**, 117, 19, 5179.
- 28.** Darden, T., York, D., Pedersen, L. *J. Chem. Phys.* **1993**, 98, 12, 10089.
- 29.** Pettersen, E. F.; Goddard, T. D.; Huang, C. C.; Couch, G. S.; Greenblatt, D. M.; Meng, E. C.; Ferin, T. E. UCSF Chimera - A visualization system for exploratory research and analysis. *J Comput Chem.* **2004**, 25, 13, 1605.
- 30.** Humphrey, W.; Dalke, A.; Schulten, K. VMD - Visual Molecular Dynamics, *J. Molec. Graphics*, **1996**, 14, 33.
- 31.** Lang, P.T.; Moustakas, D.; Brozell, S.; Carrascal, N.; Mukherjee, S.; Pegg, S.; Raha, K.; Shivakumar, D.; Rizzo, R.; Case, D.; Shoichet, B.; Kuntz, I. DOCK 6.1, University of California, San Francisco. <http://dock.compbio.ucsf.edu/> **2007**.
- 32.** Gouda, H.; Kuntz, I. D.; Case, D. A.; Kollman, P. A. *Biopolymers* **2003**, 68, 1, 16.
- 33.** Lee, M. R.; Duan, Y.; Kollman, P. A. *Struct. Funct. Genet.* **2000**, 39, 4, 309.
- 34.** Srinivasan, J.; Cheatham, T. E.; Cieplak, P.; Kollman, P. A.; Case, D. A. *J. Am. Chem. Soc.* **1998**, 120, 37, 9401.
- 35.** Kollman, P. A.; Massova, I.; Reyes, C.; Kuhn, B.; Huo, S. H.; Chong, L.; Lee, M.; Lee, T.; Duan, Y.; Wang, W.; Donini, O.; Cieplak, P.; Srinivasan, J.; Case, D. A. *Acc. Chem. Res.* **2000**, 33, 12, 889.
- 36.** Kuhn, B.; Kollman, P. A. *J. Med. Chem.* **2000**, 43, 20, 3786.
- 37.** Joruslav, K.; Jiri, D.; Emanuel, M.; Jan, B. *Magn. Res. Chem.* **2008**, 46, 5, 399.

5.1 Introduction

It is a general knowledge that the electrophilic addition of halogens to a non-conjugated alkene generate a dihalide with overall *anti* addition.^{1a,b} However It has recently been proposed that the electrophilic addition of halogens to α,β -unsaturated dicarboxylic acid salts yield products with overall *syn* additions² (Scheme 5.1), which had been thought to be proceeded corrected the missinterpatation of the stereochemistry of the product^{3a,b} (Scheme 5.2). The *syn* addition stereochemistry was explained by the existence of an α -lactone intermediate. The existence of α -lactones is undermined despite the fact that they are believed to be intermediates in many transformations. They are involved in the deamination of α -amino acids by nitrous acid and are responsible for the observed retention of configuration in the hydroxy acid products.^{4,5} Since they are so reactive it is expected that they would undergo intramolecular nucleophilic attack in aqueous solution.



Scheme 5.1-5.2 Original interpretations of the results of Tarbell and Bartlett.



Scheme 5.3 The α -lactone interpretation of the results of Tarbell and Bartlett.

In 1968, Kingsbury reported that the reactions of mesaconate and citraconate with aqueous bromine β -lactones and bromohydrin but without any definite clarification of the stereochemistry of products, though he somehow drew one for β -lactone derived from mesaconate. Premier internet to study these reactions but rather to examine the behaviour of α -halo carboxylic acids⁶

The aim of this work is to analyse the products derived from the addition of aqueous bromine to disodium salts of mesaconic and citraconic acids. The analysis by NMR and X-Ray will produce enough results to reveal the stereo and regiochemistry of products and it will ultimately give pavement to propose mechanism for the reactions.

5.2 Materials

5.2.1 Experimental

5.2.1.1 General remarks

NMR spectra were recorded on a Bruker Avance 400 MHz (1 H: 400 MHz and 13 C: 100.6 MHz) spectrometer in the deuterated solvent stated. Mesaconic and Citraconic acids were purchased from Aldrich and used without further purification. All other chemicals used were of analytical grade.

5.3 Method

5.3.1 General procedure for bromination of sodium citraconate and sodium mesaconate

Mesaconic acid or Citraconic acid (2.6 g, 0.02 mol) in 25 mL water was neutralized with sodium hydroxide (1.6 g, 0.04 mol) in 25 mL water and then bromine (3.16 g, 0.02 mol) in 50 mL was added drop-wise into the solution within 30 minutes. During the addition of bromine the flask was covered with aluminium foil. The solution was acidified with sulphuric acid (% 20) and was extracted three times with ethyl acetate. The solvent was evaporated in vacuum, producing a liquor (4.31 g from mesaconic reaction and 4.18 g from citraconic reaction). They are soluble in water, ethyl acetate, acetone, slightly soluble in chloroform, dichloromethane, petroleum ether and toluene. The presence of chloroform and dichloromethane interferes with crystallization of the lactones, and the best crystallized from petroleum ether for bromohydrines and dibromide.

Threo lactone (12): (m.p.=55-56 °C) ^1H NMR; δ [400 MHz, $(\text{CD}_3)_2\text{CO}$, δ ppm) 1.54 (s, 3H, CH_3), 4.82 (s, H) ^{13}C NMR δ [100 MHz, $(\text{CD}_3)_2\text{CO}$, δ ppm] 24.7 (CH_3), 51.73 (C-Br), 75.339 (C-O), 170.565 (C=O), 173.39 (C=O).

Erythro Bromohydrine (15): (m.p.=151-152 °C) ^1H NMR; δ [400 MHz , $(\text{CD}_3)_2\text{CO}$, δ ppm) 1.93 (s, 3H), 5.73 (s, H), ^{13}C NMR δ [100 MHz, $(\text{CD}_3)_2\text{CO}$, δ ppm] 21.13 (CH_3) 48.47 (C-Br), 81.737 (C-O), 164.114 (C=O), 168.752 (C=O).

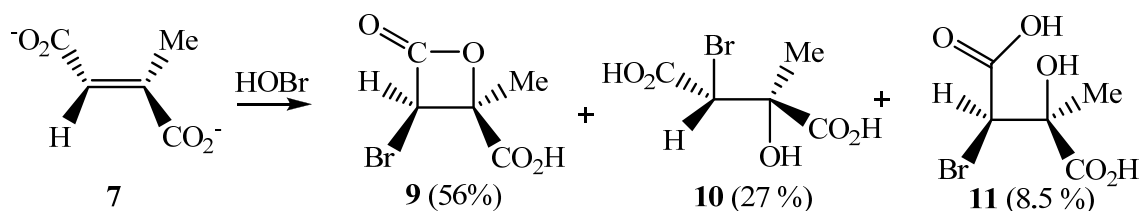
Erythro Lactone (11): (from citraconate) (m.p.=90-91 °C) ^1H NMR; δ [400 MHz , $(\text{CD}_3)_2\text{CO}$, δ ppm) 1.84 (s, 3H, CH_3), 6.04 (s, H) ^{13}C NMR δ [100 MHz, $(\text{CD}_3)_2\text{CO}$, δ ppm] 20.89 (CH_3), 50.058 (C-Br), 78.734 (C-O), 164.313 (C=O), 169.313 (s,C=O).

Threo Bromohydrine (13) : (from citraconate) (m.p.=151-152 °C) ^1H NMR; δ [400 MHz , $(\text{CD}_3)_2\text{CO}$, δ ppm) 1.64 (s, 3H), 4.70 (s, H); ^{13}C NMR δ [100 MHz, $(\text{CD}_3)_2\text{CO}$, δ ppm] 23.528 (CH_3) 52.497 (C-Br), 75.613 (C-O), 168.521 (C=O), 173.742 (C=O).

Threo Dibromide (14): (m.p.=151-152 °C) ^1H NMR; δ [400 MHz , $(\text{CD}_3)_2\text{CO}$, δ ppm) 5.11 (s, H), 2.20(s, 3H); ^{13}C NMR δ [100 MHz, $(\text{CD}_3)_2\text{CO}$, δ ppm] 23.34 (CH_3) 53.85 (C-Br), 60.20 (C-Br) 169.29 (C=O), 169.93 (C=O).

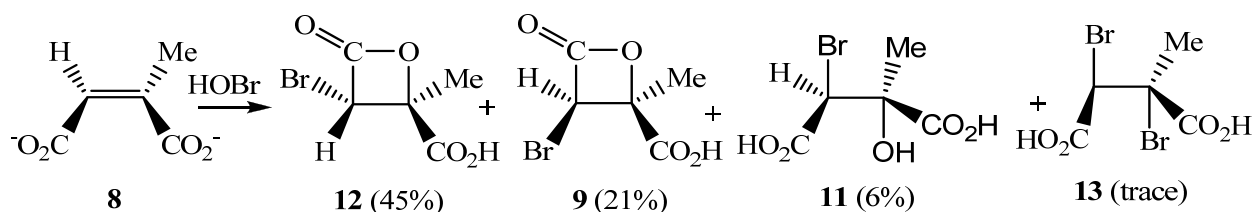
5.4 Results and Discussion

The product analysis of addition of aqueous bromine to disodium salts of mesaconic (7) and citraconic (8) acids by NMR and x-ray are summarized in Schemes 5.4 and 5.5. The yields are based on the ^1H NMR signals of each component present in the corresponding residue obtained after evaporating the organic solvent following the extraction. All products were isolated by fractional crystallization and characterized by x-ray as presented in Figures 5.6.1-5.6.5 and Tables 5.7.1-5.7.20. NMR spectra show that mesaconate (7) affords *threo* β -lactone (9) and *threo* bromohydrin (10) with overall *syn* addition and also *erythro* bromohydrin (11) with overall *anti* addition. The addition reaction of citraconate yields *erythro* β -lactone (12) with overall *syn* addition and *threo* bromohydrin, with overall *anti* addition and also *threo* β -lactone (9) with overall *anti* addition. A trace amount of the 2,3 dibromoacid (13) was isolated from the residue of the reaction of citraconate, which was hardly spotted by NMR. The formation of β -lactones from both reactions with overall *syn* addition are expected and can be rationalized by suggesting that the reactions proceed via an α -lactone intermediate to similar mechanism which is previously proposed² as illustrated in Schemes 5.5 and 5.6. The formation of α -lactone from the halonium ion is preferred over β -lactone since both individual steps, the formation of the α -lactone from the bromonium ion, followed by formation of the β -lactone, are favoured *exo* processes in the Baldwin sense.¹⁵



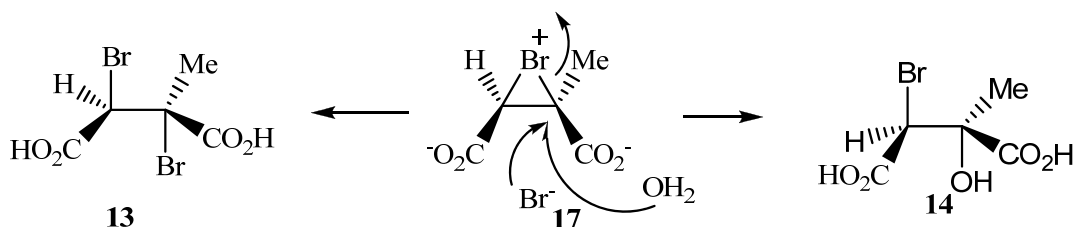
Scheme 5.4 Products of reaction of citraconate with aqueous bromide and their yield.

The yield of **12** was totally dependent on the work-up period.

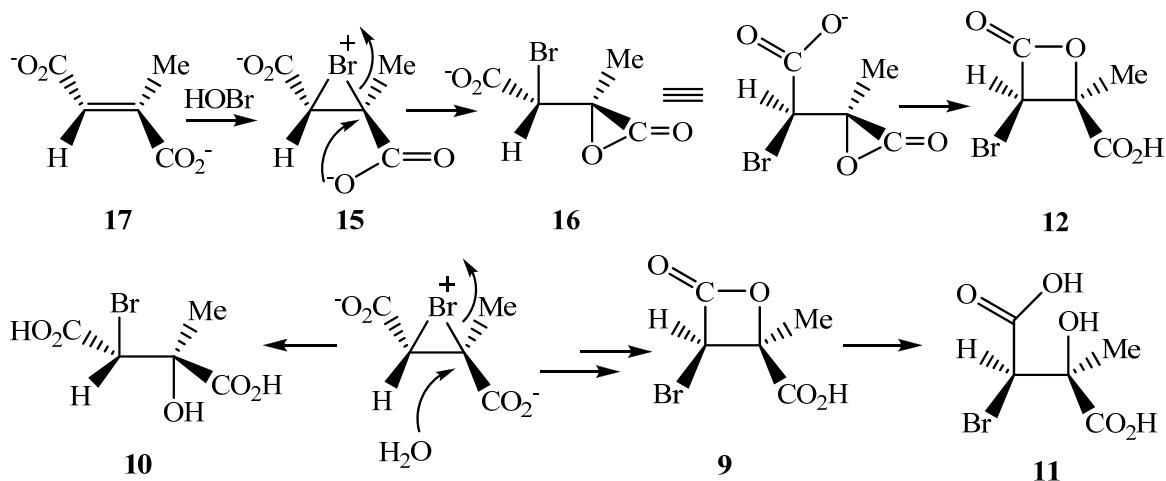


Scheme 5.5 Products of reaction of mesaconate with aqueous bromide and their yield.

The formation of the former is possibly due to intermolecular attack of water at halonium ion intermediate as illustrated in Scheme 5.6 and the later is probably driven from the hydrolysis of threo β -lactone as previously proposed. The formation of threo bromohydrin (**14**) and threo dibromide species is can be similarly ascribed to the intermolecular nucleophilic attack of water and dibromide at the halonium intermediate, resulted in overall anti addition as shown in Scheme 5.6.



Scheme 5.6 Possible mechanisms for the formation of the products from citraconate **9** in Scheme 5.5.

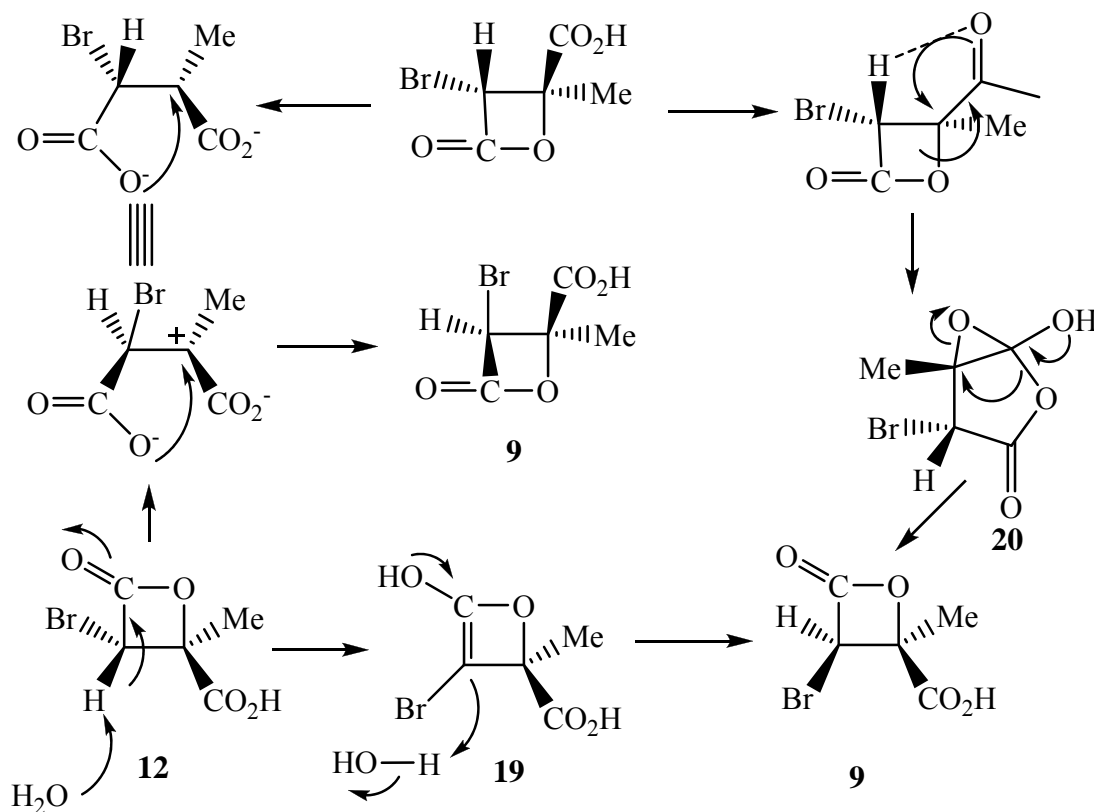


Scheme 5.7 Possible mechanisms for the formation of the products from mesaconate 7.

There is a puzzling and equally interesting question regarding the origin of the *threo* β -lactone **9** derived from the addition reaction of aqueous bromine to citraconate, which has the stereochemistry with overall *anti* addition and it is the major product from the addition reaction of aqueous bromine to mesaconate with overall *syn* addition. There are few mechanisms that may be accounted for the product. By taking it for granted that this intermediate is formed a “carbocation-like halonium” intermediate **18** obtained from the addition of bromine and hence followed by the intramolecular attack of carboxylate to form the *threo* β -lactone **9** (Scheme 5.8). There should be a driving thermodynamic force for this to happen in other words there should be an energy difference between *threo* β -lactone **9**. The coordinates taken from x-ray structures of two lactones were optimized at B3LYP/6-31+g(d) level of theory in vacuum showed that there is no much energy difference between two lactones to be accounted for the conversion. In deed it was found that *erythro* β -lactone **12** (-3066.1781957 Hartree) was slightly more stable than *threo* β -lactone **9** (-3066.1766565 Hartree). The other observation found in this work was the reaction of mesaconic and citraconic acids with aqueous bromine. Both reactions

produced similar product composition compared to corresponding reactions of this salts form. In advance, it should be mentioned that threo β -lactone, is formed by the rearrangement of erythro β -lactone **12**. The Lactone was dissolved in D_2O and monitored by NMR and hence found that **12** is rearranged to **9** very slowly. However the presence of acid or base this process is accelerated very fast. The conversion of the kinetic product *erythro* lactone **12** to the thermodynamic *threo* lactone **12** via the abstraction of hydrogen in $-CHBr-$ to form the intermediate **19** is the another possibility to account for the formation of the lactone **9** from **12**.

As just mentioned above when **12** is dissolved in D_2O it was found that it is slowly converted to **9**. If the mechanism is to be held responsible for this rearrangement then the one should observed isotope exchange in the product. Unfortunately this was not observed. Unless the intermolecular interaction of carbonyl with hydrogen as driving force to be accepted for the rearrangement, again the thermodynamics stability can not be kept responsible for the conversion and therefore this mechanism might be ruled out. The other possible mechanism which may still involve the role of the intermolecular assistance of carbonyl hydrogen interaction favouring the attack at carbonyl γ -lactone with inversion of the stereochemistry at C-Me followed by rearrangement to give threo β -lactone **9**.



Scheme 5.8 Possible mechanisms for the formation of *threo* β -lactone **9** from citraconate **8**.

Another surprising result observed in the addition reactions of aqueous bromine to **7** and **8** is the regioselectivity of the reactions. It was found that all products derived from **7** and **8** have the regioselectivity to form MeC-Nu bond, meaning that nucleophilic attack in the halonium intermediates (**5** and **7**) occurs at carbon bearing methyl group rather at the one bearing hydrogen.

If the free carboxylate is a driving force for the formation of α -lactone intermediate. A significant outcome was obtained from the product analysis by NMR. They show that reactions of aqueous bromine with citraconic and mesaconic acids give products with a similar compositions to those obtained from the reactions of salts.

5.5 Conclusion

It was quite interesting to find out that the addition of aqueous bromine to mesaconic and citraconic acids give similar product composition to these corresponding salts. It is generally accepted that carboxylate groups are the main driving force for the α -lactone mechanism and thus the overall *syn* addition.

5.6 Figures

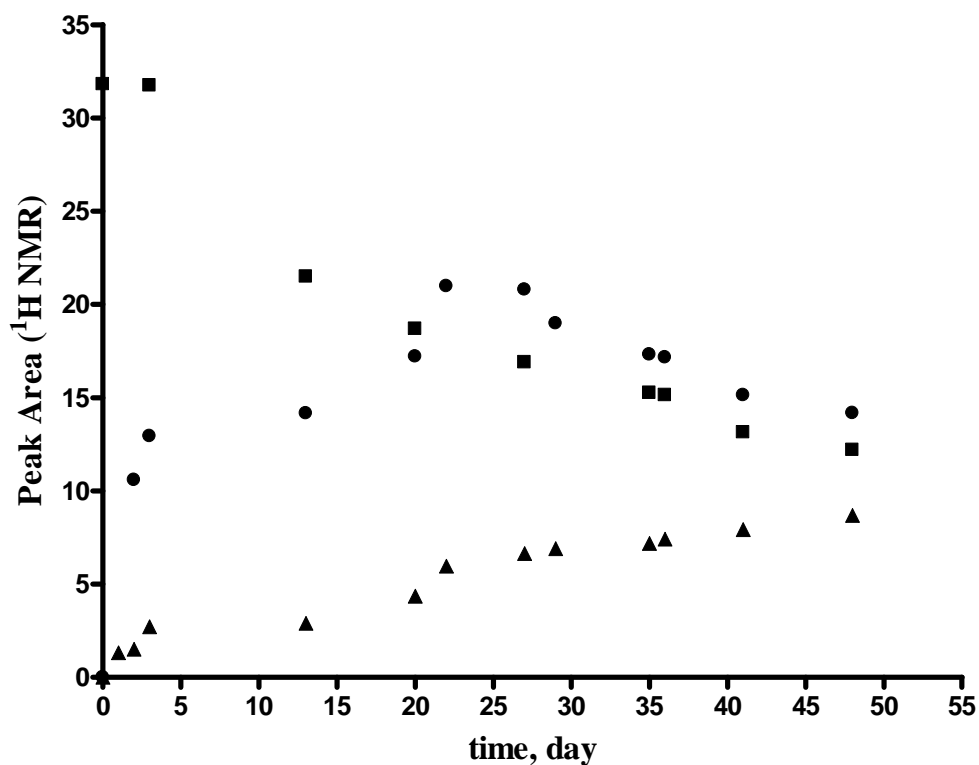


Figure 5.6.1 Time dependence ratio of ¹H NMR peaks of a solution largely involving citranonic lactone at the beginning in acetone-d₆ (the squares represents CL, circles the intermediate and semi-diamond represents ML)

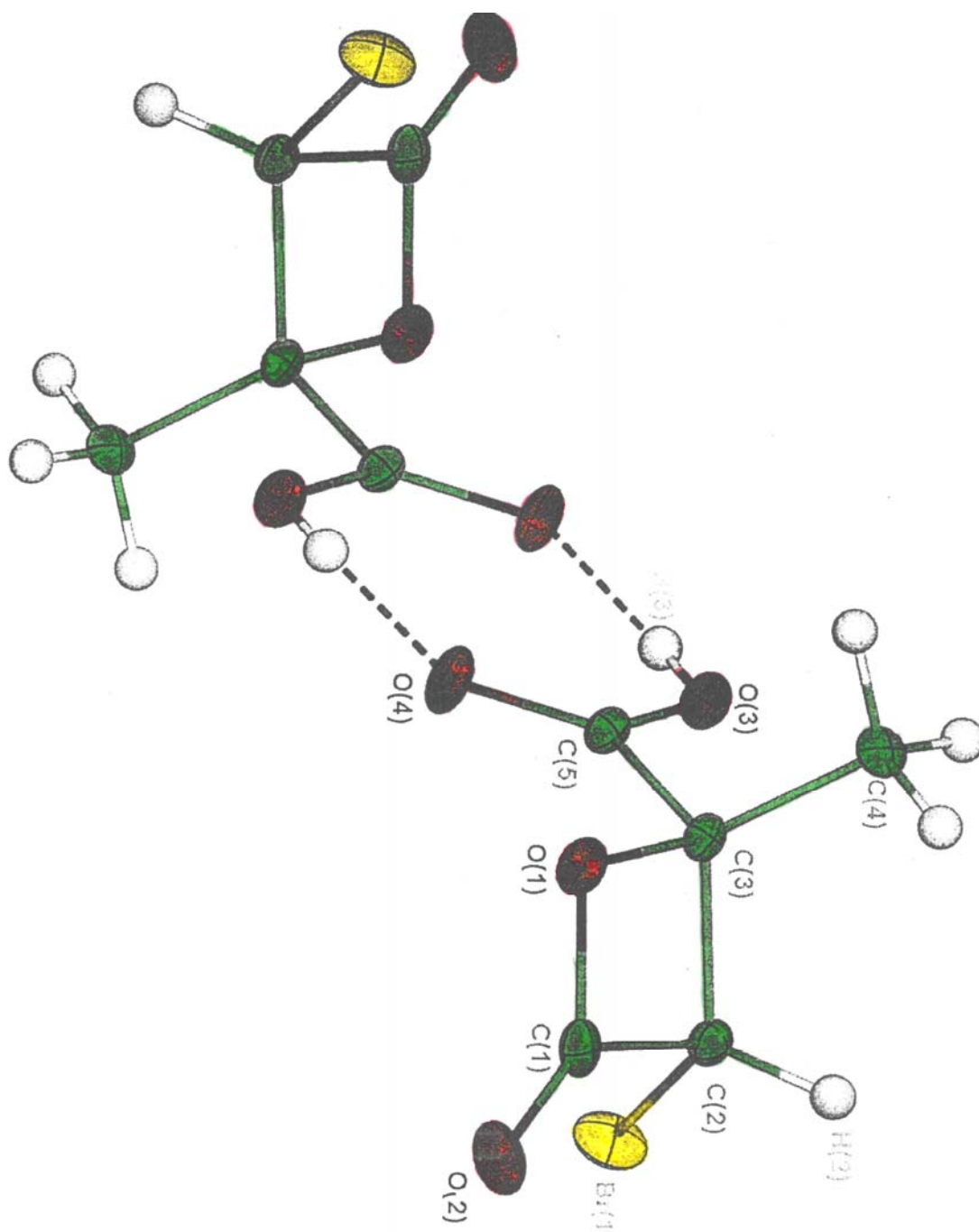


Figure 5.6.2. X-Ray crystallographic structures for *threo* bromo- β -lactone **9**.

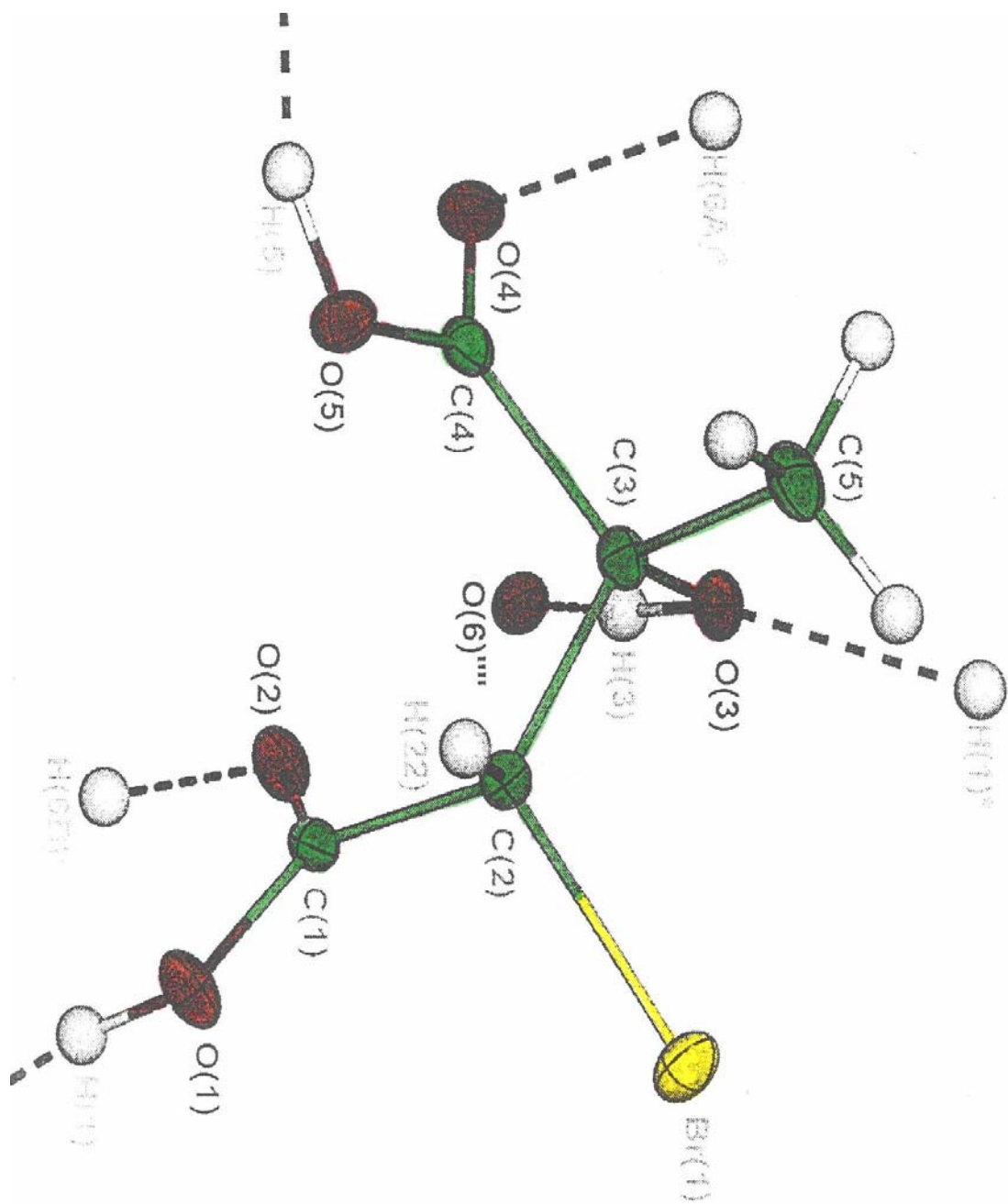


Figure 5.6.3. X-Ray crystallographic structures for *erythro* bromohydrin **10**.

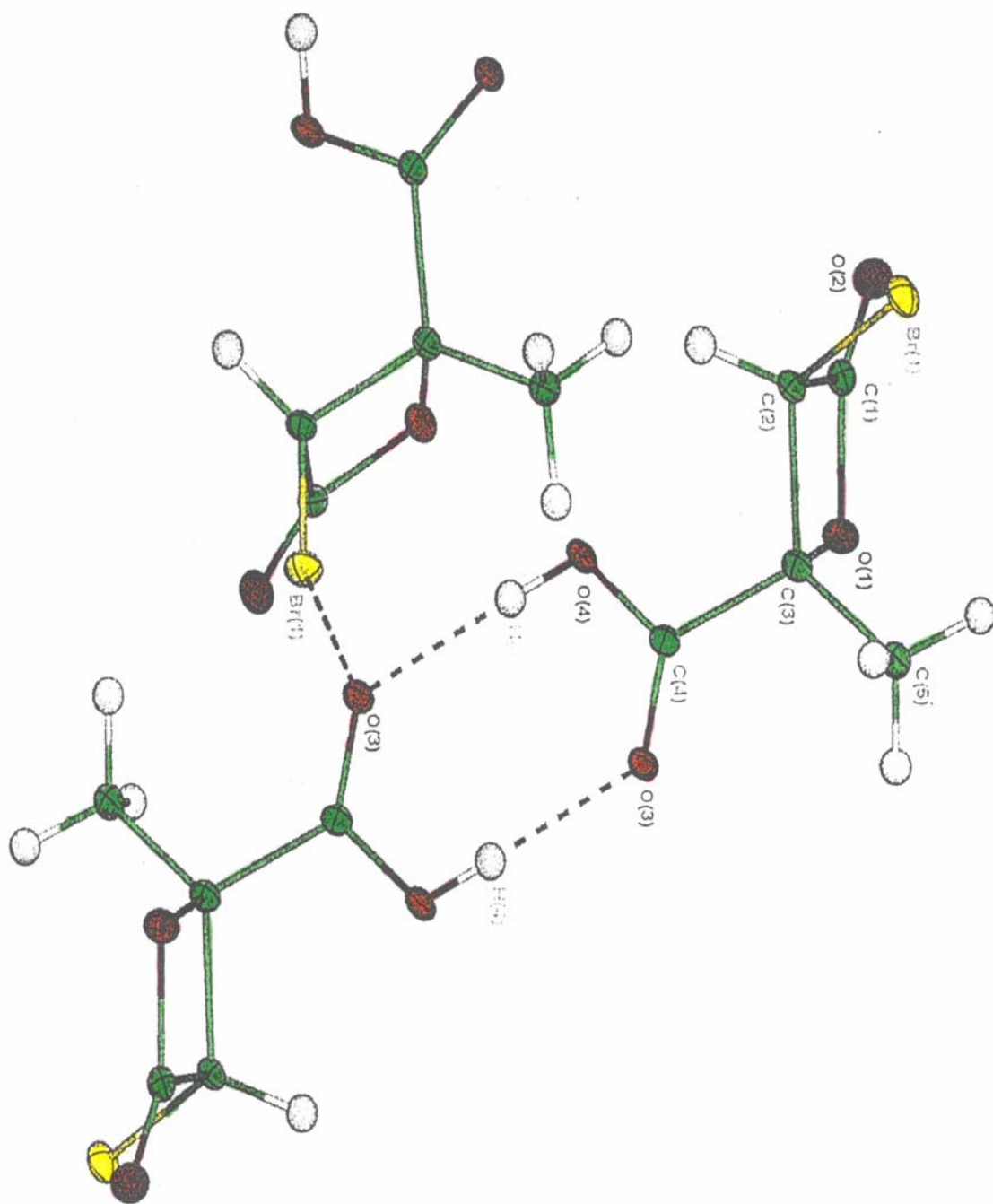


Figure 5.6.4. X-Ray crystallographic structures for *erythro* bromo- β -lactone **12**.

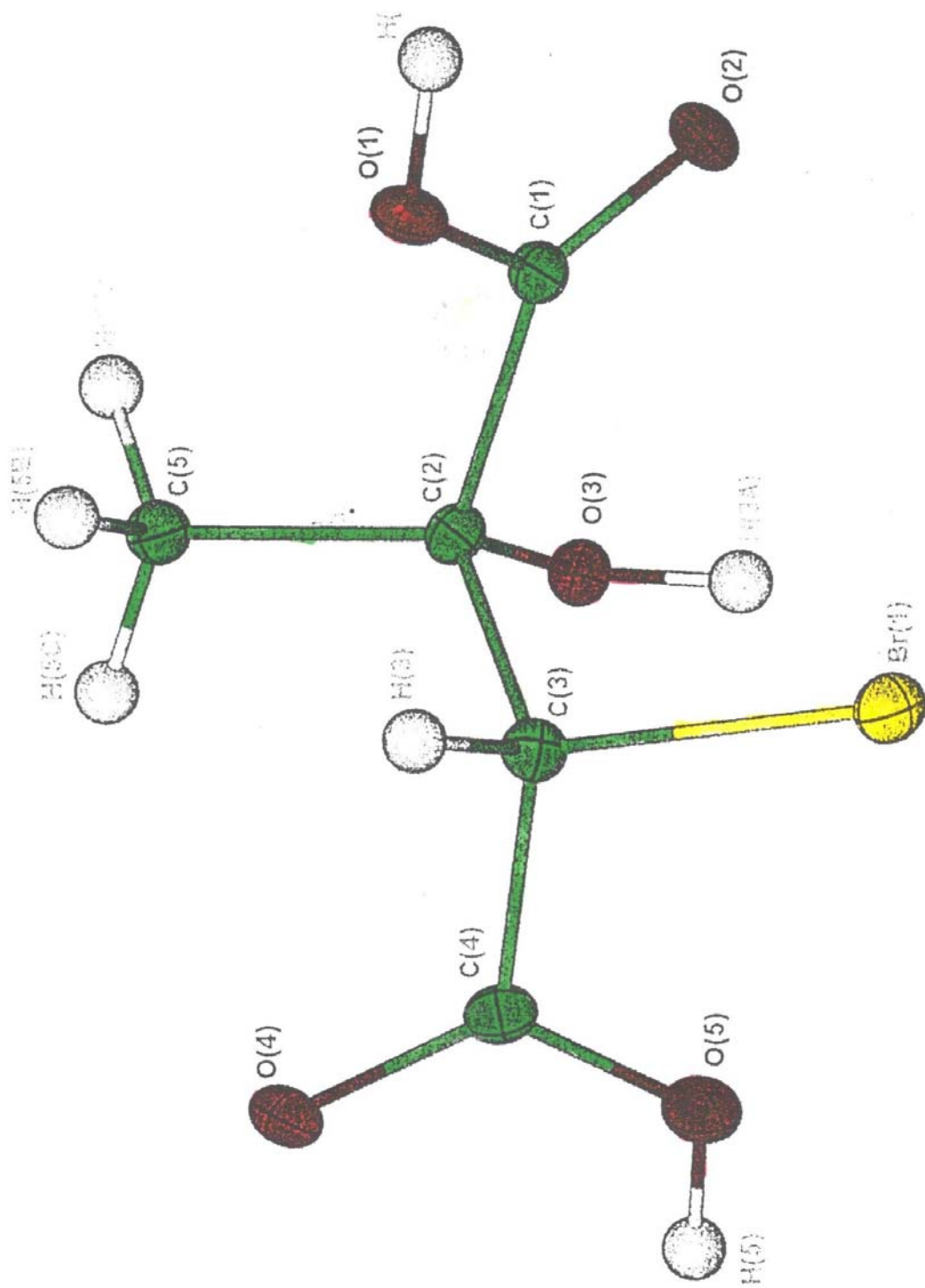


Figure 5.6.5. X-Ray crystallographic structures for *threo* bromohidrin 11.

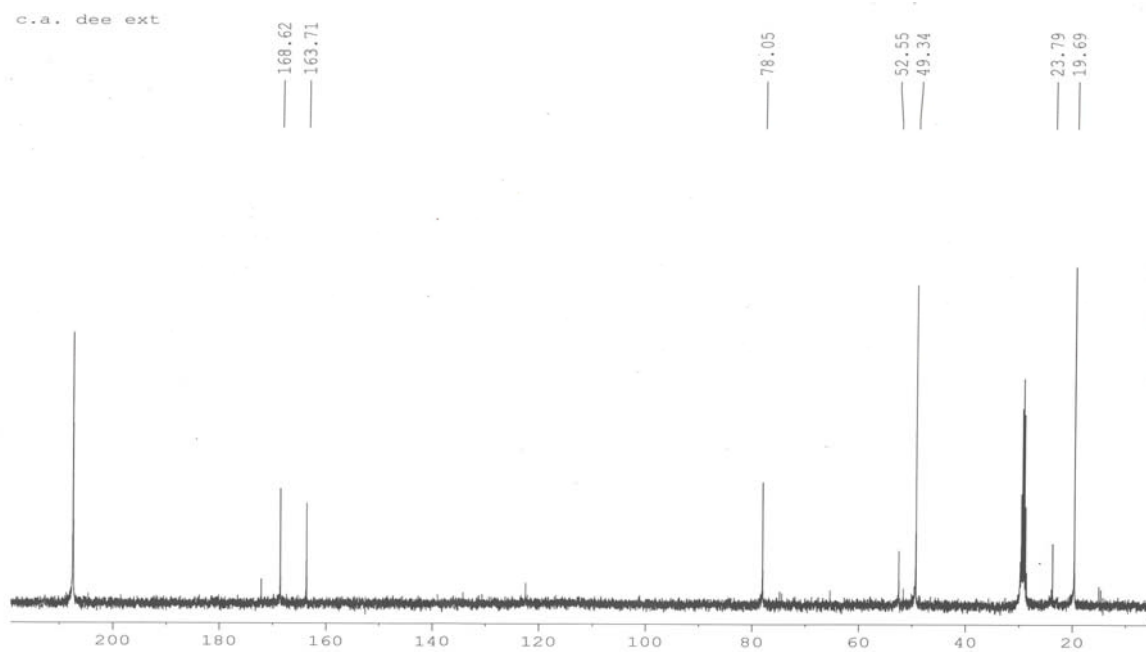


Figure 5.6.6. ^{13}C NMR spectrum of the residue from the reaction of citraconate **8** with aqueous bromine in the first day of the extraction.

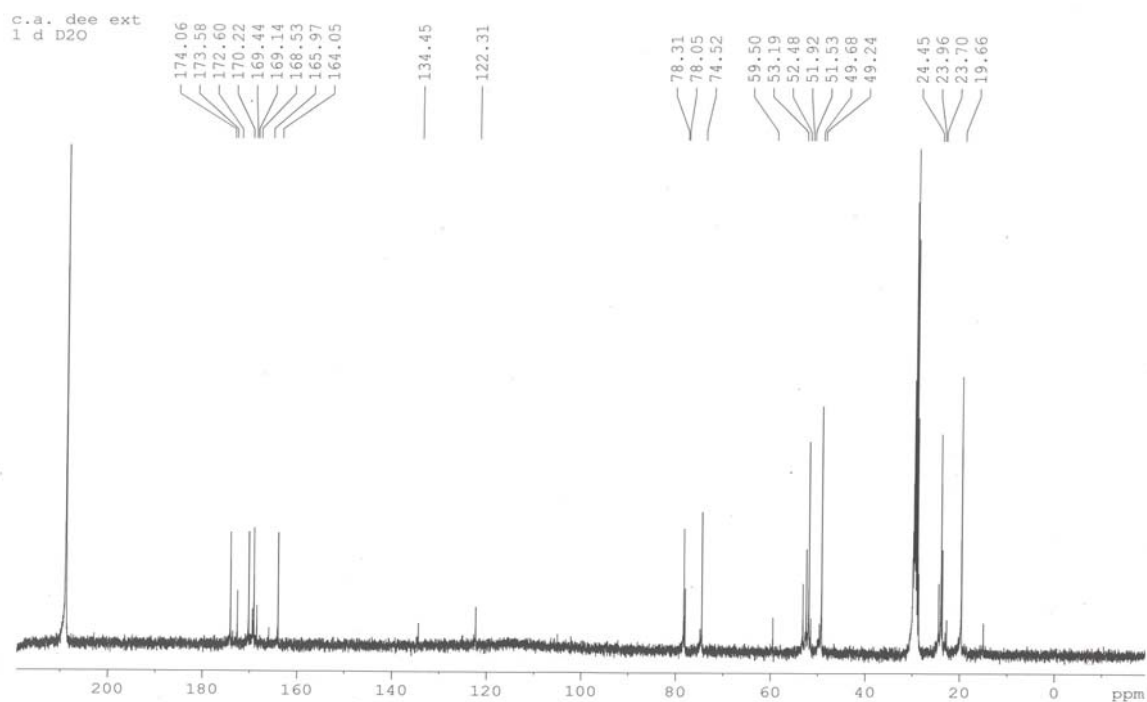


Figure 5.6.7. ^{13}C NMR spectrum of the residue from the reaction of citraconate **8** with aqueous bromine in the sixtieth day of the extraction.

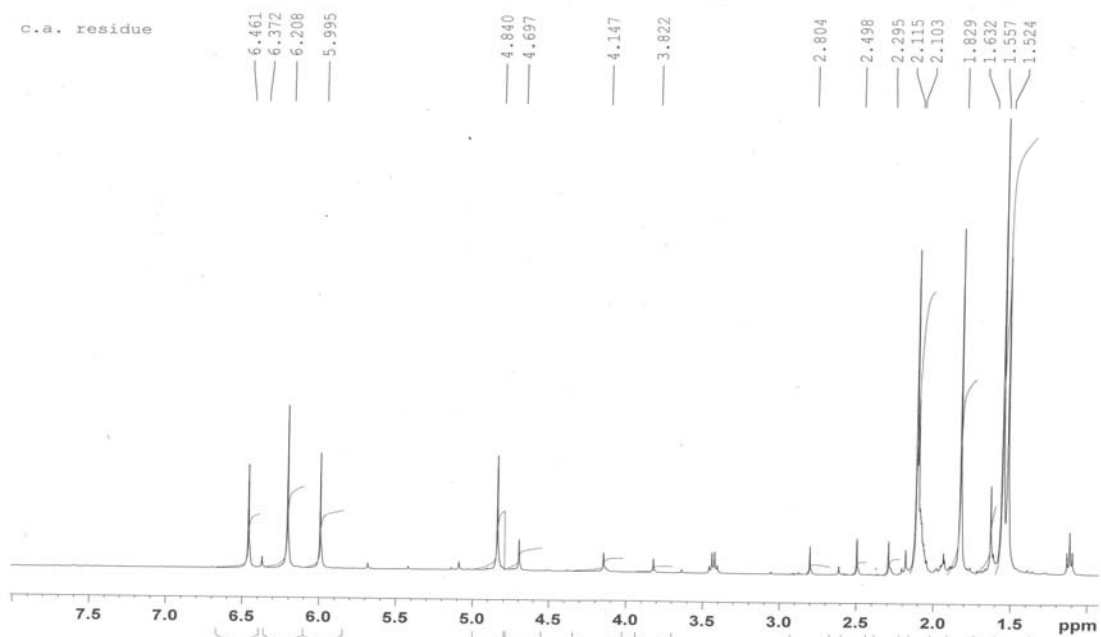


Figure 5.6.8. ^1H NMR spectrum of the residue from the reaction of citraconate **8** with aqueous bromine with a workup period of 30 minutes.

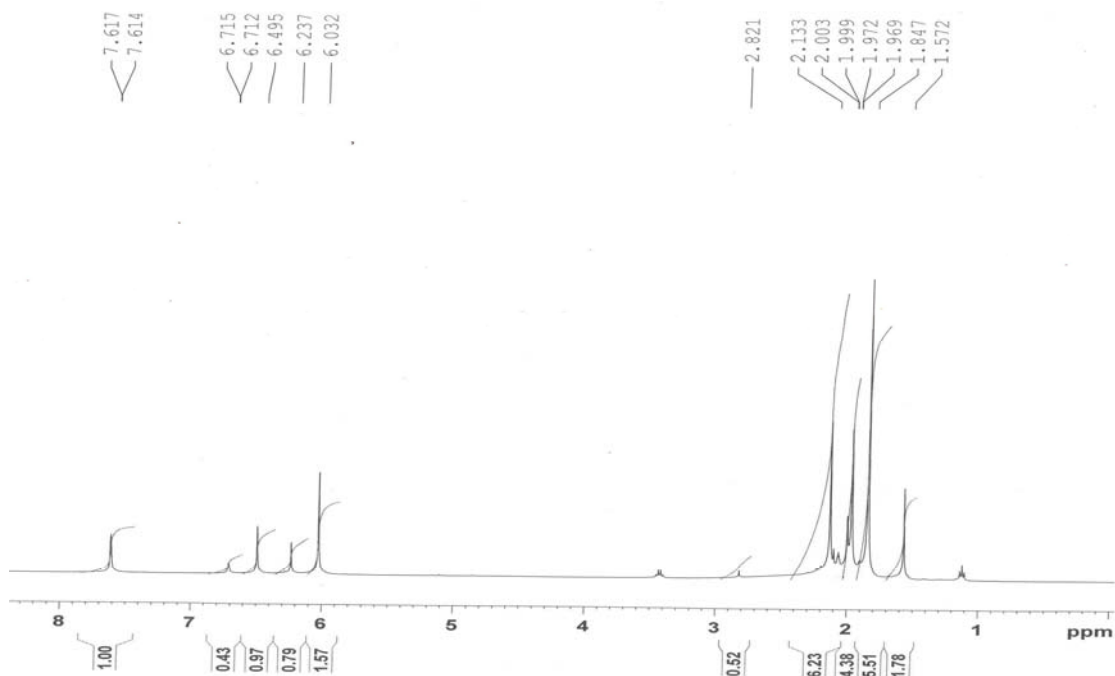


Figure 5.6.9. ^1H NMR spectrum of the residue from the reaction of citraconate **8** with aqueous bromine with a workup period of 15 minutes.

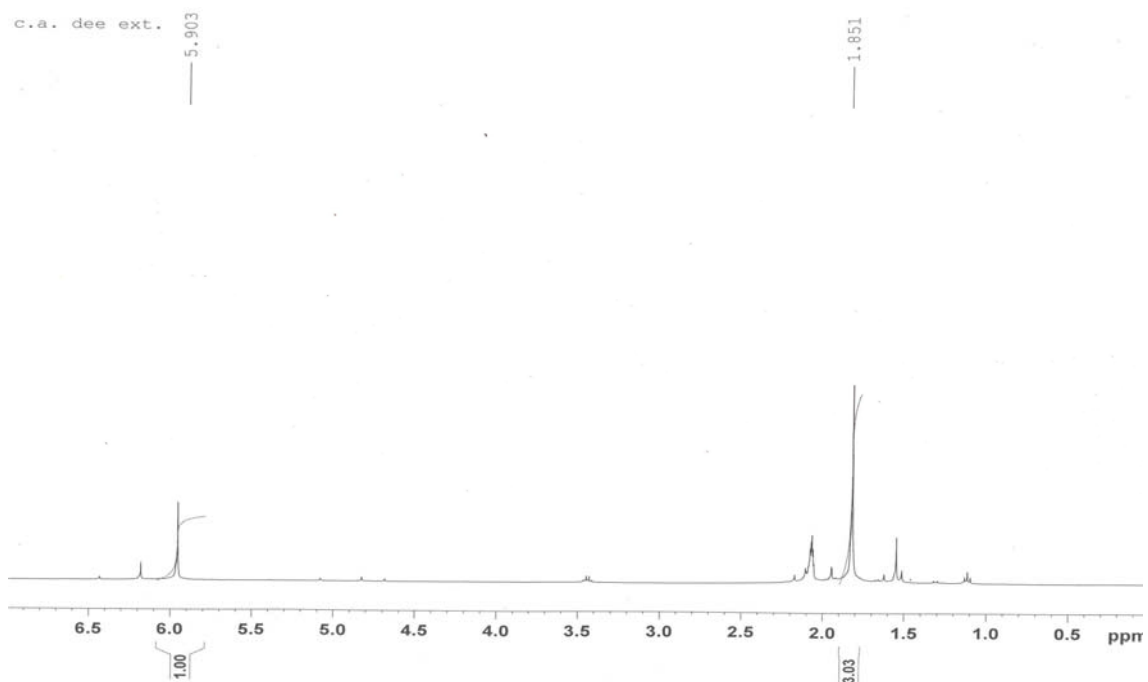


Figure 5.6.10. ^1H NMR spectrum of *threo* bromo β -lactone **12** from the reaction of citraconate **9** with aqueous bromine.

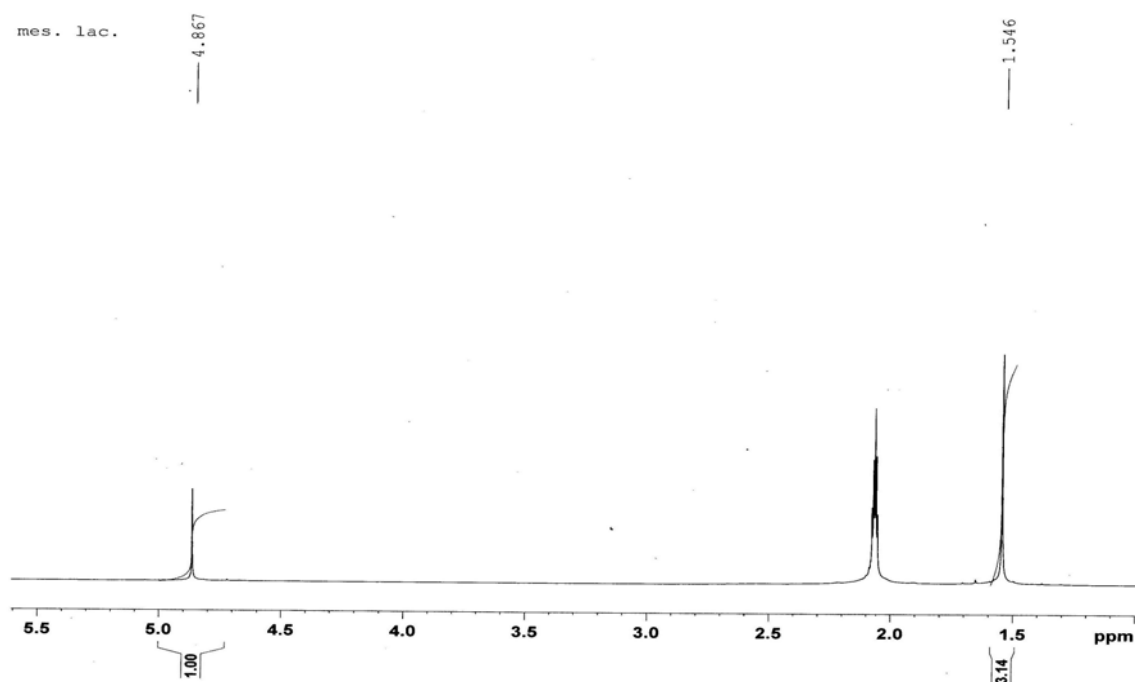


Figure 5.6.11. ^1H NMR spectrum of *erythro* bromo β -lactone **9** from the reaction of citraconate **8** with aqueous bromine.

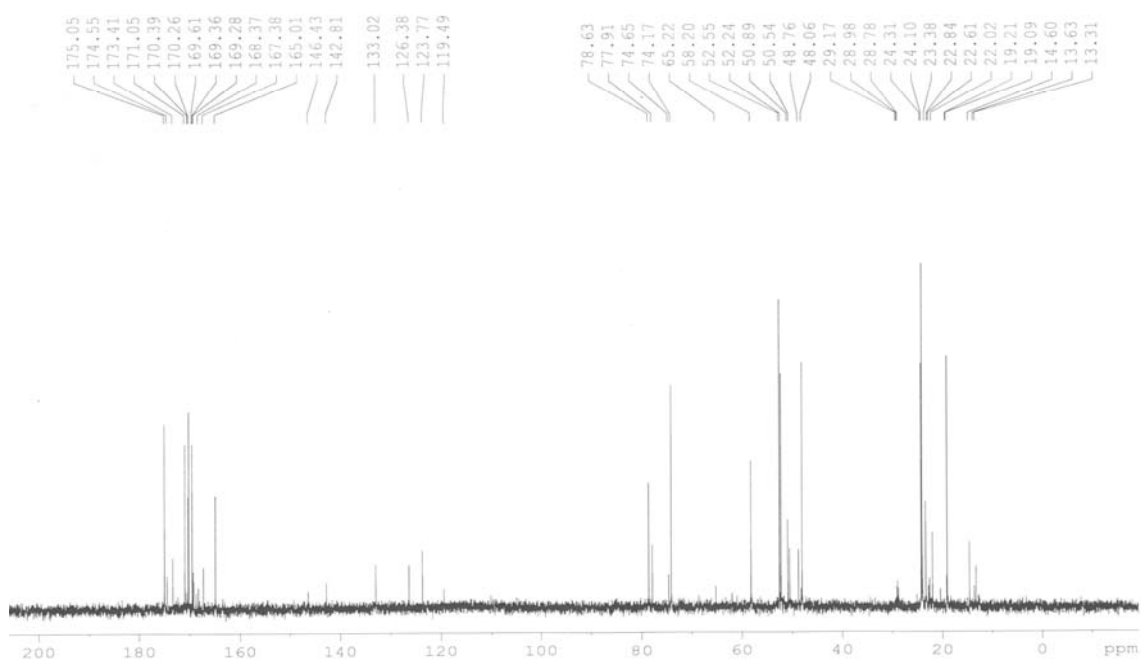


Figure 5.6.12. ^{13}C NMR spectrum of residue from the reaction of citraconic acid with aqueous bromine.

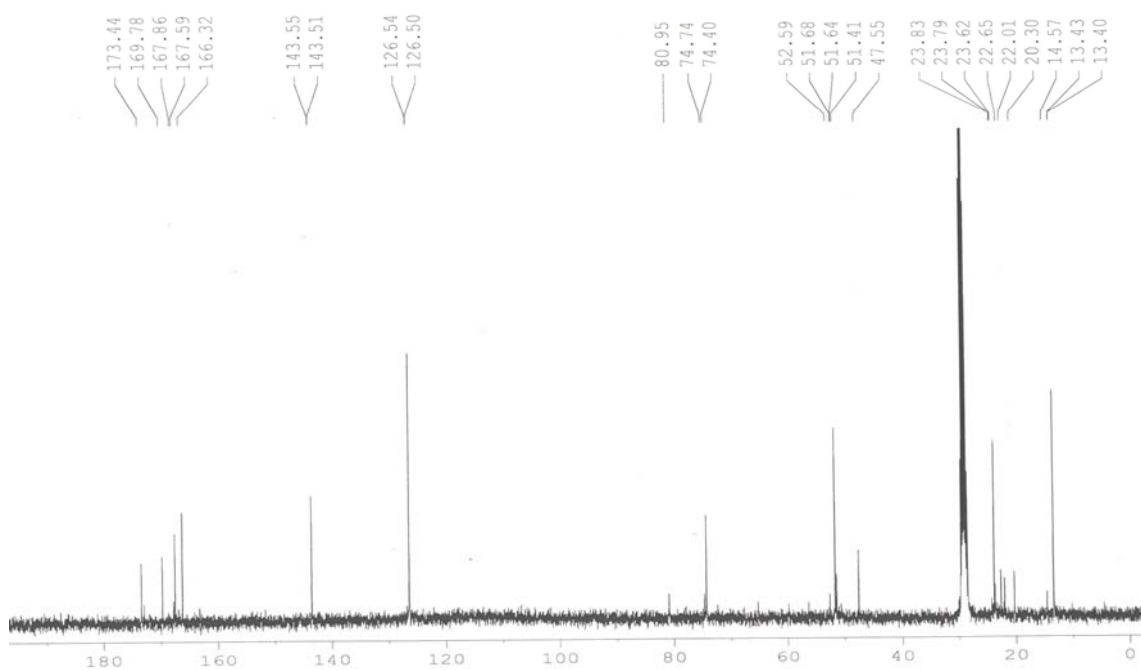


Figure 5.6.13. ^{13}C NMR spectrum of residue from the reaction of mesaconic acid with aqueous bromine.

5.7 References

1. a) Edenborough, M. *Writing Organic Reaction Mechanism, A practical Guide*, Taylor & Francis, **1994**. b) *Perspectives in Structure and Mechanism in Organic Chemistry*, Brooks/Cole, **1998**.
2. Pirinçioğlu, N.; Robinson, J. J.; Mahon, M. F.; Buchanan, J. G.; Williams, I. H., *Org. Biomol. Chem.* **2007**, *5*, 4001.
3. Tarbell, D. S.; Bartlett, P. D. *J. Am. Chem. Soc.* **1937**, *59*, 407. 2. Roberts, I.; a) Winstein, S.; Lucas, H. J. *J. Am. Chem. Soc.* **1939**, *61*, 1576. (b) Gould, E. S. *Mechanism and structure in Organic Chemistry* Holt, Rinehart and Winston: New York, **1959**, 611.
4. Kimball, G. E. *J. Am. Chem. Soc.* **1937**, *59*, 947.
5. Alt, G. H.; Barton, D. H. R. *J. Chem. Soc.*, **1954**, 4284.
6. Kingsbury, C. A. *J. Org. Chem.* **1968**, *33*, 3247. 7. Buchanan, J. G.; Sable, H. Z., *Selective Organic Transformations*; Thyagarajan, B. S., Ed.; Wiley: New York, **1972**, *12*, 1.
8. Tamelen, V. E. E.; Shamma, M. *J. Am. Chem. Soc.*, **1954**, *76*, 2315.
9. a) Winstein, S.; Lucas, H. J. *J. Am. Chem. Soc.* **1939**, *61*, 1576. b) Gould, E. Holt, Rinehart and Winston: *S. Mechanism and Structure in Organic Chemistry*; New York, 1959, 611. (c) Hine, *J. Phys. Org. Chem., McGraw-Hill*: **1962**, 217.
10. Dowle, M. D.; Davies, D. I. *Chem. Soc. Rev.* **1979**, 171.
(a) Brown, R. S. *Acc. Chem. Res.* **1997**, *30*, 131. b) Lenoir, D.; Chiappe, C. *Chem. Eur. J.* **2003**, *9*, 1037.
11. a) De La Mare, P. B. D.; Bolton, R. *Electrophilic Additions to unsaturated systems, 2nd Ed.*; Elsevier: New York, **1982**. (b) Fahey, R.C. *Topics Stereochem.*

1968, 3, 237. Harding, K. E.; Tiner, T. H., *Comprehensive Organic Synthesis*; Trost, B. M., Ed.; Pergamon: Oxford, **1991**, 4, 363.

12. Eliel, E. L.; Haber, R. G. *J. Org. Chem.* **1959**, 24, 143.

13. a) Robinson, J. J.; Buchanan, J. G.; Charlton, M. H.; Kinsman, R. G.; Mahon, M. F.; Williams, I. H. *J. Chem. Soc., Chem. Commun.* **2001**, 485. (b) Buchanan, J. G.; Charlton, M. H.; Mahon, M. F.; Robinson, J. J.; Ruggiero, G. D.; Williams, I. H. *J. Phys. Org. Chem.* **2002**, 15, 642.

14. Rodriguez, C. F.; Williams, I. H. *J. Chem. Soc. Perkin Trans.*, **1997**, 959.

15. Baldwin, J. E. *J. Chem. Soc., Chem. Commun.* **1976**, 736.

16. a) Buchanan, J. G.; Edgar, A. R., *Carbohydr. Res.* **1969**, 10, 295. b) Mills, J. A. *Adv. Carbohydr. Chem.* **1955**, 10, 1.

17. Danishefsky S.; Dynak, J.; Hatch, E.; Yamamoto, M.; *J. Am. Chem. Soc.* **1974**, 96, 1256.

18. Stork, G.; Cohen, J. *J. Am. Chem. Soc.* **1974**, 96, 5270.

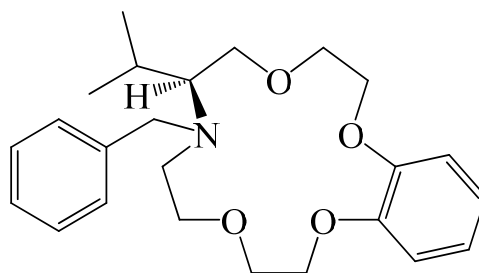
19. a) Barnett, W. E.; Sohn, W. H. *J. Chem. Soc., Chem Commun.* **1972**, 472. Barnett, W. E., Sohn, W. H. *Tetrahedron Lett.* **1972**, 1777-1780. (c) Barnett, W. E.; Needham, L. L. *J. Org. Chem.* **1975**, 40, 2843.

20. a) Holbert, G. W.; Weiss, L. B.; Ganem, B. *Tetrahedron Lett.* 1976, 4435. b) Ganem, B.; Holbert, G. W.; Weiss, L. B.; Ishizumi, I. *J. Am. Chem. Soc.*, **1978**, 100, 6483.

6.1 Introduction

Molecular recognition and thus chiral discrimination is one of the greatest challenges presented to science by nature. Therefore, studying this phenomenon is one of the most outstanding subjects of current research. However, there are still many questions to be answered in the field since it is a very difficult task to study directly the main forces behind this process in nature. So scientists have been employing models to understand insight the subject.¹ Chiral recognition is one of the most important issues in the field and greatdeal of models have been developed² and a quite large of chiral crown ether, have been employed fort he proposes.³ However, despite significant advances in modelling techniques and the comparative simplicity of host-guest systems, there is still a need to understand the molecular recognition at atomic level and to interpret experimental data by using computational tools and ultimately to help the design of new hosts for targeted molecular guests.

Molecular dynamics (MD) is one of the current methods used in the understanding of molecular recognition process occurred in organisms at atomic level, and consequently free energy calculation have become a powerful tool in estimating quantitative degree of molecular interactions in host-guest chemistry. The method has been developed for the biological systems but it has been used in supramolecular systems of organic structures.² Molecular mechanics/Poisson-Boltzmann surface area has successfully been employed in predicting the binding free energy of the complexes of macromolecules.³



1

The study involves the investigation of the complexation and discrimination ability, and hence the model binding of chiral crown ether **1** for methyl esters of alanine and valine salts. The host was previously proposed and used in literature.⁴ ¹H NMR was used to calculate the binding constants and thus the enantiomeric discrimination of the host against base pairs. Molecular dynamic and quantum mechanic computation was employed to predict the mode of complexation and the main driving forces in the discrimination. MM/PBSA was used to predict the free energy of the complexes. Theoretical data produced comparable results with those obtained by ¹H NMR.

6.2 Material and Method

All substrates and deuterated NMR solvents were obtained from commercial suppliers and used without further purification. The host **1** was a gift from Dr. Y. Turgut. Spectra were recorded on BRUKER 400 MHz NMR spectrometer at 300 K at ambient probe temperature and calibrated using tetramethylsilane as an internal reference. Graphpad PRISM software 4 version is used for non-linear curve fitting to obtain binding constants. Data were fitted to Eq. 6.2, derived from Eq. 6.1, where K_a is the dissociation constant.



$$\Delta\delta = \Delta\delta_{\text{max}} / (K_a + [\text{Guest}]_0) \quad (6.2)$$

6.3 Experimental Section

6.3.1 NMR Titration: A range of stock solution of guest ($0\text{-}10^{-4}$ M) containing constant amount of host (10^{-3} M) in chloroform-*d*1 was prepared and their ^1H NMR spectra (16 scans, sweep width of 20.7 ppm, digital resolution of 18, pulse angle of 30° , delay time of 1 sec) were collected at 300 K at ambient probe temperature and calibrated using tetramethylsilane as an internal reference. The changes in the chemical shift of methyl group of isopropyl in the host against the concentration of guests were fitted to Eq 6.1 derived from 6.2 and thus from non-linear curve fitting the binding constants for each enantiomer were calculated.

6.3.2 Computational Section

6.3.2.1 Molecular Dynamics Simulations: Molecular dynamics (MD) simulations were carried out in a Linux-Cluster system to determine conformations for the each crown ether complex studied. All simulations were conducted by using AMBER (version 9.0)⁵ suit of programs. These MD experiments were supplemented by ONIOM computations determined at the B3LYP/6-31+g(d) level for the guests and at AM1 level for the host by Gaussian 03.⁶

The host and ligands were designed by GaussView 3.09, followed by optimization with Gaussian 03 using semi-empirical AM1 method. AM1-Bcc (Austin model with Bond and charge correction)⁷ atomic partial charges for the host and guests were determined by antechamber module of AMBER (v9) package.

Charges for the ionizable residues were set at a neutral *pH*. The complex was solvated in a CHCl₃⁸ chloroform box with dimensions of 10 Å from the solute. 0.4 Å space was initially generated at the boundary of the complex and the solvent molecules during the solvation process. Cl⁻ anions were added to neutralized each complex system. The General AMBER Force Field (GAFF)⁹ was adopted in simulation because it handles small organic molecules.

The entire system was relaxed in four steps over a period of 160 ps. The system was then heated from 0 to 300 K in 100 ps and allowed to equilibration at 300 K for an other 100 ps of MD. Subsequently, MD computations were performed at through 30 ns and 2 fs of time interval was used for each iteration in all MD studies. The Particle Mesh Ewald (PME) method¹⁰ was applied to calculate long-range electrostatics interactions. The SHAKE¹¹ method was applied to constrain all of the covalent bonds involving hydrogen atoms.

To compare bound and unbound structures, additional MD simulations were performed for the host. Root-mean-square deviation (RMSD) analysis for the complex system was carried out on the trajectories by the ptraj module of AMBER (v9). Three dimensional structures were displayed using by Chimera (UCSF)¹² and VMD¹³ and RMSD graphics are shown by XMGRACE package program.

6.3.2.2 Docking Study (Molecular Docking)

In this study, dock calculations were performed to accommodate the guests within the host 1. The docking studies of the guests were carried out using the crown ether and guests parameters obtained for the minimized structures of the complexes

between the host and guests. The initial coordinates of the crown ether and guests for the docking studies were obtained via MD studies for 3 ns for the host and the 1 ns for the guests. Docking of the guests was carried out using program DOCK 6.0.¹⁴ Docking was performed with default settings to obtain a population of possible conformations and orientations for the guests at the binding site. Spheres around the centre of the binding pocket was defined as binding pocket for the docking runs. All torsion angles in each compound were allowed to rotate freely. Docking results suggested that several of these derivatives are active host with a significant preference for binding position.

6.3.2.3 MM/PBSA Calculations: This study applies a second-generation form of the Mining Minima^{15,16} algorithm, termed M2, to analyze the binding reactions of host-guest complexes in an organic solvent. The MM-PB/SA module of AMBER (v9) was applied to compute the binding free energy (ΔG_{bind}) of each complex using the MM/PBSA method. For each complex, a total number of 200 snapshots were extracted from the last 1 ns of the complex trajectories.

The vibrational entropy term (TS) was computed by using the NMODE module in the AMBER program. The computation was based on six snapshots taken from the final 1 ns of the MD trajectory with an even interval of 5 ps. Structural minimizations as well as normal mode analyses were carried out with a distance-dependent dielectric function ($\epsilon = 4 R_{ij}$) to mimic the impact of solvent.

During conformational searching and the evaluation of configuration integrals, Welec is computed with a simplified but fast generalized Born model.¹⁷ The electrostatic solvation energy of each energy well is then corrected toward a more

accurate but time-consuming finite-difference solution of the Poisson equation. The dielectric cavity radius of each atom is set to the mean of the solvent probe radius 2.4 Å for chloroform¹⁸ and the atom's van der Waals radius, and the dielectric boundary between the molecule and the solvent is the solvent-accessible molecular surface.¹⁹ The solvation calculations use a chloroform dielectric constant of 4.9. The MM/PBSA method can be conceptually summarized as:

$$\Delta G_{\text{bind}} = G_{\text{complex}} - [G_{\text{host}} + G_{\text{ligand}}] \quad (6.3)$$

$$G = E_{\text{gas}} + G_{\text{sol}} - TS \quad (6.4)$$

$$E_{\text{gas}} = E_{\text{bond}} + E_{\text{angle}} + E_{\text{torsion}} + E_{\text{vdw}} + E_{\text{ele}} \quad (6.5)$$

$$G_{\text{sol}} = G_{\text{PB}} + G_{\text{SA}} \quad (6.6)$$

$$H = E_{\text{gas}} + G_{\text{sol}} \quad (6.7)$$

$$S_{\text{tot}} = S_{\text{vib}} + S_{\text{trans}} + S_{\text{rot}} \quad (6.8)$$

$$\Delta G = \Delta H - T\Delta S \quad (6.9)$$

where G_{complex} , G_{host} , and G_{ligand} are the absolute free energies of the complex, host and the ligand species respectively as shown Eq. 6.3. Each of them is calculated by summing an internal energy in gas phase (E_{gas}), a solvation free energy (G_{sol}), and a vibrational entropy term Eq. 6.4. E_{gas} is Standard force field energy, including strain energies from covalent bonds and torsion angles as well as noncovalent van der Waals and electrostatic energies Eq. 6.5. The solvation free energy, G_{sol} , is calculated with a PB/SA model, which dissects solvation free energy as the sum of an electrostatic component (G_{PB}) and a nonpolar component (G_{SA}) as shown equation

Eq 6.6. S_{tot} is the total entropy comprising of translational (S_{trans}), vibrational (S_{vib}) and rotational (S_{rot}) entropies as gas phase for each species.

6.3.2.4 Quantum Chemical Calculations: The lowest energy structure for each complex extracted from molecular dynamic simulations was saved as pdb and used for quantum chemical calculations. The ONIOM calculations were performed at B3LYP/6-31+g(d) level for the guests and at AM1 level for the host. The preparation of the Gaussian input file for ONIOM calculations were carried by GaussView 3.09²⁰ and the computation was performed using Gaussian 03. The binding energy (ΔE_{bind}) for each complex is calculated from Eq. 6.10.

$$\Delta E_{\text{bind}} = E_{\text{com}} - (E_{\text{host}} + E_{\text{guest}}) \quad (6.10)$$

where E_{com} is the energy of complex in Hartree, E_{host} is the energy of the host in Hartree and E_{guest} is the energy of the guest in Hartree.

6.4 Results and Discussion

6.4.1 NMR Titration: The standart titration of the host **1** by methyl esters of (*R/S*)-alanine and (*R/S*)-valine hydrochloride salts demonstarted complexation between the host and the guests. Nine samples were prepared with different host/guest ratios for each of the studied methyl esters of alanine and valine, as indicated in the experimental section. The NMR spectrum was recorded for each sample. The changes in ¹H NMR shifts of the methyl group of isopropyl in the host **1** dependent on the concentration of the guests alanine and valine methyl ester salts are recorded

in Table 6.7.1. The changes are seen in Figure 6.6.1-6.6.2. The data shows that the host **1** forms 1:1 complexes with guests as proved by the Job's plots as indicated in Figure 6.6.3. Non-linear curve fitting of data to Eq. 6.2 are shown in Figures 6.6.5 and 6.6.6. The binding constants for each enantiomer derived from non-linear curve fitting are listed in Table 2. The results show that the host forms stronger complexes with methyl ester salts of alanine compared to those of valine and it preferably binds *S*-enantiomers of each salt. They also demonstrate that the host has a better capacity to discriminate enantiomers of alanine salts compared to those of valine salts. The enantiomeric discrimination factors of the host against the enantiomer pairs of methyl ester salts of alanine and valine are calculated as 17.36 and 5.22. They are obtained from the ratio of binding constants of enantiomers (S/R) and by assuming $R+S=100$. These values are small but they still indicate that the host holds one of the enantiomer more strongly than the other at least for alanine since the values for valine is too small and may be considered within the experimental error.

6.4.2 Molecular Dynamics (MD): Molecular dynamic calculations were performed to understand insight the mode of the complexation between the host and the guests and thus the deriving forces behind enantiomeric discrimination at atomic level. Starting from the right conformation of hosts forms a general problem in MD. In this study the host was computed over a period of 3 ns at 300 K in implicit solvent and few lowest energy conformers were chosen and they were minimized and further computed over 1 ns again. They are shown in Figure 6.6.6. So finally the lowest energy conformer was selected for the molecular dynamic calculations. This conformer was used to accommodate guests by using Dock 6.0 program as described

in the computational modeling section. The obtained structures were computed for MD calculations over a period of 30 ns in explicit chloroform at 300 K as described in experimental section. The root mean-square deviations (RMSD) and energies calculated for each complex are presented in Figures 6.6.7-6.6.10, indicating that MD calculations produced considerably good results over 30 ns of the period. The docking scores and energies derived from MD calculations are summarized in Table 6.7.2. The results show a parallel agreement with those of experimental ones.

The average structures of the complexes obtained from MD calculations are illustrated in Figure 6.6.11. They demonstrate that the bonded host has a rather flattened structure compared to its pre-associated uncomplexed structure (Fig. 6.6.11) and it holds the guests on the surface of the crown cavity via hydrogen bonds. Nevertheless, in the case of the complex with methyl ester of alanine salts, two phenyl rings of the host still form a sandwich-like structure, resembling its uncomplexed structure, probably due to its smaller site compare isopropyl. Thus this may be accounted for both a better binding and discrimination of the host for alanine compared to valine. CPK model of the complex of the host with *R* and *S* alanine salts is given in Figure 6.6.12. It seems that there is only small difference between two complexes. It clearly indicates that there is a steric interaction of the *N*-benzyl group of the host and the hydrogen of the guest. The rest of the complexes are quite similar. However, it is yet clearly understandable from the structures derived from MD calculations that the host would not have a great enantiomeric discrimination ability against the valine salts since it can be obviously seen that introduction of the guests flattens the structure of the host and thus there are not many steric interaction to discriminate between two enantiomers.

6.4.3 MM/PBSA Method: Estimated binding free energies (kcal mol^{-1}) of the host to guests studied by MM/PBSA are shown in Table 6.7.2. They are quite large than experimental values. This may be attributed to the fact that the guest molecules are charged and the MM/PBSA method utilizes the continuum solvation model where solute-solvent interactions are ignored. Therefore, it is expected that the method would overestimate the binding free energies of such systems. However, it is quite interesting to see that there is a parallel between the binding free energies calculated by MM/PBSA and those of experimental ones. The individual contribution of van der Waals and electrostatic interactions to the free energy of binding are listed in Table 6.7.3. They indicate that the electrostatic interactions are much favorable in the complexation and interestingly there is much difference ($0.46 \text{ kcal mol}^{-1}$) in the van der Waals interaction at least for the alanine salt pair, which may be accounted for the enantiomeric discrimination. The other remarkable result gained from MM/PBSA is that the VDW energy of valine salts is larger than those of alanine, which may be attributed to the side chain of the former.

Negative entropy values derived from NMODE calculations are obtained for all complexes, meaning that the reduction of guest and host configurational freedom upon the complexation. This is expected since it is generally acknowledged that there is entropy loss upon binding mainly due to the translation entropy loss of guest and host although there are some compensation raised from the disorder of the solvation of the solute (the guest) and the release of bonded solvent to the host to the bulk. But this will not be possible to calculate since the method, as mentioned earlier, utilizes the continuum solvation model and ignores solute-solvent interactions.

6.4.4 Quantum Mechanical Calculations: The free energies of binding of the host to the guests obtained by ONIOM calculations are presented in Table 6.7.2. They are even larger than those obtained by MM/PBSA compared to the experimental ones. However, they are in parallel with those obtained by MM/PBSA and ¹H NMR titration. The overestimated binding energies as observed in the MM/PBSA calculation may again be explained in terms of the interactions of charged molecules with the host and the effect of solvation.

6.5 Conclusion

¹H NMR titration together with theoretical calculation have produced relatively comparable results in details to understand the mode of the binding of chiral-aza-15-crown-5 ether to methyl esters of alanine and valine salts and the main driving forces for their enantiomeric discrimination. So we have the confidence to suggest that a combination of theoretical calculation (MD, MM/PBSA and QM) can be employed to estimate the binding properties of supramolecular structures.

6.6 Figures

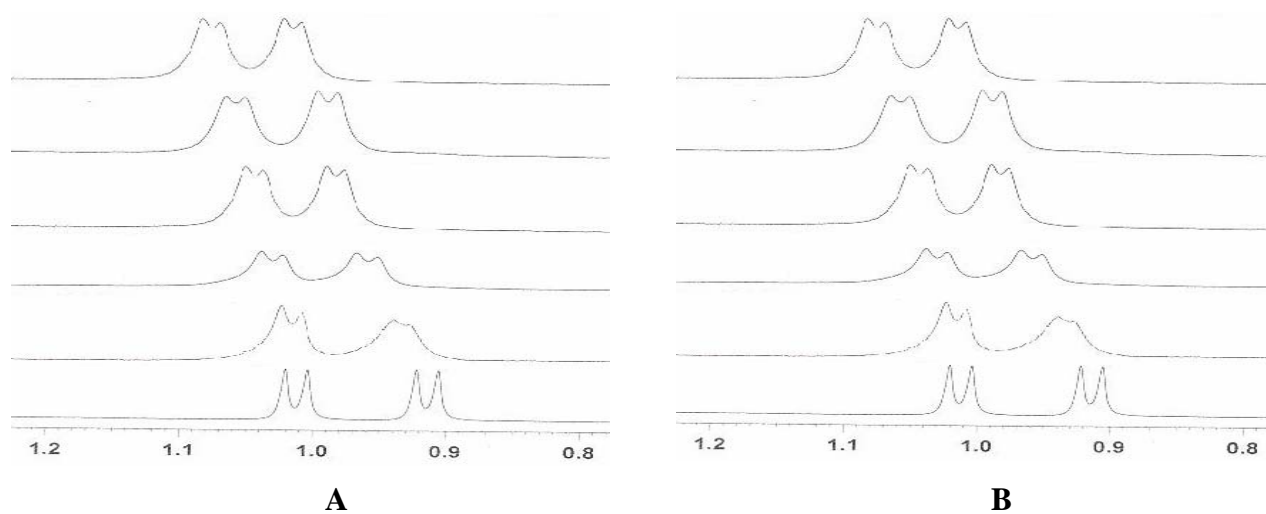


Figure 6.6.1 Dependence of ^1H NMR chemical shifts of methyl group of isopropyl in the host **1** on the concentration of the guests. **A** represents *R*-alanine methyl ester salt whereas **B** represents *S*-alanine methyl ester salt.

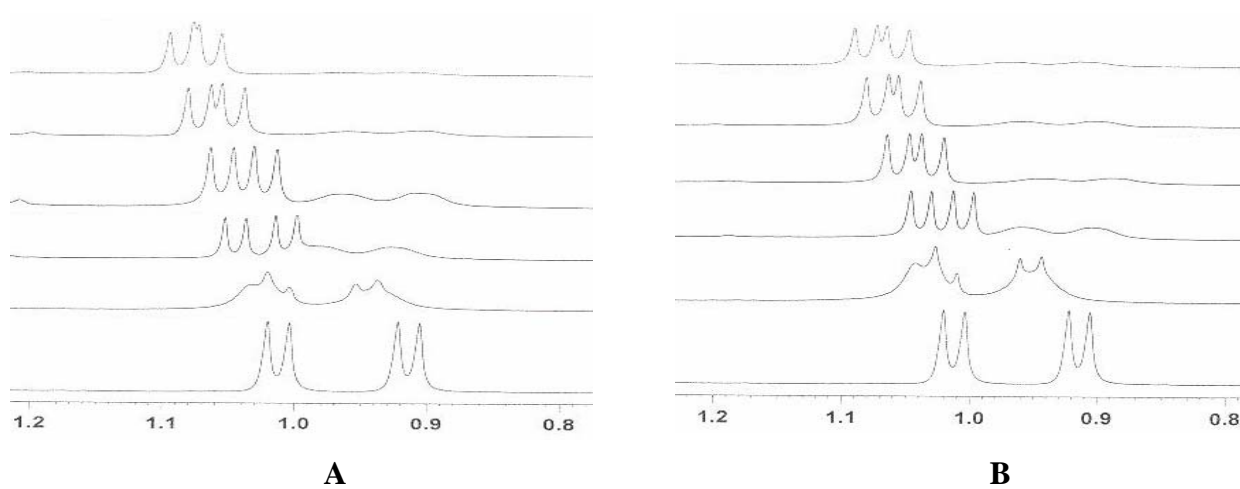


Figure 6.6.2 Dependence of ^1H NMR chemical shifts of methyl group of isopropyl in the host **1** on the concentration of the guests. **A** represents *R*-valine methyl ester salt whereas **B** represents *S*-valine methyl ester salt.

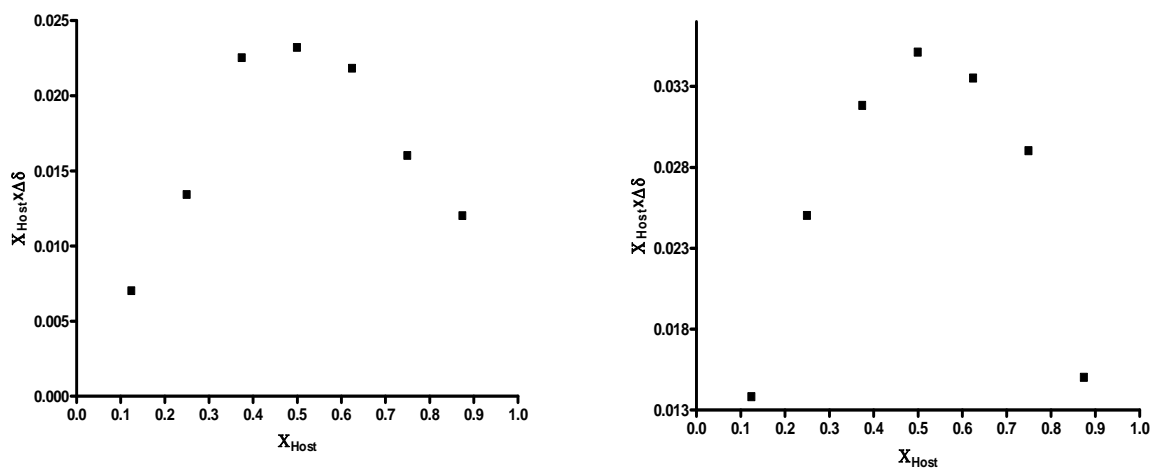


Figure 6.6.3 Job's plot diagrams for the complex of the host with methyl esters of *R*-alanine salt (on the right) and *R*-valine (on the left).

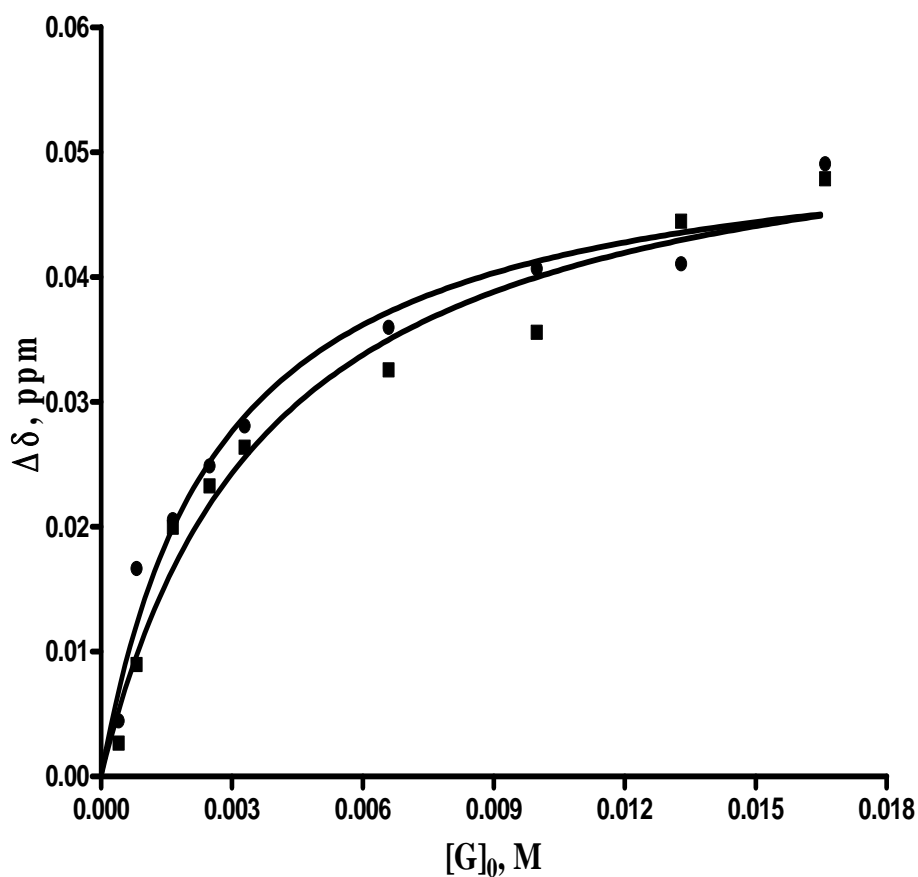


Figure 6.6.4 Non-linear dependence of ^1H NMR chemical shifts of methyl group of isopropyl in the host **1** on the concentration of the guests fitted to equation 1. The squares represent *R*-alanine methyl ester salt ($R^2 = 9682$) whereas the circles represent *S*-alanine methyl ester salt ($R^2 = 9681$). Data are taken from Table 6.6.1.

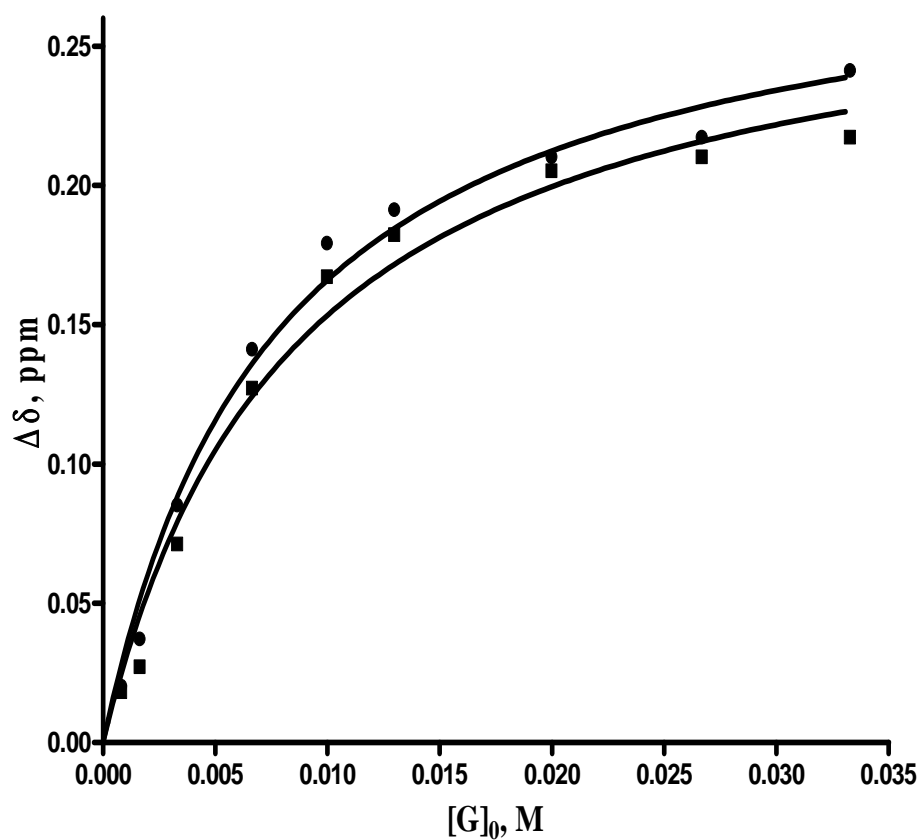


Figure 6.6.5 Non-linear dependence of ^1H NMR chemical shifts of methyl group of isopropyl in the host **1** on the concentration of the guests fitted to equation 1. The squares represent *R*-valine methyl ester salt ($R^2=9810$) whereas the circles represent *S*-valine methyl ester salt ($R^2=9871$). Data are taken from Table 6.6.1.

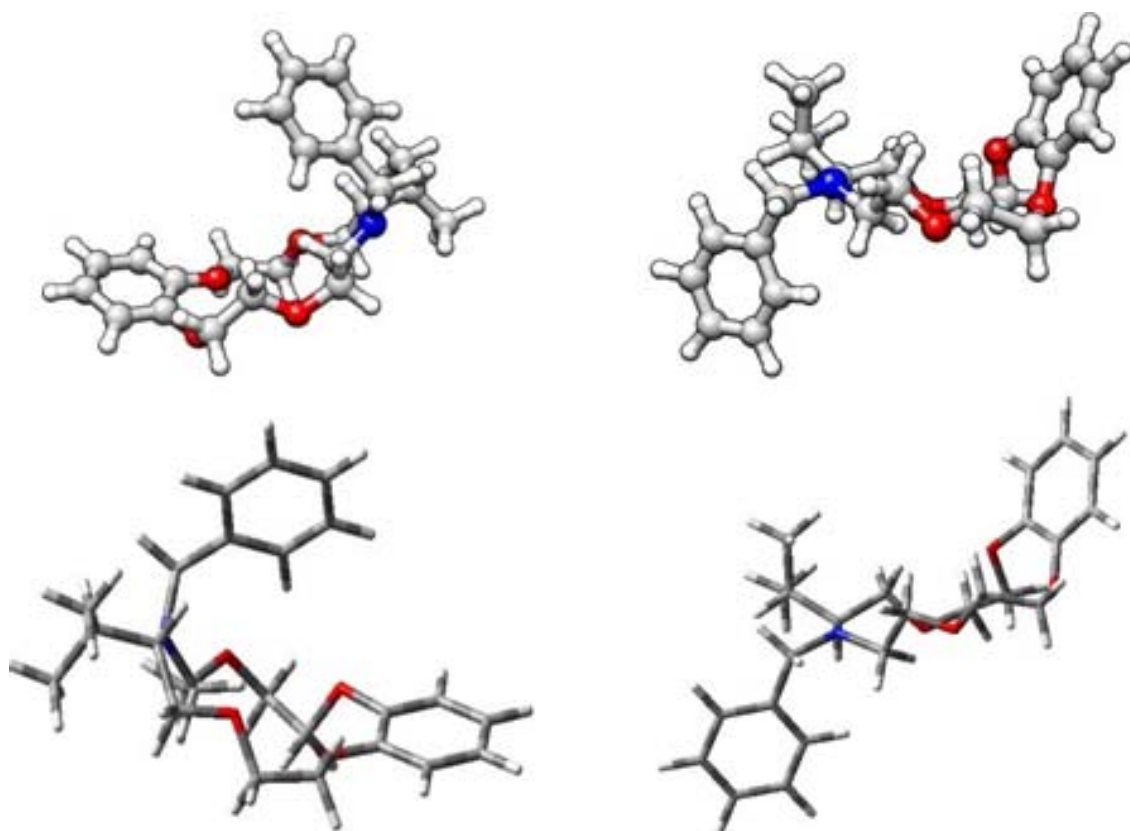


Figure 6.6.6 Structures above correspond two lowest conformers of the host **1** observed in molecular dynamic simulation in implicit solvent $94.87 \text{ kcal mol}^{-1}$ for the conformer on the left and $108.77 \text{ kcal mol}^{-1}$ for the conformer on the right and their optimized structures below at B3LYP/631+g(d) level in vacuum (-1290.03894962 Hartree for the conformer on the left and -1290.04209904 Hartree for the conformer on the right)

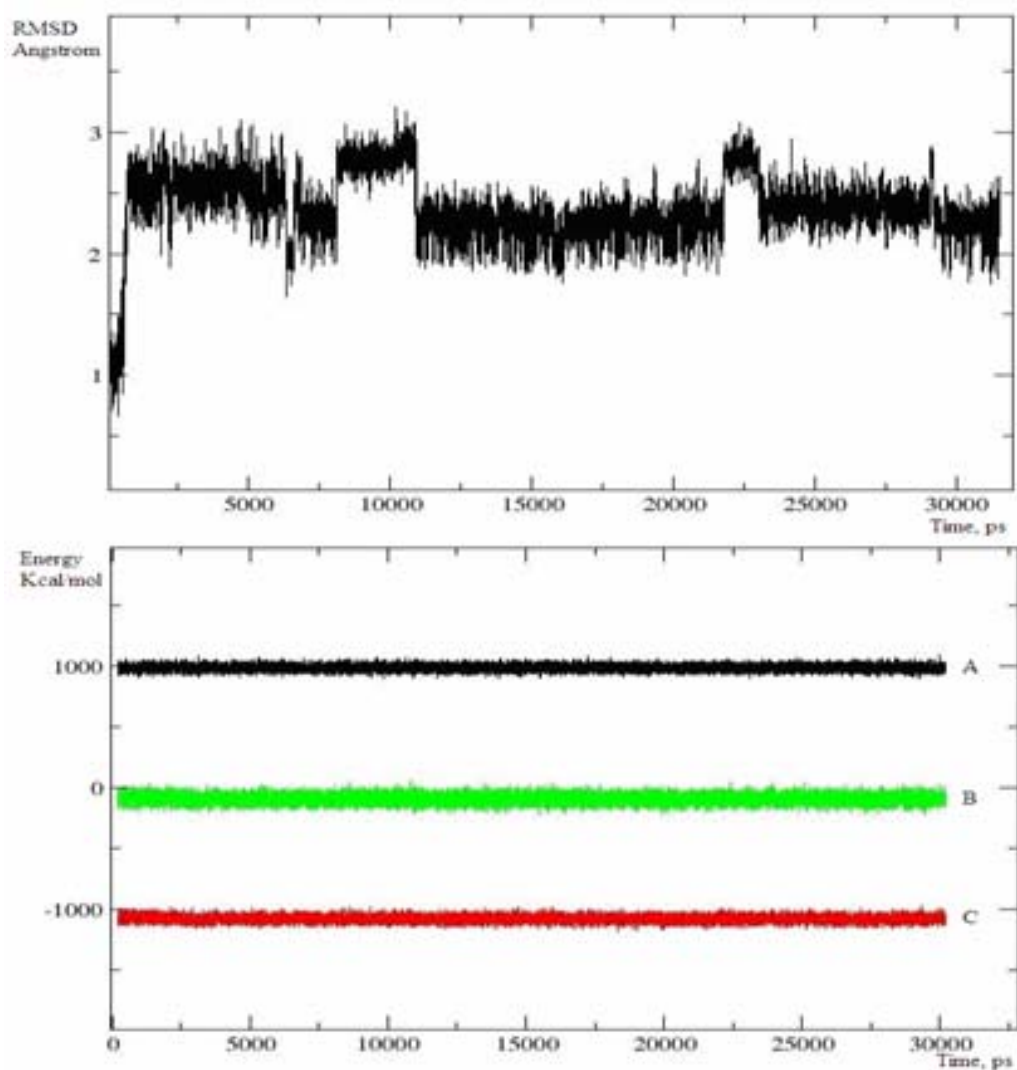


Figure 6.6.7 Root-mean square deviations (RMSD) and energy changes observed in MD simulation of the complex of the host with *R*-alanine salt. **A** represents kinetic energy, **B** represents total energy and **C** represents potential energy.

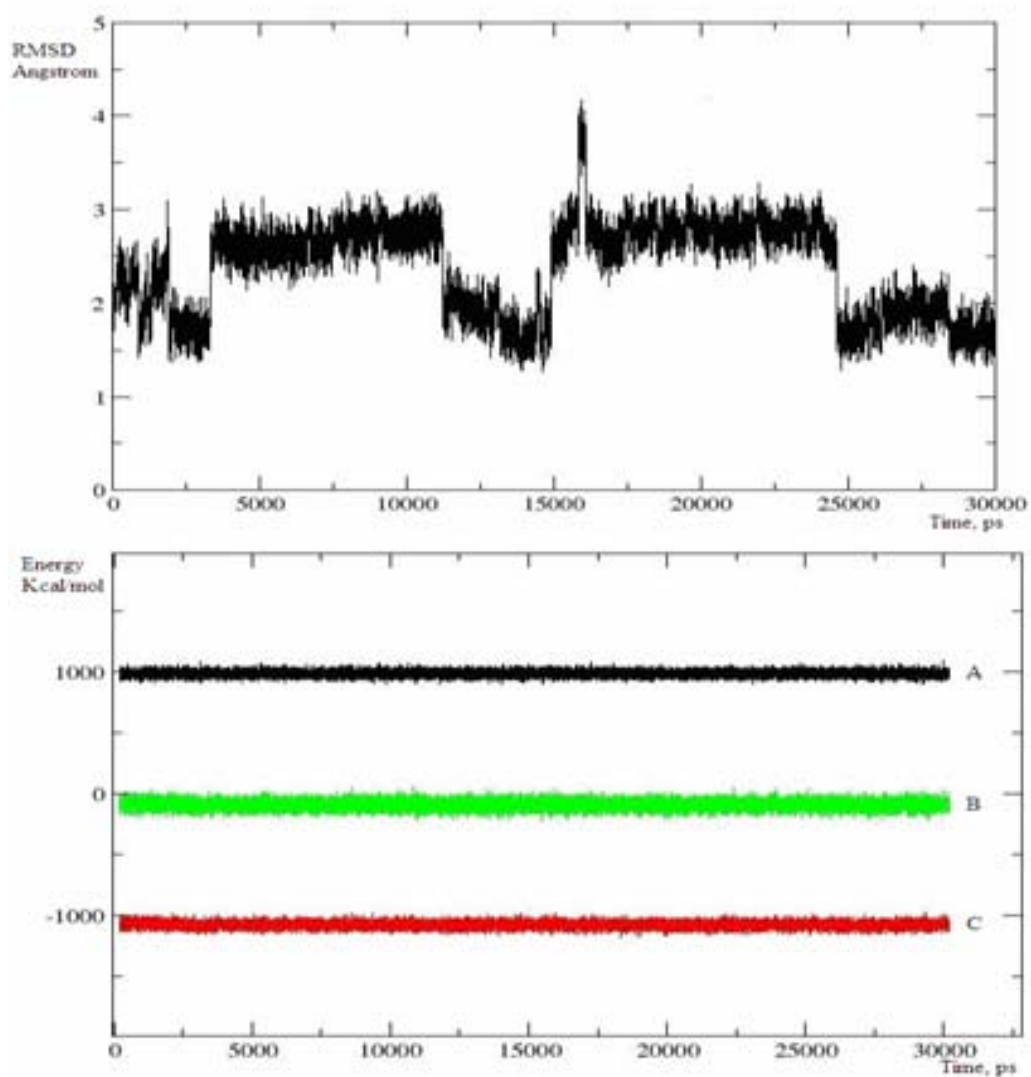


Figure 6.6.8 Root-mean square deviations (RMSD) with reference to the minimum energy conformer and energy changes observed in MD simulation of the complex of the host with *S*-alanine salt. **A** represents kinetic energy, **B** represents total energy and **C** represents potential energy.

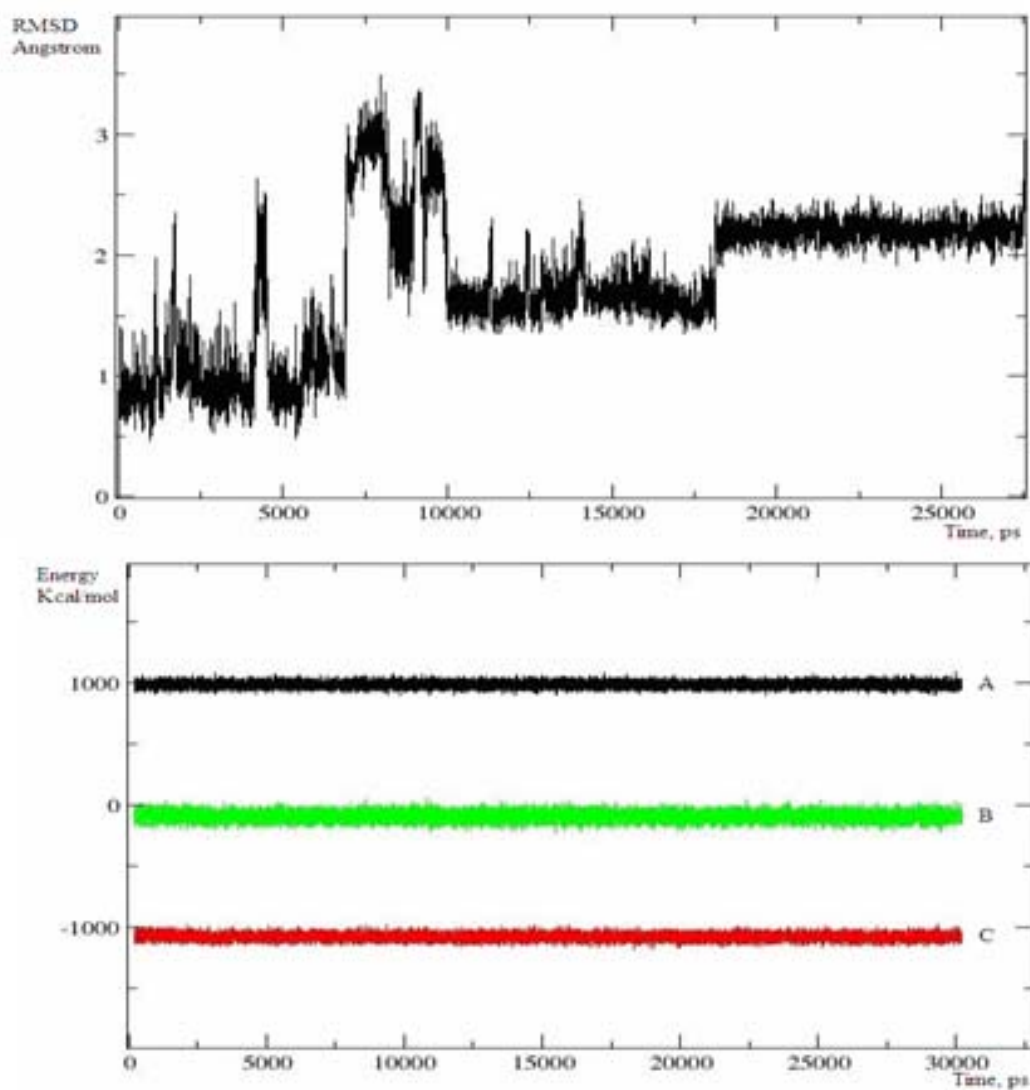


Figure 6.6.9 Root-mean square deviations (RMSD) with reference to the minimum energy conformer and energy changes observed in MD simulation of the complex of the host with *R*-valine salt. **A** represents kinetic energy, **B** represents total energy and **C** represents potential energy.

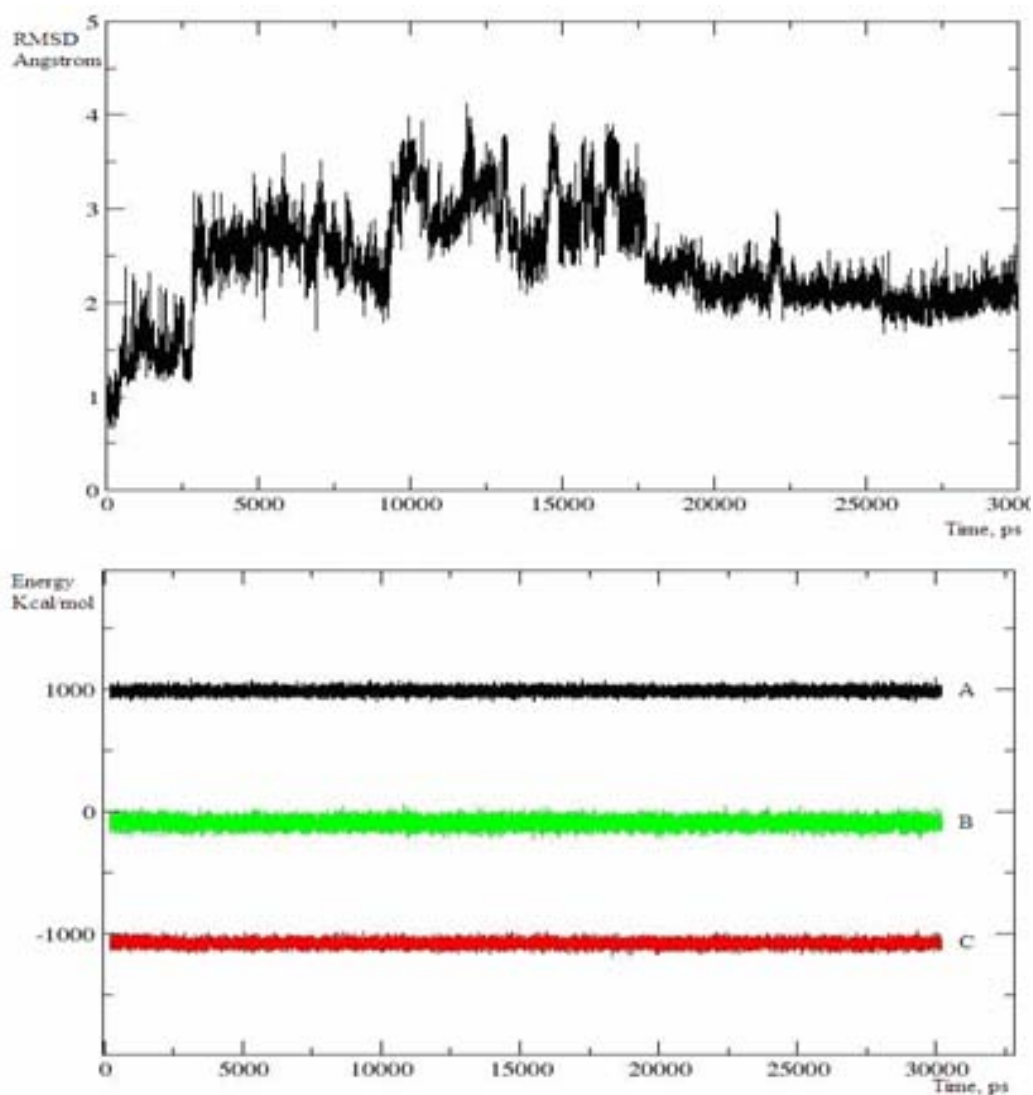


Figure 6.6.10 Root-mean square deviations (RMSD) with reference to the minimum energy conformer and energy changes observed in MD simulation of the complex of the host with *S*-valine salt. **A** represents kinetic energy, **B** represents total energy and **C** represents potential energy.

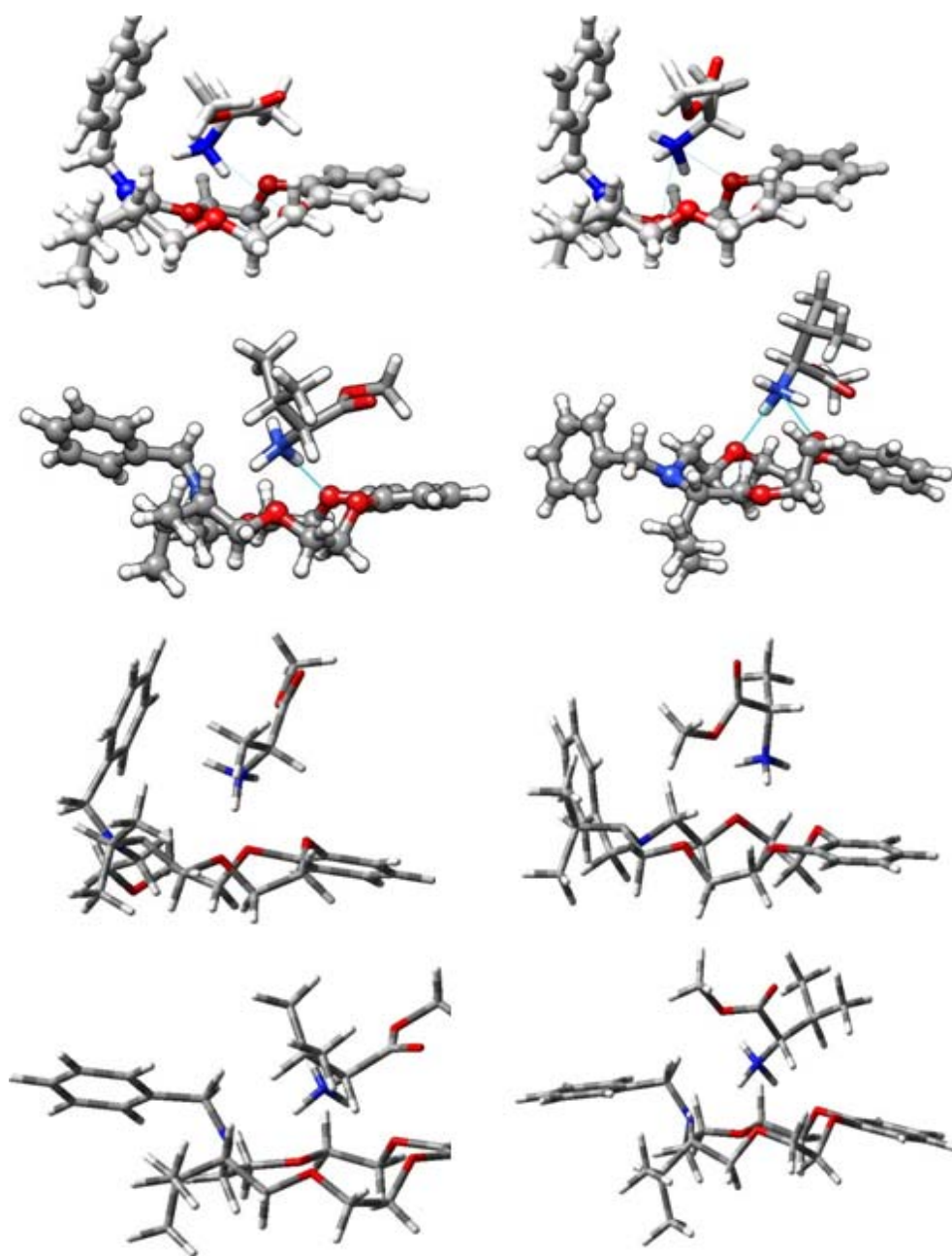


Figure 6.6.11 Graphic representation of average structures of the complexes of the host **1** with the guests obtained by MD in CHCl_3 (structures above drawn in ball and stick) and ONIOM (B3LYP/631+g(d):AM1) simulation in vacuum (structures drawn in stick). In each case the complexes on the left correspond to *R*-alanine salt (upper row) and *R*-valine salt (lower) and those on the right correspond to *S*-alanine salt (upper row) and *S*-valine salt (lower).

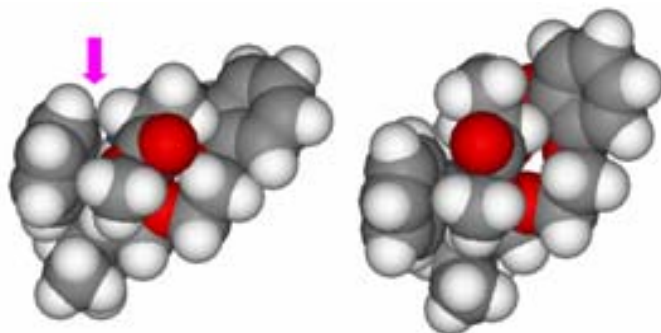


Figure 6.6.12 CPK model of the complex of the host with methyl ester salts of *R*-alanine (on the right) and *S*-alanine (on the left).

6.7 Tables

Table 6.7.1 Changes in ^1H NMR chemical shifts (400 MHz) of methyl group of isopropyl in the host dependent on the concentration of added guests at 300 K in Choloform-*d*1

Methyl ester of alanine salts			Methyl ester of valine salts		
[Guest], mM	$\Delta\delta$ for <i>R</i>	$\Delta\delta$ for <i>S</i>	[Guest], mM	$\Delta\delta$ for <i>R</i>	$\Delta\delta$ for <i>S</i>
0.4165	0.0026	0.0044	0.833	0.018	0.020
0.833	0.0089	0.0166	1.66	0.027	0.037
1.66	0.0199	0.0205	3.33	0.071	0.085
2.50	0.0232	0.0248	6.66	0.127	0.141
3.33	0.0263	0.0280	10.0	0.167	0.179
6.66	0.0325	0.0359	13.3	0.182	0.191
10.0	0.0329	0.0406	20.0	0.205	0.21
13.3	0.0444	0.0410	26.7	0.210	0.217
16.6	0.0478	0.0509	33.3	0.217	0.241

Table 6.7.2 Thermodynamic parameters derived from ^1H NMR titration and theoretical calculations.

Guests	MD ^a	DS ^b	ΔH^c	$T\Delta S^d$	ΔG_T^e	ΔE_{bind}^f	ΔG_E^g	$K_{\text{diss}} \times 10^3^h$	K_{ass}^i
<i>R</i> -Ala	-1067	-15.10	-28.74	-13.00	-15.74	-35.39	-3.32	3.84±0.78	260
<i>S</i> -Ala	-1082	-15.19	-30.14	-13.86	-16.28	-39.72	-3.53	2.69±0.48	372
<i>R</i> -Val	-1050	-13.68	-26.29	-12.96	-13.33	-31.88	-2.83	8.61±0.15	116
<i>S</i> -Val	-1062	-13.55	-27.55	-13.17	-14.38	-35.01	-2.89	7.74±0.11	129

a) Average values in kcal mol⁻¹ obtained from MD calculations over a period of 30 ns

b) Docking scores in kcal mol⁻¹

c) Enthalpy of binding calculated by MM/PBSA method in kcal mol⁻¹

d) Entropy of binding calculated by MM/PBSA method multiplied by 300 (temperature, Kelvin)

e) Theoretical binding free energy produced from $\Delta G = \Delta H - T\Delta S$

f) Complexation energy determined by ONIOM (B3LYP/6-31+g(d)//AM1) as described in experimental section.

g) Experimental binding free energy produced from $\Delta G = RT\ln K_a$ where $R = 1.987$ cal mol⁻¹ and $T = 300$ Kelvin

h) Dissociation constants of the host from the guests (M) derived from non-linear curve fitting of data in Table 6.7.1 to Eq. 6.2.

i) Binding constants (M^{-1}) between the host and each guest calculated by $1/K_d$

Table 6.7.3 The individual contribution of van der Waals and electrostatic terms (in kcal mol⁻¹) to the free energy of binding of the host to the guests at 300 K in chloroform calculated by MM/PBSA.

Term	Methyl ester of alanine salts			Methyl ester of valine salts		
	for <i>R</i>	for <i>S</i>	Delta	for <i>R</i>	for <i>S</i>	Delta
ELE	-52.32	-53.02	0.70	-47.70	-48.06	0.36
VDW	-7.00	-8.46	1.46	-8.69	-8.71	0.02

6.8 References

1. a) Cram, J. D. *Angew Chem. Int. Ed. England*, **1998**, 27, 1009. b) Pedersen, C.J. *Angew Chem. Int. Ed. England*, **1998**, 27,1021. c) Lehn, J. M. *Angew Chem. Int. Ed. England*, **1998**, 27, 87. d)Atwood J. L.; Davies, J.; E.,D.,MackNikol, D. D.; Vögtle, F. Eds.; *Elsevier Science:Oxford, UK*, **1996**, 1, 10. e) Lehn, J. M. *Supramolecular Chemistry*, VCH, Verlagsgesellschaft: Weinheim, Germany, **1995**.
2. a) Pedersen, C. J. *Am. Chem. Soc.*, **1967**, 89, 7017. b) Lehn, J. H.; Sirlin, C. J. *Chem. Soc., Chem. Commun*, **1978**, 946. c) Stoddart, J. F. *Chem. Soc. Rev.*, **1979**, 8, 85. d)Chadwick, D.J.; Cliffe, A.; Stutther, I. O. *J. Chem. Soc., Chem. Commun*, **1981**, 992. e)Nizutani, T.; Emu, T.; Tomita, T.; Kuroda, Y.; Ogoshi, H. *J. Am. Chem. Soc.*, **1994**, 116, 4240.
3. a) Hirose, K.; Ogasahara, k.;Nishioka, K.; Tobe, Y.; Naemura, K. *J. Chem. Soc. Perkin Trans2*, **2000**, 1984.
4. Turgut, Y.; Hosgoren, H. *Tet. Asym.*, **2003**, 14, 3815.
5. Case, D.A.; Cheatham III, T.E.; Darden, T.; Gohlke, H.; Luo, R. ; Merz, K.M.; Onufriev, Jr., A.; Simmerling, C.; Wang, B.; Woods, R. *J. Computat.. Chem.* **2005**, 26, 1668-1688.
6. Gaussian 03, Revision C.02, Frisch, M. J.; Trucks, G. W.; Schlegel, H. B.; Scuseria, G. E.; Robb, M. A.; Cheeseman, J. R.; Montgomery, Jr., J. A.; Vreven, T.; Kudin, K. N.; Burant, J. C.; Millam, J. M.; Iyengar, S. S.; Tomasi, J.; Barone, V.; Mennucci, B.; Cossi, M.; Scalmani, G.; Rega, N.; Petersson, G. A.; Nakatsuji, H.; Hada, M.; Ehara, M.; Toyota, K.; Fukuda, R.; Hasegawa, J.; Ishida, M.; Nakajima, T.; Honda, Y.; Kitao, O.; Nakai, H.; Klene, M.; Li, X.; Knox, J. E.; Hratchian, H. P.; Cross, J. B.; Bakken, V.; Adamo, C.; Jaramillo, J.; Gomperts, R.; Stratmann, R. E.;

Yazyev, O.; Austin, A. J.; Cammi, R.; Pomelli, C.; Ochterski, J. W.; Ayala, P. Y.; Morokuma, K.; Voth, G. A.; Salvador, P.; Dannenberg, J. J.; Zakrzewski, V. G.; Dapprich, S.; Daniels, A. D.; Strain, M. C.; Farkas, O.; Malick, D. K.; Rabuck, A. D.; Raghavachari, K.; Foresman, J. B.; Ortiz, J. V.; Cui, Q.; Baboul, A. G.; Clifford, S.; Cioslowski, J.; Stefanov, B. B.; Liu, G.; Liashenko, A.; Piskorz, P.; Komaromi, I.; Martin, R. L.; Fox, D. J.; Keith, T.; Al-Laham, M. A.; Peng, C. Y.; Nanayakkara, A.; Challacombe, M.; Gill, P. M. W.; Johnson, B.; Chen, W.; Wong, M. W.; Gonzalez, C.; and Pople, J. A.; Gaussian, Inc., Wallingford CT, 2004.

7. a) Jakalian, A.; Jack, D. B.; Bayly, C. I. *Abstr. Pap. Am. Chem. S.* **2000**, 277, 220

b) Jakalian, A.; Bush, B. L.; Jack, D. B.; Bayly, C. I., *J Comput Chem.* 2000, **21**,

132. c) Jakalian, A.; Jack, D. B.; Bayly, C. I. *J Comput Chem.* **2002**, 23(16),1623.

8. Chia-En, C.; Michael, K. G. *J. Am. Chem. Soc.* **2004**, 126, 13156.

9. Wang, J.; Wolf, R.M.; Caldwell, J.W.; Kollman, P.A.; Case, D.A. *J. Comput. Chem.*, **2004**, 25, 1157.

10. Cornell, W. D.; Cieplak, P.; Bayly, C. I.; Gould, I. R.; Merz, K. M.; Ferguson, D. M.; Spellneyer, D. C.; Fox, T.; Caldwell, J. W.; Kollman, P. A. *J Am Chem Soc* **1995**, 117, 5179.

11. Darden. T.; York, D.; Pedersen, L. *J. Chem. Phys.* **1993**, 98, 1089.

12. Pettersen, E. F.; Goddard, T. D.; Huang, C.C.; Couch, G. S.; Greenblatt, D. M.; Meng, E. C.; Ferin, T. E. *J Comput Chem.* **2004**, 25, 13, 1605.

13. Humphrey, W.; Dalke, A.; Schulten, K. *J. Molec. Graphics*, **1996**, 14, 33.

14. Lang, P. T. ; Moustakas, D. ; Brozell, S.; Carrascal, N.; Mukherjee, S.; Pegg, S.;

Raha, K.; Shivakumar, D.; Rizzo, R.; Case, D.; Shoichet, B.; Kuntz, I. **2007**. DOCK

6.1, University of California, San Francisco. <http://dock.compbio.ucsf.edu/>

15. a) Gouda, H.; Kuntz, I. D.; Case, D. A.; Kollman, P. A. *Biopolymers* **2003**, 68, 16.
b) Lee, M.R.; Duan, Y.; Kollman, P.A. *Proteins: Struct. Funct., Genet.* **2000**, 39, 309.
16. Srinivasan, J.; Cheatham, T. E.; Cieplak, P.; Kollman, P. A.; Case, D. A. *J. Am. Chem. Soc.* **1998**, 120, 9401..
17. Kuhn, B.; Kollman, P. A. *J. Med. Chem.*, 2000, 43, 3786.
18. Kuhn, B.; Gerber, P.; Schulz-Gasch, T.; Stahl, M. *J. Med. Chem.* **2005**, 48, 4040.
19. a) Lyne, P. D.; Lamb, M. L.; Saeh, J. C. *J. Med. Chem.* **2006**, 49, 4805. b) Weis, A.; Katebzadeh, K.; Soderhjelm, P.; Nilsson, I.; Ryde, U., *J. Med. Chem.* **2006**, 49, 6596.
20. Dennington II, R.; Keith, T.; Millam, J.; Eppinnett, K.; Hovell, W. L.; Gilliland, R.; Semichem, Inc., Shawnee Mission, KS, **2003** GaussView, Version 3.09.

Chapter 4 MM/PBSA Output Files

Table 4.6.3

	Complex-1		Receptor		Ligand		Delta	
	Mean	STD	Mean	STD	Mean	STD	Mean	STD
ELE	1084.26	19.55	1112.23	19.36	-29.02	0.62	1.05	6.29
VDW	13.47	6.11	10.87	4.35	5.97	1.27	-3.36	5.77
INT	184.20	9.16	163.57	8.77	20.62	3.13	0.00	0.01
GAS	1281.93	22.05	1286.67	19.31	-2.42	3.02	-2.31	7.04
PBSUR	10.63	0.90	8.51	0.13	2.65	0.02	-0.54	0.90
PBCAL	-1599.97	17.91	-1589.22	16.58	-11.43	0.53	0.68	6.05
PBSOL	-1589.34	17.63	-1580.70	16.66	-8.77	0.52	0.13	6.03
PBELE	-515.71	4.89	-476.99	4.79	-40.45	0.33	1.73	2.79
PBTOT	-307.41	9.03	-294.04	7.75	-11.20	2.92	-2.17	4.08
GBSUR	10.63	0.90	8.51	0.13	2.65	0.02	-0.54	0.90
GB	-1613.75	18.39	-1602.07	16.92	-12.59	0.52	0.91	5.97
GBSOL	-1603.13	18.08	-1593.55	17.00	-9.94	0.51	0.36	5.91
GBELE	-529.49	4.96	-489.84	4.68	-41.61	0.31	1.96	3.00
GBTOT	-321.19	8.94	-306.89	7.97	-12.36	2.93	-1.94	3.75

Table 4.6.4

	Complex-2		Receptor		Ligand		Delta	
	Mean	STD	Mean	STD	Mean	STD	Mean	STD
ELE	1099.04	16.38	1106.16	14.48	-6.22	0.60	-0.91	6.10
VDW	12.11	4.18	11.57	3.73	11.01	1.59	-10.47	1.31
INT	187.13	9.09	162.88	8.68	24.25	3.64	0.00	0.01
GAS	1298.29	17.03	1280.61	14.95	29.05	3.67	-11.37	6.52
PBSUR	10.07	0.16	8.61	0.12	3.28	0.02	-1.82	0.14
PBCAL	-1592.2	14.18	-1584.2	12.22	-14.02	0.54	5.98	5.99
PBSOL	-1582.2	14.19	-1575.6	12.31	-10.73	0.53	4.16	5.92
PBELE	-493.19	4.71	-478.03	4.30	-20.23	0.31	5.07	1.52
PBTOT	-283.87	7.92	-294.97	7.45	18.32	3.62	-7.22	1.69
GBSUR	10.07	0.16	8.61	0.12	3.28	0.02	-1.82	0.14
GB	-1605.1	14.48	-1596.7	12.19	-15.42	0.56	7.02	6.22
GBSOL	-1595.0	14.49	-1588.1	12.28	-12.13	0.54	5.21	6.15
GBELE	-506.05	4.62	-490.54	4.56	-21.63	0.30	6.12	0.94
GBTOT	-296.73	8.16	-307.48	7.68	16.92	3.64	-6.17	1.08

Table 4.6.5

	Complex-3		Receptor		Ligand		Delta	
	Mean	STD	Mean	STD	Mean	STD	Mean	STD
ELE	-21.87	5.43	-2.49	5.04	-20.55	0.63	1.18	1.36
VDW	5.24	5.09	10.34	4.29	7.97	1.60	-13.07	1.69
INT	194.46	9.86	165.97	8.63	28.49	3.92	0.00	0.01
GAS	177.83	10.61	173.81	9.48	15.90	3.86	-11.89	2.11
PBSUR	9.33	0.24	7.98	0.21	3.54	0.03	-2.18	0.17
PBCAL	-124.14	5.16	-115.84	5.06	-12.10	0.53	3.80	2.06
PBSOL	-114.81	5.04	-107.87	4.98	-8.56	0.52	1.62	1.97
PBELE	-146.01	4.73	-118.34	4.62	-32.65	0.38	4.98	1.51
PBTOT	63.02	9.65	65.95	8.47	7.34	3.80	-10.27	1.47
GBSUR	9.33	0.24	7.98	0.21	3.54	0.03	-2.18	0.17
GB	143.22	4.67	-134.69	4.40	-13.18	0.55	4.65	1.67
GBSOL	-133.89	4.58	-126.71	4.34	-9.64	0.54	2.46	1.58
GBELE	-165.09	3.93	-137.18	3.86	-33.73	0.35	5.82	1.12
GBTOT	43.93	9.42	47.10	8.23	6.26	3.82	-9.43	1.36

Table 4.6.6

	Complex-4		Receptor		Ligand		Delta	
	Mean	STD	Mean	STD	Mean	STD	Mean	STD
ELE	810.96	15.23	1127.65	18.00	25.62	0.87	-342.31	8.91
VDW	2.34	4.48	8.49	3.87	11.65	1.68	-17.80	1.40
INT	192.64	8.52	165.37	7.94	27.27	3.49	0.00	0.01
GAS	1005.94	15.08	1301.51	17.31	64.53	3.47	-360.10	8.94
PBSUR	9.15	0.11	8.33	0.12	3.49	0.02	-2.68	0.10
PBCAL	-1319.3	13.23	-1601.6	15.90	-65.30	0.77	347.61	9.19
PBSOL	-1310.1	13.27	-1593.3	15.99	-61.81	0.76	344.94	9.17
PBELE	-508.32	4.14	-473.94	4.06	-39.68	0.29	5.31	1.47
PBTOT	-304.19	8.16	-291.75	7.39	2.72	3.21	-15.17	1.96
GBSUR	9.15	0.11	8.33	0.12	3.49	0.02	-2.68	0.10
GB	-1335.4	13.37	-1614.7	15.78	-67.76	0.83	347.00	9.17
GBSOL	-1326.3	13.41	-1606.4	15.86	-64.27	0.81	344.33	9.14
GBELE	-524.48	4.27	-487.04	4.30	-42.14	0.33	4.70	0.91
GBTOT	-320.35	8.17	-304.85	7.48	0.27	3.25	-15.77	1.55

Table 4.6.7

	Complex-5		Receptor		Ligand		Delta	
	Mean	STD	Mean	STD	Mean	STD	Mean	STD
ELE	822.76	16.85	1108.42	13.30	47.65	0.76	-333.31	11.65
VDW	4.07	5.20	10.07	4.49	10.96	1.68	-16.96	1.85
INT	207.51	9.16	164.81	8.13	42.70	3.82	0.00	0.01
GAS	1034.35	17.16	1283.30	13.63	101.31	3.67	-350.27	11.82
PBSUR	9.11	0.23	8.36	0.15	3.46	0.04	-2.72	0.17
PBCAL	-1314.2	15.71	-1586.1	11.92	-62.61	0.52	334.49	11.50
PBSOL	-1305.1	15.77	-1577.7	12.04	-59.15	0.53	331.77	11.46
PBELE	-491.46	4.02	-477.68	3.91	-14.96	0.42	1.18	1.36
PBTOT	-270.76	8.06	-294.43	6.89	42.16	3.61	-18.49	2.04
GBSUR	9.11	0.23	8.36	0.15	3.46	0.04	-2.72	0.17
GB	-1327.8	15.83	-1597.2	11.79	-64.93	0.52	334.29	11.73
GBSOL	-1318.7	15.88	-1588.8	11.90	-61.47	0.52	331.58	11.69
GBELE	-505.04	4.31	-488.75	4.21	-17.27	0.49	0.98	0.98
GBTOT	-284.35	7.95	-305.50	7.09	39.85	3.63	-18.69	1.67

ELE = electrostatic energy as calculated by MM force field.

VDW = van der Waals contribution from MM.

INT = internal energy arising from bond, angle and dihedral terms in the MM force field. (this term always amounts to zero in the single trajectory approach).

GAS = total gas phase energy (sum of ELE, VDW and INT)

PBSUR/GBSUR = nonpolar contribution to the solvation free energy calculated by an empirical model.

PBCAL/GB = the electrostatic contribution to the solvation free energy calculated by PB or GB respectively.

PBSOL/GBSOL = sum of nonpolar and polar contributions to solvation.

PBELE/GBELE = sum of the electrostatic solvation free energy and MM electrostatic above. (kcal/mol)

Chapter 5 X-Ray Files

5.7 Tables

Table 5.7.1. Crystal data and structure refinement for **12**.

Identification code	h04gb2
Empirical formula	C ₅ H ₅ Br O ₄
Formula weight	209.00
Temperature	150(2) K
Wavelength	0.71073 Å
Crystal system	Monoclinic
Space group	P21/c
Unit cell dimensions	a = 6.8930(1) Å $\alpha = 90^\circ$
	b = 11.2120(3) Å $\beta = 109.793(1)^\circ$
	c = 9.4290(2) Å $\gamma = 90^\circ$
Volume	685.66(3) Å ³
Z	4
Density (calculated)	2.025 Mg/m ³
Absorption coefficient	5.945 mm ⁻¹
F(000)	408
Crystal size	0.25 x 0.20 x 0.20 mm
Theta range for data collection	3.68 to 27.51°
Index ranges	-8 ≤ h ≤ 8; -14 ≤ k ≤ 14; -11 ≤ l ≤ 12
Reflections collected	10317
Independent reflections	1565 [R(int) = 0.0573]
Reflections observed (>2σ)	1361
Data Completeness	0.997
Absorption correction	Semi-empirical from equivalents
Max. and min. transmission	0.25 and 0.13
Refinement method	Full-matrix least-squares on F ²
Data / restraints / parameters	1565/0/95
Goodness-of-fit on F ²	1.063
Final R indices [I > 2σ(I)]	R ¹ = 0.0246 wR ₂ = 0.0594
R indices (all data)	R ¹ = 0.0311 wR ₂ = 0.0617
Largest diff. peak and hole	0.392 and -0.584 eÅ ⁻³

Hydrogen bonds with H..A < r (A) + 2.000 Angstroms and <DHA > 110 deg.

D-H	d(D-H)	d(H..A)	<DHA	d(D..A)	A
O4-H4	0.840	1.838	174.74	2.675	03 [-x+2, -y+1, -z+1

Table 5.7.2. Atomic coordinates ($\times 10^4$) and equivalent isotropic displacement parameters ($\text{\AA}^2 \times 10^3$) for **12**.U(eq) is defined as one third of the trace of the orthogonalized U_{ij} tensor.

Atom	x	y	z	U(eq)
Br(1)	5999(1)	9655(1)	3179(1)	28(1)
O(1)	7861(2)	7959(1)	6669(2)	25(1)
O(2)	9243(2)	9837(2)	6977(2)	32(1)
O(3)	7575(2)	5413(1)	4622(2)	23(1)
O(4)	10364(2)	6580(1)	5522(2)	28(1)
C(1)	8514(3)	9000(2)	6221(2)	22(1)
C(2)	7942(3)	8629(2)	4584(2)	20(1)
C(3)	7114(3)	7480(2)	5092(2)	20(1)
C(4)	8371(3)	6371(2)	5053(2)	20(1)
C(5)	4830(3)	7256(2)	4549(3)	28(1)

Table 5.7.3. Bond lengths [\AA] and angles [$^\circ$] for **12**.

Br(1)-C(2)	1.9155(19)	O(1)-C(1)	1.368(3)
O(1)-C(3)	1.499(2)	O(2)-C(1)	1.183(3)
O(3)-C(4)	1.213(2)	O(4)-C(4)	1.314(2)
C(1)-C(2)	1.516(3)	C(3)-C(3)	1.550(3)
C(3)-C(5)	1.503(3)	C(3)-C(4)	1.523(3)
C(1)-O(1)-C(3)	92.13(14)	O(2)-C(2)-O(1)	27.39(19)
O(2)-C(1)-C(2)	137.9(2)	O(1)-C(1)-C(2)	94.70(16)
C(1)-C(2)-C(3)	84.76(15)	C(1)-C(2)-Br(1)	114.77(14)
C(3)-C(2)-Br(1)	117.92(13)	O(1)-C(3)-C(5)	111.50(17)
O(1)-C(3)-C(4)	108.03(15)	C(5)-C(3)-C(4)	113.22(17)
O(1)-C(3)-C(2)	88.30(14)	C(5)-C(3)-C(2)	119.12(17)
C(4)-C(3)-C(2)	113.52(16)	O(3)-C(4)-O(4)	124.99(19)

Atom	X	y	z	U(eq)
H(4)	10990	5961	5418	40(8)
H(2)	9184	8472	4290	23
H(5A)	4121	7957	4758	42
H(5B)	4535	6561	5073	42
H(5C)	4344	7104	3461	42
O(3)-C(4)-C(3)	122.36(17)	O(4)-C(4)-C(3)	112.65(17)	

Symmetry transformations used to generate

Table 5.7.4. Anisotropic displacement parameters ($\text{Å}^2 \times 10^3$) for **12**. The anisotropic factor exponent takes the form: $-2 \text{ gpi}^2 [h^2 a^* \cdot U_{11} + \dots + 2 h k a^* b^* U$

Atom	U11	U22	U33	U23	U13	U12
Br(1)	32(1)	23(1)	29(1)	8(1)	9(1)	9(1)
O(1)	33(1)	22(1)	20(1)	-2(1)	10(1)	-4(1)
O(2)	36(1)	29(1)	32(1)	-10(1)	13(1)	-9(1)
O(3)	22(1)	18(1)	27(1)	-1(1)	5(1)	-1(1)
O(4)	21(1)	15(1)	42(1)	-1(1)	5(1)	1(1)
CO)	22(1)	21(1)	25(1)	-1(1)	9(1)	1(1)
C(2)	22(1)	15(1)	20(1)	3(1)	6(1)	3(1)
C(3)	24(1)	17(1)	19(1)	-1(1)	7(1)	-1(1)
C(4)	23(1)	18(1)	17(1)	2(1)	6(1)	0(1)
C(5)	25(1)	22(1)	38(1)	-2(1)	12(1)	0(1)

Table 5.7.5. Hydrogen coordinates ($\times 10^4$) and isotropic displacement parameters ($\text{Å}^2 \times 10^3$) for **11**.

Table 5.7.6. Crystal data and structure refinement for **11**.

Identification code	h04gb1
Empirical formula	C ₅ H ₉ BrO ₆
Formula weight	245.03
Temperature	150(2) K
Wavelength	0.71073 Å
Crystal system	Triclinic
Space group	P-1
Unit cell dimensions	a = 6.1630(2) Å α = 97.308(1)°
	b = 7.1410(2) Å β = 93.115(1)°
	c = 10.7000(4) Å γ = 113.713(2)°
Volume	424.75(2) Å ³
Z	2
Density (calculated)	1.916 Mg/m ³
Absorption coefficient	4.830 mm ⁻¹
F(000)	244
Crystal size	0.30x0.25x0.20 mm
Theta range for data collection	3.70 to 27.43°
Index ranges	-7 ≤ h ≤ 7; -9 ≤ k ≤ 9; -13 ≤ l ≤ 13
Reflections collected	7533
Independent reflections	1928 [R(int) = 0.0545]
Reflections observed (>2σ)	1609
Data Completeness	0.992
Absorption correction	None
Refinement method	Full-matrix least-squares on F ²
Data / restraints / parameters	1928/4/128
Goodness-of-fit on F ²	1.044
Final R indices [I > 2σ(I)]	R ¹ = 0.0330 wR ₂ = 0.0751
R indices (all data)	R ¹ = 0.0478 wR ₂ = 0.0802
Largest diff. peak and hole	0.980 and -0.958 e Å ⁻³

Notes: Carboxylate and water hydrogens located in penultimate difference Fourier map, and refined at 0.89 Å from relevant parent atoms.

Hydrogen bonds with $H \dots A < r(A) + 2.000$ Angstroms and $\langle DHA \rangle > 110$ deg.

D-H	d(D-H)	d(H..A)	$\langle DHA \rangle$	d(D..A)	A
O4-H3A	0.840	1.838	174.74	2.675	03 [-x+2, -y+1, -z+1]
O3-H3A	0.840	2.931	112.71	3.346	Br1
O1-H1	0.873	1.782	172.20	2.650	06
O5-H5	0.893	1.775	164.60	2.647	O4 [-x, -y, -z+1]
O6-H6B	0.872	1.918	169.15	2.780	O2 [-x+2, -y+1, -z]
O6-H6A	0.885	1.888	169.80	2.763	O2 [-x+1, -y+1, -z]

Table 5.7.7. Atomic coordinates ($\times 10^4$) and equivalent isotropic displacement parameters ($\text{\AA}^2 \times 10^3$) for **11**. U(eq) is defined as one third of the trace of the orthogonalized U_{ij} tensor.

Atom	X	y	z	U(eq)
Br(1)	6300(1)	836(1)	2797(1)	29(1)
O(1)	7553(3)	5774(3)	1993(2)	27(1)
O(2)	5579(4)	3261(3)	326(2)	29(1)
O(3)	1702(3)	1628(3)	1551(2)	23(1)
O(4)	2054(4)	2391(3)	4944(2)	28(1)
O(5)	1558(4)	-603(3)	3760(2)	36(1)
O(6)	10692(3)	7663(3)	469(2)	23(1)
CO	5725(5)	4103(4)	1409(3)	24(1)
C(2)	3702(5)	3291(4)	2255(3)	22(1)
C(3)	4658(5)	2555(4)	3375(3)	24(1)
C(4)	2609(5)	1382(4)	4105(3)	24(1)
O(5)	2947(5)	5031(5)	2734(3)	25(1)

Table 5.7.8. Bond lengths [Å] and angles [°] for **11**.

Br(1)-C(3)	1.946(3)	O(1)-C(1)	1.317(3)
O(2)-C(1)	1.218(3)	O(3)-C(2)	1.411(3)
O(4)-C(4)	1.228(3)	O(5)-C(4)	1.291(4)
C(1)-C(2)	1.544(4)	C(2)-C(5)	1.534(4)
C(2)-C(3)	1.547(4)	C(3)-C(4)	1.526(4)
O(2)-C(1)-O(1)	125.4(3)	O(2)-C(1)-C(2)	122.2(3)
O(1)-C(1)-C(2)	112.4(2)	O(3)-C(2)-C(5)	108.4(2)
O(3)-C(2)-C(1)	110.2(2)	C(5)-C(2)-C(1)	109.5(2)
O(3)-C(2)-C(3)	110.1(2)	C(5)-C(2)-C(3)	110.9(2)
C(1)-C(2)-C(3)	107.8(2)	C(4)-C(3)-C(2)	109.9(2)
C(4)-C(3)-Br(1)	110.58(19)	C(2)-C(3)-Br(1)	111.52(18)
O(4)-C(4)-O(5)	125.3(3)	O(4)-C(4)-C(3)	118.0(3)
O(5)-C(4)-C(3)	116.6(2)		

Symmetry transformations used to generate equivalent atoms.

Table 5.7.9. Anisotropic displacement parameters ($\text{Å}^2 \times 10^3$) for **11**. The anisotropic displacement factor exponent takes the form: $-2 \pi^2 [h^2 a^{*2} U_{11} + \dots + 2 h k a^* b^*]$

Atom	U11	U22	U33	U23	U13	U12
Br(1)	25(1)	33(1)	37(1)	12(1)	7(1)	16(1)
O(1)	21(1)	31(1)	25(1)	6(1)	7(1)	5(1)
O(2)	32(1)	36(1)	24(1)	3(1)	8(1)	17(1)
O(3)	20(1)	22(1)	24(1)	1(1)	-2(1)	8(1)
O(4)	26(1)	31(1)	23(1)	3(1)	7(1)	8(1)
O(5)	35(1)	29(1)	37(1)	6(1)	14(1)	4(1)
O(6)	21(1)	29(1)	21(1)	5(1)	3(1)	12(1)
C(1)	27(2)	25(2)	24(2)	7(1)	5(1)	15(1)
C(2)	20(1)	20(2)	25(1)	4(1)	1(1)	8(1)
C(3)	22(1)	25(2)	25(2)	4(1)	3(1)	9(1)
C(4)	21(1)	26(2)	22(1)	7(1)	0(1)	7(1)
C(5)	25(2)	26(2)	28(2)	6(1)	5(1)	13(1)

Table 5.7.10. Hydrogen coordinates ($\times 10^4$) and isotropic displacement parameters ($\text{Å}^2 \times 10^3$) for **11**.

Atom	x	y	z	U(eq)
H(3A)	2080	657	1289	27
H(3)	5823	3806	3961	29
H(5A)	2472	5550	2009	38
H(5B)	4288	6163	3272	38
H(5C)	1598	4292	3228	38
H(1)	8690(50)	6390(50)	1540(30)	39(10)
H(5)	220(70)	-1370(80)	4070(60)	130(20)
H(6B)	11970(40)	7480(50)	310(30)	39(10)
H(6A)	9990(120)	7790(110)	-240(40)	160(30)

Table 5.7.11. Crystal data and structure refinement for **9**.

Identification code	k03gb2
Empirical formula	C ₅ H ₅ BrO ₄
Formula weight	209.00
Temperature	150(2) K
Wavelength	0.71073 Å
Crystal system	Triclinic
Space group	P-1
Unit cell dimensions	a = 5.0470(2)Å alpha = 91.142(2)°
	b = 6.7130(3)Å beta = 96.891(2)°
	c = 10.8060(6)Å gamma = 103.043(4)°
Volume	353.67(3) Å ³
Z	2
Density (calculated)	1.963 Mg/m ³
Absorption coefficient	5.763 mm ⁻¹
F(000)	204
Crystal size	0.25 x 0.20 x 0.08 mm
Theta range for data collection	4.18 to 27.53°
Index ranges	-6<=h<=6; -8<=k<=8; -13<=l<=14
Reflections collected	4558
Independent reflections	1578 [R(int) = 0.0384]
Reflections observed (>2sigma)	1390
Data Completeness	0.968
Absorption correction	Semi-empirical from equivalents
Max. and min. transmission	0.70 and 0.55
Refinement method	Full-matrix least-squares on F ²
Data / restraints / parameters	1578/0/97
Goodness-of-fit on F ²	1.095
Final R indices [I>2sigma(I)]	R1 = 0.0456 wR2 = 0.1140
R indices (all data)	R1 = 0.0521 wR2 = 0.1191
Largest diff. peak and hole	1.086 and -1.064 eÅ ⁻³

Hydrogen bonds with H..A < r (A) + 2.000 and <DHA> 110 deg.

D-H	d(D-H)	d(H..A)	<DHA	d(D..A)	A
O3-H3	0.721	1.936	177.18	2.656	04 [-x+1, -y-1, -z]

Table 5.7.12. Atomic coordinates ($\times 10^4$) and equivalent isotropic displacement parameters ($\text{\AA}^2 \times 10^3$) for **9**. $U(\text{eq})$ is defined as one third of the trace of the orthogonalized U_{ij} tensor.

Atom	X	y	z	U(eq)
Br(1)	2672(1)	101(1)	1351(1)	47(1)
O(1)	6508(4)	-2368(4)	3632(2)	31(1)
O(2)	7246(6)	1057(5)	4104(3)	45(1)
O(3)	2272(5)	-4932(4)	882(3)	31(1)
O(4)	6825(5)	-3825(5)	1346(2)	40(1)
CO)	5897(7)	-499(6)	3644(3)	30(1)
C(2)	3080(6)	-1265(5)	2878(3)	27(1)
C(3)	3884(6)	-3349(5)	2859(3)	23(1)
C(4)	2215(7)	-5024(5)	3530(3)	30(1)
C(5)	4464(6)	-4072(5)	1605(3)	25(1)

Table 5.7.13. Bond lengths [\AA] and angles [$^\circ$] for **9**.

Br(1)-C(2)	1.916(3)	O(3)-C(5)	1.286(4)
O(1)-C(1)	1.358(5)	O(1)-C(3)	1.484(4)
O(4)-C(5)	1.233(4)	O(2)-C(1)	1.174(5)
C(5)-C(3)	1.514(4)	C(3)-C(4)	1.500(4)
C(3)-C(2)	1.542(4)	C(2)-C(1)	1.531(5)
C(1)-O(1)-C(3)	93.1(2)	O(4)-C(5)-O(3)	125.7(3)
O(4)-C(5)-C(3)	121.4(3)	O(3)-C(5)-C(3)	112.9(3)
O(1)-C(3)-C(4)	111.4(2)	O(1)-C(3)-C(5)	109.5(2)
C(4)-C(3)-C(5)	113.0(3)	O(1)-C(3)-C(2)	88.6(2)
C(4)-C(3)-C(2)	116.6(2)	C(5)-C(3)-C(2)	115.1(2)
C(1)-C(2)-C(3)	84.4(2)	C(1)-C(2)-Br(1)	113.2(2)
C(3)-C(2)-Br(1)	119.3(2)	O(2)-C(1)-O(1)	128.4(3)
O(2)-C(1)-C(2)	137.6(4)	O(1)-C(1)-C(2)	93.9(3)

Symmetry transformations used to generate

Table 5.7.14. Anisotropic displacement parameters ($\text{\AA}^2 \times 10^3$) for **9**. The anisotropic displacement factor exponent takes the form: $-2 \text{ gpi}^2 [\text{h}^2 \text{ a}^{*2} \text{ U11} + \dots + 2 \text{ h k a}^* \text{ b}^*$

Atom	U11	U22	U33	U23	U13	U12
Br(1)	69(1)	37(1)	37(1)	15(1)	-1(1)	17(1)
O(1)	27(1)	46(2)	21(1)	-2(1)	0(1)	11(1)
O(2)	44(2)	48(2)	33(1)	-6(1)	9(1)	-10(1)
O(3)	30(1)	43(2)	21(1)	-10	2(1)	11(1)
O(4)	26(1)	61(2)	33(1)	-9(1)	10(1)	10(1)
C(1)	30(2)	40(2)	19(2)	1(1)	10(1)	3(1)
C(2)	28(2)	31(2)	26(2)	4(1)	8(1)	10(1)
C(3)	23(1)	32(2)	16(1)	4(1)	4(1)	10(1)
C(4)	43(2)	29(2)	21(2)	11(1)	13(1)	9(1)
C(5)	27(2)	31(2)	21(2)	3(1)	5(1)	12(1)

Table 5.7.15. Hydrogen coordinates ($\times 10^4$) and isotropic displacement parameters ($\text{\AA}^2 \times 10^3$) for **9**.

Atom	X	y	z	U(eq)
H(2)	1544	-1263	3383	33
H(3)	2540(110)	-5300(80)	290(50)	52(15)
H(4A)	3213	-6107	3684	45
H(4B)	457	-5591	3017	45
H(4C)	1883	-4467	4328	45

Table 5.7.16. Crystal data and structure refinement for **10**.

Identification code	h03gb1
Empirical formula	C ₅ H ₉ BrO ₆
Formula weight	245.03
Temperature	150(2) K
Wavelength	0.71073 Å
Crystal system	Monoclinic
Space group	C2/c
Unit cell dimensions	a = 26.0020(5) Å α = 90°
	b = 6.3360(2) Å β = 116.807(1)°
	c = 12.2820(3) Å γ = 90°
Volume	1805.98(8) Å ³
Z	8
Density (calculated)	1.802 Mg/m ⁻¹
Absorption coefficient	4.544 mm ⁻¹
F(000)	976
Crystal size	0.15 x 0.15 x 0.10 mm
Theta range for data collection	3.79 to 27.49°
Index ranges	-33 ≤ h ≤ 33; -8 ≤ k ≤ 8; -15 ≤ l ≤ 15
Reflections collected	15130
Independent reflections	2058 [R(int) = 0.0503]
Reflections observed (>2σ)	1743
Data Completeness	0.996
Absorption correction	Semi-empirical from equivalents
Max. and min. transmission	1.00 and 0.25
Refinement method	Full-matrix least-squares on F ²
Data / restraints / parameters	2058 / 5 / 131
Goodness-of-fit on F ²	1.070
Final R indices [I > 2σ(I)]	R ¹ = 0.0268 wR ₂ = 0.0635
R indices (all data)	R ¹ = 0.0373 wR ₂ = 0.0673
Largest diff. peak and hole	0.631 and -0.667 eÅ ⁻³

Notes: Asymmetric unit contains 1 molecule of water in addition to 1 molecule of the title compound. Lattice dominated by H-bonding.

Hydrogenbonds with H. A < r(A) + 2.000 Angstroms d(H..A) and <DHA > 110 deg.

D-H	d(D-H)	d(H...A)	<DHA	d(D...A)	A
5-H5	0.871	1.843	156.88	2.666	06
O1-H1	0.874	1.743	173.17	2.613	03 [x, -y, z-1/2]
O3-H3	0.870	1.877	155.59	2.694	06 [x, y+1, z]
O3-H3	0.870	2.425	119.51	2.952	02
O6-H6B	0.870	1.923	169.28	2.782	02 [-x, y-1, -z-1/2]
O6-H6A	0.861	1.923	168.76	2.773	04 [-x, -y-1, -z]

Table 5.7.17. Atomic coordinates ($\times 10^4$) and equivalent isotropic displacement parameters ($\text{\AA}^2 \times 10^3$) for **10.U**(eq) is defined as one third of the trace of the orthogonalized U_{ij} tensor.

Atom	X	y	z	U(eq)
Br(1)	2176(1)	184(1)	441(1)	37(1)
O(1)	1533(1)	-1406(3)	-2335(1)	35(1)
O(2)	769(1)	-517(3)	-2049(1)	32(1)
O(3)	1021(1)	-468(2)	547(1)	27(1)
O(4)	235(1)	-3489(2)	-585(1)	33(1)
O(5)	860(1)	-5400(2)	-969(2)	33(1)
O(6)	99(1)	-8299(2)	-1058(1)	28(1)
C\$ (1)	1250(1)	-1204(3)	-1683(2)	24(1)
C(2)	1594(1)	-1981(3)	-390(2)	23(1)
C(3)	1228(1)	-2367(3)	285(2)	25(1)
C(4)	713(1)	-3787(3)	-487(2)	27(1)
C(5)	1587(1)	-3499(4)	1499(2)	38(1)

Table 5.7.18. Bond lengths [Å] and angles [°] for **10**.

Br(1)-C(2)	1.9540(19)	O(1)-C(1)	1.314(2)
O(2)-C(1)	1.204(2)	O(3)-C(3)	1.414(2)
O(4)-C(4)	1.208(2)	O(5)-C(4)	1.321(2)
C(1)-C(2)	1.511(3)	C(2)-C(3)	1.538(3)
C(3)-C(5)	1.535(3)	C(3)-C(4)	1.535(3)
O(2)-C(1)-O(1)	125.46(17)	O(2)-C(1)-C(2)	122.24(17)
O(1)-C(1)-C(2)	112.29(16)	C(1)-C(2)-C(3)	113.66(15)
C(1)-C(2)-Br(1)	105.80(12)	C(3)-C(2)-Br(1)	110.60(12)
O(3)-C(3)-C(5)	107.66(16)	O(3)-C(3)-C(4)	108.86(15)
C(5)-C(3)-C(4)	107.75(16)	O(3)-C(3)-C(2)	112.32(15)
C(5)-C(3)-C(2)	110.23(16)	C(4)-C(3)-C(2)	109.89(15)
O(4)-C(4)-O(5)	124.63(19)	O(4)-C(4)-C(3)	122.80(18)
O(5)-C(4)-C(3)	112.49(17)		

Symmetry transformations used to generate equivalent atoms.

Table 5.7.19. Anisotropic displacement parameters ($\text{Å}^2 \times 10^3$) for **10**. The anisotropic displacement factor exponent takes the form: $-2 \pi^2 [h^2 a^{*2} U_{11} + \dots + 2 h k a^* b^* U_{12}]$

Atom	U11	U22	U33	U23	U13	U12
Br(1)	25(1)	40(1)	42(1)	-10(1)	12(1)	-7(1)
O(1)	36(1)	46(1)	30(1)	11(1)	21(1)	13(1)
O(2)	26(1)	46(1)	26(1)	6(1)	12(1)	8(1)
O(3)	30(1)	28(1)	23(1)	-3(1)	12(1)	3(1)
O(4)	34(1)	30(1)	43(1)	-3(1)	24(1)	-3(1)
O(5)	34(1)	26(1)	45(1)	-7(1)	23(1)	-5(1)
O(6)	27(1)	28(1)	33(1)	-8(1)	17(1)	-3(1)
CO	26(1)	22(1)	25(1)	1(1)	14(1)	-1(1)
C(2)	22(1)	23(1)	25(1)	0(1)	11(1)	2(1)
C(3)	29(1)	23(1)	24(1)	2(1)	13(1)	3(1)
C(4)	36(1)	23(1)	26(1)	3(1)	17(1)	0(1)
C(5)	49(1)	40(1)	26(1)	9(1)	17(1)	5(1)

Table 5.7.20. Hydrogen coordinates ($\times 10^4$) and isotropic displacement parameters ($\text{Å}^2 \times 10^3$) for **10**.

Atom	X	y	z	U(eq)
H(22)	1792	-3325	-405	28
H(5A)	1917	-2618	2015	58
H(5B)	1725	-4851	1343	58
H(5C)	1348	-3753	1916	58
H(5)	583(10)	-6330(40)	-1210(20)	61(9)
H(1)	1348(11)	-870(50)	-3067(18)	53(8)
H(3)	740(11)	10(40)	-120(20)	53(9)
H(6B)	-166(10)	-9120(40)	-1580(20)	55(8)
H(6A)	-52(10)	-7750(40)	-630(20)	49(7)

Chapter 6 MM/PBSA Output Files

Table 6.6.4

r-ala	Complex-1		Receptor		Ligand		Delta	
	Mean	STD	Mean	STD	Mean	STD	Mean	STD
ELE	60.71	3.93	55.46	2.09	57.57	1.51	-52.32	4.70
VDW	3.79	3.11	8.98	2.24	1.82	0.94	-7.00	1.73
INT	79.41	6.30	66.93	5.65	12.80	3.34	-0.32	0.22
GAS	143.91	7.20	131.36	5.78	72.20	3.33	-59.64	4.44
PBSUR	5.27	0.09	4.82	0.04	2.11	0.02	-1.66	0.09
PBCAL	-35.68	1.15	-12.85	1.01	-55.39	0.74	32.56	1.63
PBSOL	-30.41	1.14	-8.03	1.00	-53.28	0.73	30.90	1.61
PBELE	25.03	3.20	42.61	1.76	2.19	1.41	-19.76	3.52
PBTOT	113.51	6.77	123.33	5.61	18.92	3.02	-28.74	3.17
GBSUR	5.27	0.09	4.82	0.04	2.11	0.02	-1.66	0.09
GB	-37.71	1.36	-13.35	1.18	-55.75	0.81	31.40	1.97
GBSOL	-32.43	1.33	-8.53	1.16	-53.64	0.80	29.74	1.93
GBELE	23.01	3.16	42.10	1.61	1.82	1.59	-20.92	3.18
GBTOT	111.48	6.72	122.83	5.69	18.55	3.07	-29.90	2.91
TSTRA	13.35	0.00	13.15	0.00	11.94	0.00	-11.74	0.00
TSROT	11.16	0.02	10.92	0.03	8.32	0.00	-8.08	0.02
TSVIB	44.71	0.35	31.18	0.17	6.70	0.15	6.82	0.47
TSTOT	69.22	0.37	55.25	0.16	26.97	0.15	-13.00	0.48

Table 6.6.5

s-ala	Complex-2		Receptor		Ligand		Delta	
	Mean	STD	Mean	STD	Mean	STD	Mean	STD
ELE	60.84	4.31	56.54	2.46	57.33	1.44	-53.02	5.87
VDW	2.93	3.17	9.52	2.31	1.87	0.93	-8.46	1.94
INT	81.10	6.46	68.18	5.67	13.28	3.04	-0.36	0.21
GAS	144.88	7.09	134.24	5.96	72.48	3.01	-61.85	5.31
PBSUR	5.09	0.09	4.87	0.04	2.11	0.01	-1.89	0.09
PBCAL	-34.99	1.39	-13.13	1.22	-55.45	0.68	33.60	2.04
PBSOL	-29.90	1.41	-8.27	1.22	-53.35	0.68	31.71	2.07
PBELE	25.86	3.51	43.41	2.05	1.87	1.28	-19.42	4.31
PBTOT	114.98	6.62	125.98	5.65	19.14	2.78	-30.14	3.71
GBSUR	5.09	0.09	4.87	0.04	2.11	0.01	-1.89	0.09
GB	-37.64	1.79	-14.41	1.35	-55.71	0.78	32.48	2.67
GBSOL	-32.55	1.80	-9.54	1.33	-53.61	0.77	30.59	2.68
GBELE	23.21	3.42	42.14	1.63	1.61	1.40	-20.54	3.78
GBTOT	112.32	6.51	124.71	5.69	18.88	2.85	-31.26	3.20
TSTRA	13.35	0.00	13.15	0.00	11.94	0.00	-11.74	0.00
TSROT	11.07	0.02	10.80	0.04	8.32	0.00	-8.06	0.04
TSVIB	44.63	0.54	31.96	0.37	6.73	0.15	5.94	0.39
TSTOT	69.05	0.54	55.91	0.39	27.00	0.15	-13.86	0.40

Table 6.6.6

r-val	Complex-4		Receptor		Ligand		Delta	
	Mean	STD	Mean	STD	Mean	STD	Mean	STD
ELE	66.92	3.20	55.04	2.20	59.59	1.41	-47.70	4.13
VDW	2.75	2.99	8.74	2.34	2.70	1.26	-8.69	1.47
INT	85.53	6.63	67.47	5.73	18.38	3.64	-0.32	0.21
GAS	155.20	6.79	131.25	5.87	80.66	3.62	-56.71	3.69
PBSUR	5.50	0.06	4.83	0.03	2.41	0.02	-1.74	0.05
PBCAL	-34.18	0.91	-13.09	1.02	-51.99	0.72	30.90	1.45
PBSOL	-28.68	0.92	-8.26	1.02	-49.58	-49.58	29.16	1.46
PBELE	32.74	2.71	41.94	1.58	7.60	1.29	-16.80	3.07
PBTOT	126.52	6.56	122.99	5.65	31.08	3.35	-27.55	2.56
GBSUR	5.50	0.06	4.83	0.03	2.41	0.02	-1.74	0.05
GB	-36.90	1.09	-13.40	1.17	-52.18	0.81	28.67	1.64
GBSOL	-31.40	1.08	-8.56	1.17	-49.77	0.80	26.93	1.63
GBELE	30.02	2.82	41.64	1.44	7.40	1.45	-19.02	3.03
GBTOT	123.80	6.63	122.68	5.71	30.89	3.37	-29.77	2.57
TSTRA	13.40	0.00	13.15	0.00	12.16	0.00	-11.90	0.00
TSROT	11.24	0.01	10.92	0.01	8.77	0.01	-8.46	0.01
TSVIB	47.72	0.28	31.17	0.16	9.35	0.04	7.19	0.24
TSTOT	72.35	0.28	55.24	0.16	30.28	0.05	-13.17	0.25

Table 6.6.7

s-val	Complex-3		Receptor		Ligand		Delta	
	Mean	STD	Mean	STD	Mean	STD	Mean	STD
ELE	66.53	3.74	54.82	2.42	59.78	1.37	-48.06	4.57
VDW	2.62	2.91	8.67	2.12	2.66	1.22	-8.71	1.55
INT	84.95	6.82	67.34	5.86	17.91	3.65	-0.30	0.20
GAS	154.11	7.01	130.82	5.73	80.35	3.42	-57.07	4.32
PBSUR	5.47	0.07	4.83	0.04	2.41	0.02	-1.77	0.08
PBCAL	-34.20	1.03	-12.76	1.11	-53.99	0.64	32.56	1.71
PBSOL	-28.73	1.04	-7.93	1.11	-51.58	0.64	30.78	1.72
PBELE	32.34	3.14	42.06	1.79	5.78	1.27	-15.51	3.31
PBTOT	125.37	6.76	122.89	5.53	28.77	3.22	-26.29	3.02
GBSUR	5.47	0.07	4.83	0.04	2.41	0.02	-1.77	0.08
GB	-36.31	1.13	-13.01	1.25	-54.34	0.77	31.04	1.93
GBSOL	-30.84	1.11	-8.18	1.25	-51.93	0.76	29.27	1.92
GBELE	30.22	3.23	41.81	1.67	5.44	1.43	-17.02	3.12
GBTOT	123.26	6.66	122.64	5.63	28.42	3.23	-27.80	2.93
TSTRA	13.40	0.00	13.15	0.00	12.16	0.00	-11.90	0.00
TSROT	11.23	0.02	10.92	0.01	8.78	0.01	-8.48	0.02
TSVIB	48.08	0.33	31.25	0.33	9.42	0.12	7.42	0.45
TSTOT	72.71	0.34	55.31	0.33	30.35	0.13	-12.96	0.46

ELE = electrostatic energy as calculated by MM force field.

VDW = van der Waals contribution from MM.

INT = internal energy arising from bond, angle and dihedral terms in the MM force field. (this term always amounts to zero in the single trajectory approach).

GAS = total gas phase energy (sum of ELE, VDW and INT)

PBSUR/GBSUR = nonpolar contribution to the solvation free energy calculated by an empirical model.

PBCAL/GB = the electrostatic contribution to solvation free energy calculated by PB or GB respectively.

PBSOL/GBSOL = sum of nonpolar and polar contributions to solvation.

PBELE/GBELE = sum of the electrostatic solvation free energy and MM electrostatic above.(kcal/mol)

TSTRA = translational entropy (as calculated by nmode)

TSROT = rotational entropy (as calculated by nmode)

TSVIB = vibrational entropy (as calculated by nmode)

Curriculum Vitae

Surname: OZHAN KOCAKAYA **Name:** Safak
Date of Birth: 18.01.1980 **Place of Birth:** Eskisehir (Turkey)
Marital status: Married

Current address: **Telephone:** +90 412 2488406 -3198 (work)
University of Dicle
Faculty of Science & Art **e-mail :** safakozhan@dicle.edu.tr
Department of Chemistry
21280 Diyarbakır, TURKEY

Work Experience

2005 **Research Assistant**, University of Dicle, Diyarbakır-Turkey.
Working as a research assistant in Organic Chemistry I involved in teaching of a variety of courses in undergraduate.

Education

2004- **Ph.D.**, University of Dicle in Organic Chemistry under the supervision of Professor Necmettin PIRINCCIOGLU, Studying “ Experimental And Thereotical Investigation of Various Chemical Processes.”

2002 - 2004 **M.Sc. in Chemistry**, University of Dicle in Organic Chemistry under the supervision of Professor Necmettin PIRINCCIOGLU, “Studying Addition of Aqueous Bromine to Disodium Salts of Mesaconate and Citraconate”.

1998 - 2002 **B.Sc. in Chemistry** , University of Dicle, Diyarbakır.

2001 (10 weeks)

I have attended to general English course at
Hilderstone College, Broadstairs, England.

Other Skills

Routinely use P.C computers for word processing, on-line searches etc. I have extensive 'hands-on' experience with NMR equipment (Bruker 400 MHz and also Gaussian 03 and AMBER v9, Dock v 6.0.

Interests and Activities

My interests including reading, cinema and jogging.